JOURNAL OF THERMOPHYSICS AND HEAT TRANSFER
Vol. 19, No. 3, July–September 2005

Transport Properties for the Chemical Oxygen–Iodine Laser

Drew A. Copeland*
The Boeing Company, Wast Hills, California 91304

Transport models for computing the diffusivity, viscosity, and thermal conductivity of mixtures over a broad range of temperatures of interest to chemical oxygen–iodine lasers are presented. The individual species transport models are based on the corresponding states correlations for the rare gases and several non- or weakly polar polyatomic molecules developed by Mason, Kestin, and coworkers and extended by Paul to treat strongly polar molecules and the Thijsse expression for conductivity. New polynomial extensions for the molecular collision integrals to allow their computation for $0 < T^* \leq 1$ are developed. The potential and molecular parameters for the atomic and diatomic halogens are derived from viscosity data if available, estimated using the Tang–Toennies potential model and the Cambi potential parameter correlations, or obtained from the literature as appropriate. Results are compared to both experimental and theoretical data when available, and good agreement is obtained. Binary interaction potential parameters with which to compute the mixture viscosity and conductivity using the Chapman–Enskog theory are presented for 14 species. New approximate mixture rules that use only the pure species properties are also discussed. Parametric representations of the species viscosities and conductivities are provided for temperatures ranging from 50 to 1000 K.

Nomenclature

A^*, B^*, C^*, E^*	=	collision integral ratios, dimensionless
a	=	effective rigid-core diameters, Å
a_0	=	Bohr radius, 0.529177 Å
C	=	internal contribution to the molar specific heat, erg/mol · K
C_P	=	molar specific heat at constant pressure, erg/mol · K
C_{spn}	=	empirical spin-polarization coefficient, dimensionless
C_V	=	molar specific heat at constant volume, erg/mol · K
C_{2n}	=	long-range dispersion coefficients, erg · cm^{2n}
C^*_{2n}	=	reduced long-range dispersion coefficients $C_{2n}/\varepsilon\sigma^{2n}$, dimensionless
$\hat{C}_{2n}$	=	effective reduced long-range dispersion coefficient $C_{2n}/\hat{\varepsilon}\hat{\sigma}^{2n}$, dimensionless
$\tilde{C}_{2n}$	=	reduced long-range dispersion coefficient $C_{2n}/\varepsilon r_M^{2n}$, dimensionless
c_i	=	parametric fit coefficients
D	=	binary mass or internal energy diffusion coefficient, cm^2/s
d	=	number of rotational degrees of freedom, dimensionless
F, G, H	=	symmetric, positive definite matrix describing mixture transport properties
f_{ij}, f_η, f_λ	=	Kihara binary mass diffusion, viscosity, and conductivity correction factor, dimensionless
g	=	quantum mechanical summation in the rotational exchange corrections, dimensionless
$\hbar$	=	Planck constant, $h/2\pi$, 1.054592 × 10^{-27} erg · s
I	=	rotational moment of inertia, g · cm^2
k_B	=	Boltzmann constant, 1.380622 × 10^{-16} erg/particle · K
N_A	=	Avogadro's number, 6.022169 × 10^{23} particles/mol
N_B, N_{NB}	=	number of molecular bond and nonbond electrons
N_E	=	effective number of electron oscillators
N_I, N_O	=	number of inner and outer atomic electrons
N_S	=	number of species in the gas mixture
N_T	=	total number of atomic or molecular electrons
P	=	gas pressure, torr
R	=	universal gas constant, 8.31434 × 10^7 erg/particle · K
$\boldsymbol{R}_a$	=	ath atom position relative to the molecular center of mass, Å
r	=	intermolecular separation, Å
r_M	=	intermolecular equilibrium separation, Å
r^2	=	ratio of the internal to translational heat capacity, $2C_{\text{int}}/5R$, dimensionless
s^2	=	ratio of the rotational to translational heat capacity, $2C_{\text{rot}}/5R$, dimensionless
T	=	gas temperature, K
T_B	=	boiling point temperature, K
T^*_{crs}	=	crossover temperature for uncorrected rotational energy correlation, dimensionless
T^*	=	reduced gas temperature, k_BT/ε, dimensionless
$\hat{T}$	=	effective gas temperature, $k_BT/\hat{\varepsilon}$, dimensionless
U	=	intermolecular interaction potential, erg
U^*	=	reduced intermolecular interaction potential, U/ε, dimensionless
$\hat{U}$	=	effective intermolecular interaction potential, $U^*\xi^{-2}$, dimensionless
V	=	Born–Mayer repulsive potential strength, erg
V^*, $\tilde{V}$	=	reduced repulsive potential strength, V/ε, dimensionless
$\hat{V}$	=	effective reduced repulsive potential strength, $V^*\xi^{-2}$, dimensionless
W	=	molecular weight, g/mol
W_{ij}	=	reduced molecular weight, $W_iW_j/(W_i + W_j)$, g/mol
x	=	normalized intermolecular separation, r/r_M, or mole fraction, dimensionless
Z	=	collision number for energy relaxation, dimensionless

Presented as Paper 2004-2261 at the 35th Plasmadynamics and Lasers Conference, Portland, OR, 28 June–1 July 2004; received 14 July 2004; revision received 16 November 2004; accepted for publication 7 November 2004.

*Senior Scientist/Engineer, Technology Development, Laser and Electro–Optical Systems, 8531 Fallbrook Avenue. Member AIAA.

α = static molecular polarizability, Å^3
α^* = reduced static molecular polarizability, α/σ^3, dimensionless
γ = formal expansion parameter in thermally averaged interaction potential
Δ = deviation of viscosity or conductivity from present value, %, or total exchange correction
Δ_{spn} = spin-polarization correction factor, dimensionless
$\Delta_{\mu\mu}$, $\Delta_{\mu\Theta}$, $\Delta_{\Theta\Theta}$ = exchange correction for dipole–dipole, dipole–quadrupole, and quadrupole–quadrupole collisions, dimensionless
δ^* = reduced dipole–dipole interaction parameter, $\mu^2/2\varepsilon\sigma^3$, dimensionless
ε = intermolecular interaction potential well-depth, erg
$\hat{\varepsilon}$ = effective intermolecular interaction potential well-depth, $\varepsilon\xi^2$, erg
η, η_V = shear and volume viscosity coefficient, μPa · s
Θ = magnitude of the quadrupole moment, B, where $1\text{B} = 10^{-26}$ esu · cm^2
$\boldsymbol{\Theta}$ = total molecular quadrupole tensor, B
$\boldsymbol{\Theta}_a$ = total atom molecular quadrupole tensor, B
Θ^* = $\Theta/\sqrt{\varepsilon\sigma^5}$, reduced quadrupole moment, dimensionless
θ, ϕ = intermolecular interaction potential orientation angles, rad
θ_R = rotational temperature, $\hbar^2/2k_B I$, K
Λ^* = de Boer parameter, $h/\sigma\sqrt{m\varepsilon}$, dimensionless
λ = thermal conductivity, mW/m · K
μ = magnitude of the dipole moment, D, where $1\text{D} = 10^{-18}$ esu · cm
$\boldsymbol{\mu}$ = total molecular dipole moment vector, D
$\boldsymbol{\mu}_a$ = total atom dipole moment vector, D
μ_{ij} = interaction dipole moment, $\sqrt{\mu_i\mu_j}$, D
μ^* = reduced dipole moment, $\mu/\sqrt{\varepsilon\sigma^3}$, dimensionless
ν_0 = mean relative velocity of the collision partners, cm/s
ξ = temperature–dependent effective well-depth parameter, dimensionless
ρ = Born–Mayer repulsive range, Å, or gas density, g/cm^3
ρ^* = reduced repulsive range, ρ/σ, dimensionless
$\tilde{\rho}$ = reduced repulsive range, ρ/r_M, dimensionless
$\hat{\rho}$ = effective reduced repulsive range, $\rho^*\xi^{+1/6}$, dimensionless
σ = rigid-sphere collision diameter, Å
$\hat{\sigma}$ = effective rigid sphere collision diameter, $\sigma\xi^{-1/6}$, Å
τ_D = duration time of a collision, s
τ_R = rotational period of a molecule, s
χ^* = reduced dipole-induced dipole interaction parameter, dimensionless
$\Omega_{ij}^{(l,s)^*}$ = reduced collision integral, dimensionless

Subscripts

int = internal
i, j = species
ele = electronic
rot = rotational
vib = vibrational

Superscripts

(M) = monatomic value
T = transpose operation
298 = value at 298.15 K
∞ = value in high-temperature limit

Miscellaneous

$\mathcal{P}$ = mixture viscosity, μPa · s, or conductivity, mW/m · K
$\mathfrak{S}_{20}$ = Thijsse cross section for momentum transfer, cm^2
$\mathfrak{S}_{1000}$ = Thijsse cross section for the mass self-diffusion, cm^2
$\mathfrak{S}_{10E}$ = Thijsse cross section for total energy flux, cm^2
$\mathfrak{S}_{10D}$ = Thijsse cross section for total energy flux difference, cm^2
$\mathfrak{S}_{10D}^{10E}$ = Thijsse coupling cross section between the total energy flux and the energy flux difference, cm^2
$\mathfrak{S}_{1010}$ = Thijsse cross section for the decay of the translational energy flux, cm^2
$\mathfrak{S}_{100\varepsilon}$ = Thijsse cross section for the decay of the internal energy flux, cm^2
$\mathfrak{S}_{100\varepsilon}^{1010}$ = Thijsse coupling cross section between the translational and the internal energy fluxes, cm^2
$\mathfrak{S}_{0001}$ = Thijsse cross section for the relaxation of internal energy, cm^2
$\mathfrak{S}_{0010}$ = Thijsse cross section for the exchange of translational and internal energy, cm^2

I. Introduction

THERMOCHEMICAL models of the species heat capacity, enthalpy, and entropy and transport property models of mass diffusion, viscosity, and thermal conductivity are crucial to describe the mass, momentum, and energy transport within flowing, reacting, dilute gas mixtures and to ensure that the aerodynamics of the flow is accurately described by the model. In the modeling of chemical laser performance, such as that of the chemical oxygen–iodine laser (COIL), this is important during both the testing phase when subscale test data are used to validate the performance models and, later, during the design phase when the performance models are used to design and scale such laser systems for applications. Ensuring that the aerodynamics within the cavity is accurately represented by the transport models significantly reduces and shifts validation concerns to the mixing, turbulence, chemical kinetics, and gain models used to describe laser performance, about which there is often considerably more uncertainty and debate. Although there has been considerable experimental and theoretical progress in the understanding of dilute-gas transport properties during the last 35 years, computational fluid dynamics (CFD) models often use transport models developed in the early part of the last century or the 1950s and 1960s when manned space flight was becoming a reality. For example, the Sutherland model is often used to estimate and/or parameterize the viscosity and thermal conductivity of the individual gas species, the Eucken or modified Eucken model is frequently used to estimate the thermal conductivity, whereas the Wilke rules (see Refs. 1 and 2) are often used to describe the gas mixtures viscosity and conductivity. Comparisons of the species viscosities and conductivities computed using the Sutherland model with those computed using the present transport models shows, for several species, significant disagreement over the temperature range of present interest (see Ref. 3). In addition, recent work has suggested that the Wilke mixture rules for dilute gases, which date to the late 1940s, can be substantially improved for multicomponent gas mixtures with little or no increase in computational cost (see Refs. 4–6). Whereas there exist extensive experimental transport data for the rare gases, N_2, and O_2, the available experimental transport data for Cl_2, I_2, H_2O, and H_2O_2 are more limited, and experimental transport data for ICl, Cl, and I are unavailable. Furthermore, although there exist numerous tabulations and functional fits to much of the species transport data, a major drawback is that it often does not span the temperature range, ~50–1000 K, of present interest for modeling conventional and ejector COIL performance. Also, recent transport property work has focused on higher temperatures where molecular dissociation

and ionization can become important.[5–7] Thus, models are needed to extrapolate intelligently experimental data to the required temperature ranges or provide estimates in absence of data. Indeed, although initially transport theory achieved prominence and importance for the wealth of information and understanding it shed on the interaction potentials between molecules, today its importance stems more from the need to predict and estimate the transport properties of species outside the range of available data and for the infinitude of gas mixtures of interest to industrial applications.[8] These needs have prompted significant refinements and improvements in the theories used to estimate, predict, and compute the transport properties of both individual species and mixtures. The present work was motivated, in part, by the need to describe accurately these species and mixture transport properties to model the COIL medium over a wide range of temperatures for which experimental data did not exist or, in a few cases, for which little or no data existed.

For COIL modeling purposes, we consider the following 14 species: the rare gases He, Ne, Ar, Kr, and Xe, atomic iodine and chlorine I and Cl, the diatomics N_2, O_2, I_2, Cl_2, and ICl, and the polyatomics H_2O and H_2O_2. Although most practical COIL mixes use He or N_2 as the buffer gas, occasionally Ar has been used and, for completeness, all of the rare gases are included. Reliable, well-validated computational models for the transport properties of the rare gases, N_2, O_2, and several other molecules, not of specific interest to COIL, and their mixtures over a broad range of temperatures have been developed by Kestin et al.,[9] Boushehri et al.,[10] Bzowski et al.,[11] and Mason and Uribe.[12] Their model of viscosity and binary mass diffusivity for the dilute gases is based on the Chapman–Enskog statistical mechanical theory of transport, an extended principle of corresponding states, some knowledge of the intermolecular potentials, and a set of combination rules. For the present application, an important result of their work was to provide a set of analytic functionals to compute the transport collision integrals for the noble gases for $T^* > 0$ and for molecular gases for $T^* \geq 1$, as well as a consistent, well-validated set of potential parameters for the rare gases, N_2, and O_2. Although these models were limited in application to non- or weakly polar molecules, Paul[13] and Paul and Warnatz[14] recently provided a model to extend these functionals to strongly polar molecules, such as water, and gave polynomial extensions for the molecular collision integrals for $0.2 \leq T^* \leq 1$. In the present work, new polynomial extensions for these integrals for $0 < T^* \leq 1$ are developed. Paul[13] also suggested a methodology to estimate the required potential parameters for additional molecules not included in the original database that has been employed, in part, to determine the potential parameters for the remaining species of interest to COIL, namely, I, Cl, I_2, Cl_2, and ICl. For the diatomic halogens, experimental viscosity data are used to determine the potential well parameters for low to intermediate temperatures, whereas the Tang and Toennies[15,16] potential model is used to obtain the repulsive potential parameters required for high temperatures. For the atomic halogens and the interhalogen ICl, in lieu of experimental viscosity data, the Cambi et al.[17] potential well parameter correlations and the Tang and Toennies[15,16] model are used to determine all of the required potential parameters. For completeness, the fluorine and bromine halogen atoms and molecules, although not of interest to COIL applications, have been included to facilitate an assessment of the trends in the halogen potential parameters obtained here and a comparison of the computed viscosities and conductivities with those of other workers; good agreement is obtained.

The thermal conductivity model for the species is based on the Thijsse total energy formulation of species conductivity (see Refs. 18–20) rather than the more traditional two-flux or Hirschfelder–Eucken formulation that was employed by Uribe et al.[21,22] to develop a correlation to predict the thermal conductivity of several polyatomic gases. When the internal mechanical modes are assumed to be independent, new approximate expressions for the internal energy diffusion coefficient and collision number are developed that use the Uribe et al.[21,22] correlation for the rotational energy diffusion coefficient and the classical Parker[23] Brau–Jonkman[24] expression for the rotational collision number. Corrections for near-resonant rotational exchange collisions on the rotational diffusion coefficient and spin-polarization effects, although small, are included as appropriate. In addition to the species molecular weight and potential parameters required for the viscosity coefficients, the thermal conductivity model requires several additional molecular parameters including the species heat capacity, moments of inertia, quadrupole moments, and rotational collision number. For the halogen diatomics, reliable values of these parameters are available from the literature with the notable exception of the rotational collision number, which, in the spirit of Uribe et al.,[21,22] is treated as an adjustable parameter to correlate the available diatomic halogen conductivity data. Results are compared to both experimental and theoretical data when available, and the model provides a very satisfactory correlation. With suitable estimates of the quadrupole moments for the weakly polar interhalogen ICl and polyatomic hydrogen peroxide H_2O_2, the model is then used to obtain their conductivities. Because the Uribe et al.[21,22] rotational energy diffusion correlation is not applicable to strongly polar molecules, H_2O was treated using the same model but assuming that its rotational collision number was temperature independent and using the Sandler high-temperature expression for the rotational diffusion coefficient.[25] For water, a reasonable correlation with available experimental data was obtained.

This paper is organized as follows. In Sec. II, the transport property correlations of Kestin et al.,[9] Boushehri et al.,[10] Bzowski et al.,[11] and Mason and Uribe,[12] the combination rules used to obtain the binary interaction potential parameters for unlike species, and the Paul[13] and Paul and Warnatz[14] extension of the correlation to treat strongly polar molecules are briefly reviewed. The discussion is intended primarily to summarize the more practical aspects of these models for the purpose of their application, but where appropriate, the limitations and applicability of Paul's thermally averaged interaction potential model for viscosity and the Thijsse conductivity model are briefly discussed. For a more complete justification and/or validation of the models, the reader is referred to the original papers. Then the methodology to determine the intermolecular potential parameters for the halogen species is discussed, and the required binary potential parameters are derived and compared with available data. The section concludes with a summary of the binary interaction potential parameters for species of interest to COIL. In Sec. III, the Thijsse conductivity model is reviewed, and the formal expression for the conductivity is recast in terms of the internal energy diffusion coefficient and collision number. Practical expressions for the latter are described, and the additional molecular parameters required for the halogens, the interhalogen ICl, and the polyatomics H_2O and H_2O_2 are determined and comparisons are made to the available data. Molecular parameters for species of interest to COIL are summarized. In Sec. IV, the Chapman–Enskog theory of mixture viscosity and conductivity for dilute gases is summarized, and new approximate expressions for these transport mixture properties, which require only pure species properties and parameters, are presented. To facilitate their application in practical CFD programs, parametric representations of the species viscosities and conductivities over the temperature range of interest to COILs are also given. The work is summarized in Sec. V. For completeness, the formulas to compute the collision integrals and the new polynomial extensions for the molecular collision integrals are summarized in the Appendix.

II. Mass Diffusivity and Viscosity

A. Review

It follows from the Chapman–Enskog solution of the Boltzmann equation for dilute gases that the binary mass diffusion coefficient D_{ij} for species i diffusing in species j (or vice versa) and the viscosity η_i of species i can be written as (see Refs. 9–12, 26, and 27),

$$D_{ij} \equiv \frac{3}{8}\frac{RT}{P}\frac{1}{N_A}\frac{(\pi RT/2W_{ij})^{\frac{1}{2}}}{\pi\sigma_{ij}^2\Omega_{ij}^{(1,1)^*}} f_{ij} \tag{1a}$$

$$\eta_i \equiv \frac{5}{16}\frac{1}{N_A}\frac{(\pi RTW_i)^{\frac{1}{2}}}{\pi\sigma_i^2\Omega_i^{(2,2)^*}} f_\eta \tag{1b}$$

Whereas both of the correction factors f_{ij} and f_η depend on the gas temperature and are very nearly unity, only f_{ij} depends on the gas composition.[3,26,27] Expressions for f_{ij} are available,[3,26,27] whereas $f_\eta = 1 + (3/196)(8E^* - 7)^2$. The reduced transport collision integrals $\Omega_{ij}^{(l,s)^*}$ and $\Omega_i^{(l,s)^*} \equiv \Omega_{ii}^{(l,s)^*}$, which depend on the gas temperature and several other parameters characterizing the shape of the interaction potential, will be further discussed.

Early work often attempted to correlate transport data using a specific representation of the molecular interaction potential such as the well-known Lennard–Jones (L–J) potential. Because only pairwise interactions are significant for dilute gases, the principle of corresponding states suggests that even the properties of dilute multicomponent gases could be expressed in terms of the properties of its pure components plus functionals corresponding only to binary interactions. The two-parameter principle of corresponding states expresses the equilibrium and transport properties in terms of nearly universal functions when written in terms of appropriate scale factors representing the pairwise molecular interaction range and energy. This was confirmed in the early 1970s for mixtures of the noble gases by Kestin et al.[28] However, through advances in experimental techniques for measuring noble gas scattering at thermal- and high-energies and the development of numerical methods for direct inversion of the measured transport properties to determine the potential without any explicit assumption about its functional form, it became apparent by the 1980s that the potentials for the noble gases did not scale perfectly using two parameters. To improve the corresponding states description at low and high temperatures, the correlations had to describe better and to distinguish between the shapes of the potentials of the individual noble gases. At low temperatures, this required accounting for the long-range attractive part of the interaction potential that was achieved by using the van der Waals potential,

$$U(r) = -C_6/r^6 \tag{2}$$

characterized by an effective dispersion coefficient C_6. At high temperatures, this required improving the description of the short-range repulsive potential, which was achieved using the Born–Mayer repulsive potential,

$$U(r) = V \exp(-r/\rho) \tag{3}$$

characterized by a repulsive range ρ (not to be confused with the gas density) and strength V. A schematic of the interaction potential is shown in Fig. 1. Thus, the extended five-parameter principle of corresponding states developed by Najafi et al.[29] is based on the following form of the molecular interaction potential energy:

$$U(r) = \varepsilon U^*\left(r/\sigma, \rho^*, V^*, C_6^*\right) \tag{4}$$

Here ε is an energy scale parameter chosen to be the depth of the potential well; σ, sometimes referred to as the collision diameter, is a distance parameter chosen to be the intermolecular separation r at which the potential energy is zero; $\rho^* \equiv \rho/\sigma$ and $V^* \equiv V/\varepsilon$ characterize the range and strength of the repulsive potential, respectively; and $C_6^* \equiv C_6/\varepsilon\sigma^6$ characterizes the long-range dispersion forces. The corresponding reduced collision integrals $\Omega^{(l,s)^*}$ are functions of the reduced gas temperature T^* and the potential shape parameters ρ^*, V^*, and C_6^*.

From a knowledge of the asymptotic forms of the collision integrals, which are dictated by the corresponding asymptotic forms of the potential in the low- and high-temperature regimes, and the use of a two-parameter correlation for the temperatures in between, Kestin et al.[9] developed a five-parameter corresponding states correlation for mixtures of the noble gases describing their binary mass diffusion, viscosity, and conductivity coefficients. For practical purposes, the temperature range was divided into three specific regions. In the middle temperature range, $1.2 \le T^* \le 10$, a two-parameter correlation parameterized by σ and ε was used, whereas in the cryogenic temperature range, $0 < T^* \le 1.2$, the parameter C_6^* was included, and in the high-temperature range, $T^* \ge 10$, the parameters ρ^* and V^* were included. Through a complex iterative process, Kestin et al.[9] determined the mathematical form of the collision integral functionals and a consistent set of material parameters σ, ε, ρ^*, and V^*, which will be summarized in Sec. II.C. The resulting functionals for the reduced collision integrals $\Omega^{(l,s)^*}$ are continuous and have continuous first and second derivatives at the crossover points $T^* = 1.2$ and $T^* = 10$, possess the correct asymptotic behavior as $T \to 0$ and $T \to \infty$, and satisfy the recursion relations imposed on them by theory; see the Appendix. For reduced temperatures T^* ranging from 0.01 to 100, the noble gas reduced collision integrals $\Omega^{(1,1)^*}$ and $\Omega^{(2,2)^*}$ are shown in Figs. 2 and 3, respectively. The splitting of these curves at low temperatures is indexed by the long-range dispersion parameter C_6^* and at high temperatures by the repulsive range and strength parameters ρ^* and V^*, respectively. For comparison, the corresponding L–J collision integrals are also shown, from which it is apparent that they are only a good approximation for temperatures ranging from about $T^* = 1$ to $T^* = 10$.

The principle of corresponding states is more limited for polyatomic molecules than for noble gases.[12] This is caused in part by a lack of knowledge of the interaction potentials and inelastic collisions, as well as by a less extensive, accurate experimental database for the transport properties. Although unable to encompass low temperatures, which are dominated by the attractive wells and tails of the potential and its intrinsic antisotopic character, Boushehri et al.[10] were able to develop an extended four-parameter principle of corresponding states correlation, describing viscosities and mass self-diffusion coefficients, for several non- or weakly polar molecular species valid when $T^* \ge 1$ that ensures that quantum effects between collision partners remain small. For $1 \le T^* \le 10$, $\Omega^{(2,2)^*}$ is the same as that for the noble gases, but $\Omega^{(1,1)^*}$ was adjusted slightly to achieve better agreement with the few available, accurate measurements of the binary mass diffusion coefficient.[12] For $T^* \ge 10$, the molecular transport collision integrals $\Omega^{(1,1)^*}$ and $\Omega^{(2,2)^*}$ are identical with those for the noble gases. Because the resulting collision integrals represent, in effect, an effective spherical interaction potential between molecules, they have been referred to as universal spherical-potential collision integrals.[4]

For the present application, the molecular collision integrals for T^* less than 1 are required to be able to compute transport properties down to temperatures of 50 K for strongly polar species such as water or nonpolar species such as I_2 for which $\varepsilon/k_B \approx 500$ K and the minimum reduced temperature is about 0.1. To ensure quantum effects are negligible when computing the collision integrals requires that a molecules de Broglie wavelength be small compared to its collision diameter or $\Lambda^*/T^{*1/2} \ll 1$, where $\Lambda^* \equiv h/\sigma\sqrt{m\varepsilon}$ is the de Boer parameter (see Ref. 26) to within factors of order unity.

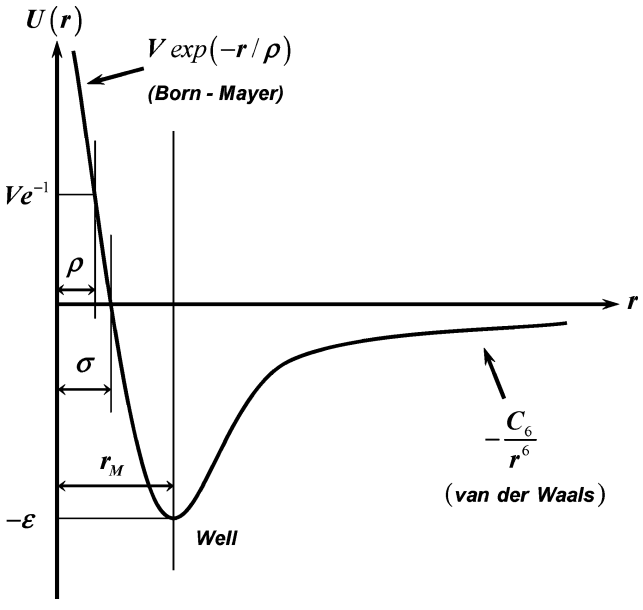

Fig. 1 Schematic of interaction potential.

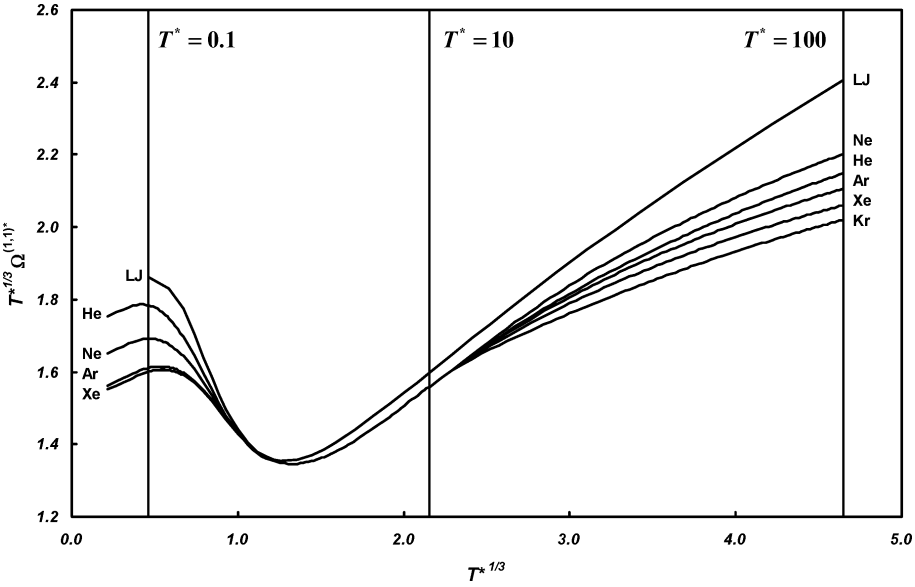

Fig. 2 Noble gas collision integrals $\Omega^{(1,1)^*}$ vs reduced temperature T^*.

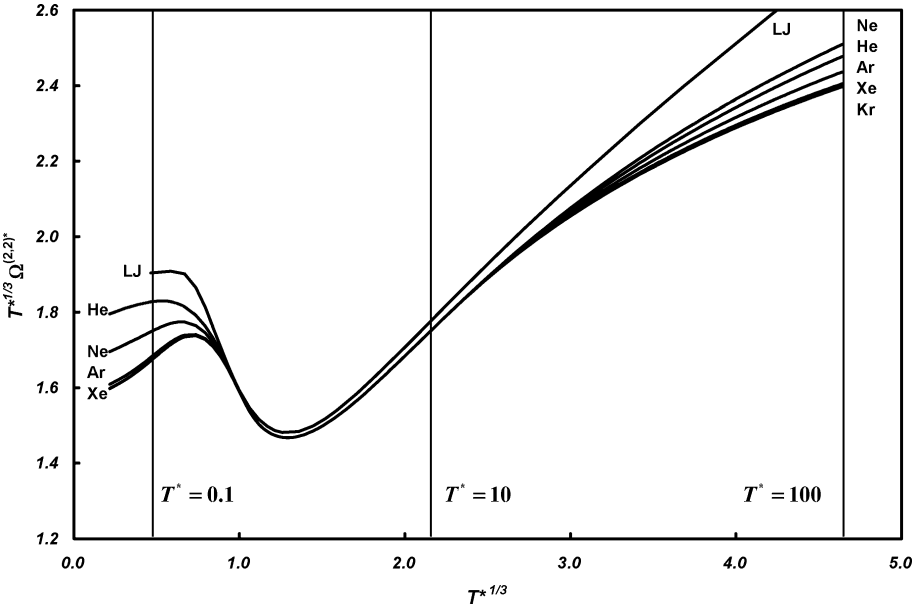

Fig. 3 Noble gas collision integrals $\Omega^{(2,2)^*}$ vs reduced temperature T^*.

In other words, for temperatures such that

$$T^* \gg \Lambda^{*2} \tag{5}$$

quantum effects can be neglected. For the present molecular species of interest, this constraint is most significant for water for which $\Lambda^* \approx 0.167$ so that $T^* \gg 0.028$ or $T \gg 15$ K. Here the temperatures of interest are well in excess of this temperature. Unfortunately, at present, below $T^* = 1$ there is no consistent means of treating the collision integrals for other than the noble gases.[13] To circumvent this problem, new polynomial extensions of the molecular collision integrals $\Omega^{(1,1)^*}$ and $\Omega^{(2,2)^*}$, which are analytic to second order with the collision integrals given by Bzowski et al.[11] at $T^* = 1$, have been developed for $0.1 \leq T^* \leq 1$. Also a scaled extrapolation method, taking into account the known mathematical behavior of the collision integrals near zero, has been employed for $0 < T^* \leq 0.1$; for details see the Appendix. These extensions are based on the remarkable similarity of the universal molecular collision integrals $\Omega^{(1,1)^*}$ and $\Omega^{(2,2)^*}$ for $1 \leq T^* \leq 10$ to those for an L–J potential, which are compared in Fig. 4 for reduced temperatures T^* ranging from 0.1 to 10. Although this mathematical extrapolation scheme allows one to extrapolate down to $T^* \approx 0.01$, the temperature dependence is, at best, only qualitatively described. Indeed, for $T^* \leq 1$ the errors due to neglecting the shape and asymmetry of the molecular interaction potential are probably larger and more important than the errors caused by any physically and mathematically reasonable extrapolation procedure.

Bzowski et al.[11] extended the work of Kestin et al.[9] for the rare gases and Boushehri et al.[10] for 11 polyatomic species to allow the computation of the binary mass diffusion and viscosity coefficients for mixtures of these 16 species. Because of the problems associated with the molecular potentials at low temperatures, as in the work of Boushehri et al.,[10] the correlations of Bzowski et al.[11] were limited to temperatures satisfying $T^* \geq 1$. Unlike the correlations developed for the noble gases, in which the binary interaction potential parameters for unlike interactions between collision partners could be determined directly from a wealth of accurate experimental data, because a comparable body of data does not exist for the molecular species they considered, the essential means to achieve the correlation was the use of accurate combination rules to determine the unlike species interaction parameters given the like species interaction parameters. Because combination rules have yet

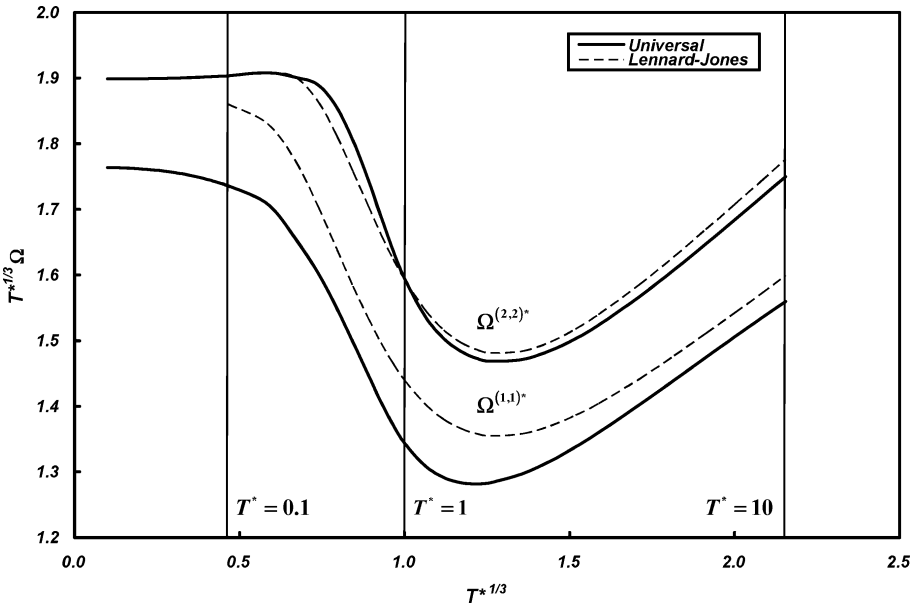

Fig. 4 Molecular gas collision integrals $\Omega^{(i,i)^*}$ vs reduced temperature T^*.

to be devised that are completely accurate in all cases, there is some loss of accuracy in the resulting predictions of mixture properties; however, these errors are small and more than offset by the ability to operate in an entirely predictive mode. An additional minor complication occurs because, as already mentioned, the reduced collision integral $\Omega^{(1,1)^*}$ is somewhat different for the molecular gases than that for the noble gases, which raises the issue of which integral to use for the mixed interaction $\Omega_{ij}^{(1,1)^*}$ between a noble gas and a molecular gas species. Because the differences between these integrals are small, the arithmetic mean of the two is used in such cases, although any sensible averaging procedure could be used.[11]

The resulting combination rules, based on the work of Tang and Toennies[15] and Bzowski et al.,[30] are quite easy to use. The interaction collision diameter σ_{ij} is calculated from the expression

$$\sigma_{ij} - a_{ij} = \frac{1}{2}[(\sigma_i - a_i) + (\sigma_j - a_j)] \times \left[1 + \frac{1}{2}(\ell_n(\sigma_{ij} - a_{ij}) - \frac{1}{7}\,\ell_n(E))\right] \tag{6a}$$

$$\ell_n(E) = \frac{1}{2}\,\ell_n(\varepsilon_i\varepsilon_j) + 3\,\ell_n[(\sigma_i - a_i)(\sigma_j - a_j)] - \frac{(\sigma_i - a_i)}{(\sigma_i - a_i) + (\sigma_j - a_j)}\,\ell_n\left(\frac{\varepsilon_i}{(\sigma_i - a_i)}\right) - \frac{(\sigma_j - a_j)}{(\sigma_i - a_i) + (\sigma_j - a_j)}\,\ell_n\left(\frac{\varepsilon_j}{(\sigma_j - a_j)}\right) \tag{6b}$$

where the effective interaction rigid-core diameter a_{ij} is

$$a_{ij} = \tfrac{1}{2}(a_i + a_j) \tag{6c}$$

and the effective rigid-core diameters for each species a_i are computed according to the rule

$$a_i = \begin{cases} \sigma_i\left[1 - \left(C_{6i}^*/2.2\right)^{\frac{1}{6}}\right] & \text{for} \quad C_{6i}^* < 2.2 \\ 0 & \text{for} \quad C_{6i}^* \geq 2.2 \end{cases} \tag{6d}$$

Because the last factor in brackets in Eq. (6a) is close to unity, it is straightforward to iterate Eq. (6) functionally to determine σ_{ij}. To a first approximation, in which the second bracketed factor is taken to be unity, we obtain the conventional arithmetic-mean combination rule, that is, $\sigma_{ij} = \frac{1}{2}(\sigma_i + \sigma_j)$, which may be used as a starting value for the iteration process. The combination rule for ε_{ij} requires knowledge of the long-range interaction dispersion coefficient C_{6ij}. Although experimental values of C_{6ij} are sometimes known, it is easier to use the following well-tested combination rule:

$$\alpha_i\alpha_j/C_{6ij} = \tfrac{1}{2}\left[\alpha_i^2/C_{6i} + \alpha_j^2/C_{6j}\right] \tag{7}$$

which can be derived from the Slater–Kirkwood expression for the long-range dispersion constant and is accurate to about 1% (see Refs. 11 and 15). The value of ε_{ij} is computed from the expression

$$\varepsilon_{ij} = (\varepsilon_i\varepsilon_j)^{\frac{1}{2}}\left[\frac{(\sigma_i - a_i)^3(\sigma_j - a_j)^3}{(\sigma_{ij} - a_{ij})^6}\right]\frac{C_{6ij}}{(C_{6i}C_{6j})^{\frac{1}{2}}} \tag{8}$$

The first factor represents the conventional geometric-mean rule, and the other factors give corrections. The introduction of the rigid-core diameters typically changes the value of σ_{ij} by less than 1%. However, ignoring the effect of the rigid-core parameters can have a large effect on the interaction well-depth parameter ε_{ij}; changes up to 10% can occur for typical systems.[11] Once σ_{ij} and ε_{ij} have been obtained, the normalized long-range interaction dispersion coefficient is $C_{6ij}^* \equiv C_{6ij}/\varepsilon_{ij}\sigma_{ij}^6$. Finally, because the transport properties are dominated by the effective spherical repulsive potential at high temperatures, the scale factors σ and ε are replaced by ρ and V and combination rules for these parameters are also required. Following Bzowski et al.[11] the (unnormalized) interaction repulsive potential parameters for unlike species can be obtained from the individual (unnormalized) like species repulsive potential range, $\rho_i \equiv \rho_i^*\sigma_i$, and strength, $V_i \equiv V_i^*\varepsilon_i$ using the simple combination rules

$$\rho_{ij} = \tfrac{1}{2}(\rho_i + \rho_j) \tag{9a}$$

$$(V_{ij}/\rho_{ij})^{2\rho_{ij}} = (V_i/\rho_i)^{\rho_i}(V_j/\rho_j)^{\rho_j} \tag{9b}$$

after which the normalized repulsive potential parameters are computed according to their definitions,

$$\rho_{ij}^* \equiv \rho_{ij}/\sigma_{ij} \tag{10a}$$

$$V_{ij}^* = V_{ij}/\varepsilon_{ij} \tag{10b}$$

These combination rules are to be employed to compute the binary interaction parameters σ_{ij}, ε_{ij}, ρ_{ij}^*, V_{ij}^*, and C_{6ij}^* for unlike rare gas–molecule or molecule–molecule interactions, whereas for unlike

rage gas–rare gas interactions these parameters, tabulated by Kestin et al.,[9] were derived from the database as part of the correlation procedure.

Paul[13] and Paul and Warnatz[14] provide a model to extend the correlations of Kestin et al.,[9] Boushehri et al.,[10] and Bzowski et al.[11] to other molecular species, including strongly polar species not contained in the original correlations. First, they tacitly recognized that the reduced universal collision integrals, within the temperature range $1 \le T^* \le 10$, where the two-parameter corresponding states correlation works quite well, are very similar to those obtained if the L–J interaction potential is used (Figs. 2–4). Second, they recognized that an effective spherical potential could be obtained by thermally averaging the interaction potential between neutral but polar species over all molecular orientations. This allows the incorporation of the dipole–dipole and dipole–induced-dipole interaction terms into the reduced collision integrals by defining an effective interaction potential separation $\hat{\sigma}_{ij}$ and well-depth energy $\hat{\varepsilon}_{ij}$. The Stockmayer potential, augmented with the appropriate dipole–induced-dipole potential interaction terms, can be written as (see Refs. 26 and 31)

$$U(r;\theta_i,\theta_j,\phi) = 4\varepsilon_{ij}\left[(\sigma_{ij}/r)^{12} - (\sigma_{ij}/r)^6\right] - \left(\mu_i\mu_j/r^3\right)\zeta_{\mu\mu}(\theta_i,\theta_j,\phi) - \left(\alpha_i\mu_j^2/2r^6\right)\zeta_{\alpha\mu}(\theta_j) - \left(\alpha_j\mu_i^2/2r^6\right)\zeta_{\alpha\mu}(\theta_i) \tag{11}$$

where $\zeta_{\mu\mu}(\theta_i,\theta_j,\phi) \equiv (2\cos\theta_i\cos\theta_j - \sin\theta_i\sin\theta_j\cos\phi)$ and $\zeta_{\alpha\mu}(\theta_i) \equiv (3\cos^2\theta_i + 1)$ are angle-dependent functions that describe the dependence of the potential on molecular orientation. Whereas the dipole–dipole interaction energy can be attractive or repulsive depending on the relative orientation of the molecules, the dipole–induced-dipole interaction energy is always attractive. The average potential energy, denoted $U(r)$, is obtained by thermally averaging the potential (11) over all molecular orientations, which proceeding as described by Maitland et al.,[31] can be written as

$$U(r) = 4\varepsilon_{ij}\left\{(\sigma_{ij}/r)^{12} - \left[1 + \chi_{ij}^* + (2\gamma/3)\left(\delta_{ij}^{*2}/T^*\right)\right](\sigma_{ij}/r)^6\right\} \equiv 4\hat{\varepsilon}_{ij}\left[(\hat{\sigma}_{ij}/r)^{12} - (\hat{\sigma}_{ij}/r)^6\right] \tag{12a}$$

where

$$\chi_{ij}^* \equiv \left(\alpha_i\mu_j^2 + \alpha_j\mu_i^2\right)/4\varepsilon_{ij}\sigma_{ij}^6 \tag{12b}$$

$$\delta_{ij}^* \equiv \mu_{ij}^2/2\varepsilon_{ij}\sigma_{ij}^3 \tag{12c}$$

Here $\mu_{ij} \equiv \sqrt{\mu_i\mu_j}$ defines the interaction dipole moment, and a formal expansion parameter, γ, has been introduced to account for the strength of the thermally averaged dipole–dipole term. The last identity of definition (12a) serves to identify the effective temperature-dependent potential parameters

$$\hat{\sigma}_{ij} \equiv \sigma_{ij}\xi_{ij}^{-\frac{1}{6}} \tag{12d}$$

$$\hat{\varepsilon}_{ij} \equiv \varepsilon_{ij}\xi_{ij}^2 \tag{12e}$$

$$\xi_{ij} \equiv 1 + \chi_{ij}^* + (2\gamma/3)\left(\delta_{ij}^{*2}/T^*\right) \tag{12f}$$

Hence, at low temperatures, the potential well is deeper for strongly polar species. The dimensionless interaction parameter χ_{ij}^* measures the dipole–induced-dipole interaction energy (at the separation at which the potential energy is zero) relative to the potential well-depth energy and is zero only if both species are nonpolar. Similarly, the dimensionless Stockmayer parameter δ_{ij}^* measures the dipole–dipole interaction energy relative to the potential well-depth energy and is zero if either species is nonpolar. Notice that the orientation-averaged dipole–dipole interaction term is always attractive. Although, formally $\gamma \equiv 1$, this value tends to overestimate the contributions of the dipole–dipole term, and Paul[13] argues that the low-order terms in an expansion for the effective central potential should match those in an expansion for the thermodynamic properties and the centers pair-correlation function of a system that actually has a central potential. This imposes the constraint that $\frac{1}{4} \le \gamma \le \frac{1}{2}$. By empirically testing the ability of the model to fit viscosity data, Paul[13] found that $\gamma = \frac{1}{4}$ worked best to fit the viscosity data of 20 different polar species encompassing Stockmayer parameters ranging from 0.03 to 2.40, which is far beyond the range that Mason and Monchick[32] applied in their model.

Before continuing, let us examine the conditions under which such a potential model is applicable. There are three distinct issues. First, under what conditions can we replace the orientation-dependent molecular interaction potential, which in the case of the dipole–dipole interactions can be attractive or repulsive depending on orientation, by a thermally averaged, spherically symmetric potential? Second, when the thermally averaged potential is used, under what conditions can we drop the higher-order multipole moment interactions? Third, under what conditions can we retain only the lowest-order terms that result when the molecular potential is thermally averaged over all orientations? Two different times are generally used to characterize molecular encounters between rotating polyatomic molecules[33–35]: the duration time of the collision, denoted τ_D, and the rotational period of the molecule, denoted τ_R. When $\tau_D \ll \tau_R$, the molecules rotate very slowly throughout the collision and we can assume a fixed relative orientation, compute the collision integrals for each fixed orientation, and then average them over the initial distribution of orientations, which in practice is assumed to be uniformly distributed.[32] In this case, rotational energy transfer between the collision partners can be quite efficient. In the opposite limit, when $\tau_D \gg \tau_R$, because the molecules rotate very rapidly throughout the collision, each colliding molecular partner "sees," in effect, an effective spherical potential and the intermolecular potential can be preaveraged over all orientations, which are assumed to be thermally distributed, to obtain an effective spherically symmetric but temperature-dependent potential. In this case, rotation–translational energy transfer is much less efficient. Thus, by estimating the ratio of the collisional duration time to the rotational period, we can establish, at least approximately, when the use of such an orientation-averaged potential is justified. When the range of the intermolecular forces is characterized by the collision diameter and the approach velocity is characterized by the mean thermal velocity, the duration of a collision is approximately $\tau_D \approx \sigma/(8k_BT/\pi m)^{1/2}$. Similarly, when the rotational thermal energy is equated to the classical rotational energy of a rigid body, the rotational period is about $\tau_R \approx 2\pi/\sqrt{(dk_BT/I)}$, where $d = 2$ and $d = 3$ for diatomic and polyatomic molecules, respectively. Thus, the criterion $\tau_D/\tau_R \gg 1$ for when a thermally averaged interaction potential is applicable becomes

$$\sqrt{\frac{d}{2}}\frac{2\sigma k_B\theta_R}{h}\Bigg/\left(\frac{8}{\pi}\frac{k_B\theta_R}{m}\right)^{\frac{1}{2}} \gg 1 \tag{13}$$

which is independent of gas temperature because in this approximation both the duration of the collision and the rotational period scale as $T^{-1/2}$. As applied to the polar molecules H_2O, H_2O_2, and ICl, this parameter is 1.88, 1.18, and 0.6, respectively, and the thermally average potential model is apparently most suited for water, less so for hydrogen peroxide, and poor for iodine chloride. However, because both hydrogen peroxide and iodine chloride are weakly polar, the thermally averaged model might also be expected to apply. Although this kinematic criterion is suggestive of when a thermally averaged potential is applicable, it says nothing about the collision dynamics, that is, the relative magnitude of the intermolecular multipole forces or the orientation biasing that may occur because these forces are attractive or repulsive depending on the relative orientation and temperature of the colliding molecules. Unfortunately, this is a difficult question to answer with a simple analysis such as that used to obtain criterion (13) and Paul[13] takes a more empirical approach, which is justified a posteriori by the ability of the model to fit polar species viscosity data. This approach has the additional advantage that it accounts, albeit empirically, for other limitations of the thermally averaged potential model such as dropping the higher-order multipole and orientation-averaging terms, which are now discussed.

To simplify the following analysis, we consider like species, but the results are easily generalized to unlike species. It follows from Maitland et al.[31] that the thermally averaged interaction potential for two like polar species can be written as

$$U(r) = 4\varepsilon\Big\{(\sigma/r)^{12} - \Big[1 + \alpha^*\delta^* + \tfrac{2}{3}(\delta^{*2}/T^*)\Big](\sigma/r)^6 - (3\alpha^*\Theta^{*2} + \delta^*\Theta^{*2}/T^*)(\sigma/r)^8 - \cdots\Big\} \tag{14}$$

Here the first two terms are the usual L–J potential, the third and fourth terms are the thermally averaged induced-dipole–dipole and dipole–dipole interaction terms, and the fifth and sixth terms are the thermally averaged induced-dipole–quadrupole and dipole–quadrupole interaction terms, respectively. Observe that 1) the thermally averaged potential is spherically symmetric, 2) the dipole–dipole and dipole–quadrupole terms are temperature dependent, and 3) all of the thermally averaged potential terms are attractive. Demanding that the third term be small compared to the second term at the equilibrium separation, $r \approx 2^{1/6}\sigma$, and using $2^{1/3} \approx \frac{5}{4}$ yields the requirement that

$$(3\alpha^*\Theta^{*2} + \delta^*\Theta^{*2}/T^*) \ll \tfrac{5}{4}\Big[1 + \alpha^*\delta^* + \tfrac{2}{3}(\delta^{*2}/T^*)\Big] \tag{15a}$$

which ensures that the thermally averaged quadrupole interaction terms may be neglected. For nonpolar molecules, that is, those that do not have a permanent dipole moment, this requirement becomes

$$3\alpha^*\Theta^{*2} \ll \tfrac{5}{4} \tag{15b}$$

which is well satisfied for all of the molecular species of present interest. For polar molecules, this requirement implies that

$$T^* \gg \frac{\left(\delta^*\Theta^{*2} - \frac{5}{6}\delta^{*2}\right)}{\frac{5}{4}(1 + \alpha^*\delta^*) - 3\alpha^*\Theta^{*2}} \tag{15c}$$

This condition is most severe for ICl for which $T^* \gg 0.039$ or $T \gg 15$ K, whereas for both water and hydrogen peroxide this condition simply requires $T^* \gg 0$. For the present applications, the temperatures of interest greatly exceed these lower bounds. Finally, let us determine when the higher-order terms that result when the potential is thermally averaged over all orientations can be neglected. Again when the interaction of like species is considered it follows that the Stockmayer potential augmented with the induced dipole–dipole interaction terms, orientation averaged to second order in the interaction potential, is

$$U(r) = 4\varepsilon[(\sigma/r)^{12} - (\sigma/r)^6 - \alpha^*\delta^*(\sigma/r)^6 - (2/5T^*)(\alpha^*\delta^*)^2(\sigma/r)^{12} - (2\gamma/3)(\delta^{*2}/T^*)(\sigma/r)^6 + (8\gamma^2/25)(\delta^{*4}/T^{*3})(\sigma/r)^{12}\cdots] \tag{16}$$

where Paul's formal expansion parameter has been inserted into the dipole–dipole interaction terms. Observe that both of the induced-dipole–dipole terms are attractive, whereas for the dipole–dipole terms the lowest-order term is attractive and the next-order term is repulsive, which reflects that for some orientations the dipole–dipole interaction potential is attractive and for others it is repulsive. Demanding that the second-order induced dipole–dipole term be small compared to the corresponding first-order term at the equilibrium separation requires that

$$T^* \gg \tfrac{1}{5}\alpha^*\delta^* \tag{17a}$$

which is most severe for water and implies that $T^* \gg 0.019$ or $T \gg 10$ K. Similarly, to neglect the second-order dipole–dipole terms at the equilibrium separation requires that

$$T^* \gg \sqrt{7/150}\,\delta^* \tag{17b}$$

when $\gamma = \frac{1}{4}$. For water, this implies that the second-order dipole–dipole term can be neglected when $T^* \gg 0.265$ or $T \gg 140$ K. For weakly polar species, this requirement is much less severe, for example, for H_2O_2 the second-order dipole–dipole term can be neglected when $T^* \gg 0.123$ or $T \gg 45$ K and for ICl $T^* \gg 0.045$ or $T \gg 17$ K. Thus, it is the neglect of higher terms in the orientation averaging of the dipole–dipole interaction potential that set the limits of applicability on the thermally averaged potential model, although for temperatures not too far below these limits, the model is at least qualitatively correct and, hence, reasonable for present applications.

Finally, after this long digression, because the Born–Mayer repulsive potential is assumed at high energies, the interaction parameters ρ^* and V^* must be replaced by the new normalized parameters

$$\hat{\rho}_{ij} \equiv \rho_{ij}/\hat{\sigma}_{ij} = \rho^*_{ij}\xi^{+\frac{1}{6}}_{ij} \tag{18a}$$

$$\hat{V}_{ij} \equiv V_{ij}/\hat{\varepsilon}_{ij} = V^*_{ij}\xi^{-2}_{ij} \tag{18b}$$

whereas at low energies, because the long-range van der Waal's potential is used, the interaction parameter C_6^* is replaced by the new normalized parameter

$$\hat{C}_{6ij} \equiv C_{6ij}\big/\hat{\varepsilon}_{ij}\hat{\sigma}^6_{ij} = C^*_{6ij}\xi^{-1}_{ij} \tag{18c}$$

In other words, instead of the molecular interaction potential energy (4), the potential can be written as

$$U(r) = \hat{\varepsilon}\hat{U}(r/\hat{\sigma}, \hat{\rho}, \hat{V}, \hat{C}_6) \tag{19}$$

and the corresponding reduced collision integrals are functions of an effective reduced temperature $\hat{T} \equiv k_B T/\hat{\varepsilon}$ and shape parameters $\hat{\rho}$, $\hat{V}$, and $\hat{C}_6$.

In summary, given the seven pure species potential parameters σ_i, ε_i, ρ_i^*, V_i^*, C_{6i}^*, α_i^*, and μ_i^*, one uses the combination rules [Eqs. (6–10)] to compute the binary interaction potential parameters σ_{ij}, ε_{ij}, ρ_{ij}^*, V_{ij}^*, and C_{6ij}^* and Eqs. (12) to compute the additional binary interaction potential parameters χ_{ij}^* and δ_{ij}^* for each collision pair. Then Eqs. (12) and (18) are used to compute the effective temperature-dependent interaction potential parameters $\hat{\sigma}_{ij}$, $\hat{\varepsilon}_{ij}$, $\hat{\rho}_{ij}$, $\hat{V}_{ij}$, and $\hat{C}_{6ij}$ for each collision pair with which the reduced universal interaction collision integrals can then be evaluated as a function of gas temperature. Of course, when computing the viscosity or conductivity of a pure species, only the pure species parameters $\hat{\sigma}_i$, $\hat{\varepsilon}_i$, $\hat{\rho}_i$, $\hat{V}_i$, and $\hat{C}_{6i}$ are required.

B. Potential Parameters for the Halogens

In this section, the potential parameters for the halogen atoms F, Cl, Br, and I, the halogen molecules F_2, Cl_2, Br_2, and I_2, and the weakly polar interhalogen ICl are determined using a methodology recommended, in part, by Paul.[13] The species index will be suppressed, except when necessary for clarity, because the primary concern is with the potential parameters for a pure species. The preferred approach to obtain the potential parameters for a species is to begin with its measured polarizability α, dipole moment μ, and viscosity η and determine the potential well parameters, σ, ε, and δ^* from a fit of the viscosity data, restricted to the temperature range $1 \le T^* \le 10$, where the two-parameter correlation is applicable. Next C_6^* is determined from these fit parameters, and an experimental value of the van der Waals coefficient C_6, which if unavailable, can be estimated from the Slater–Kirkwood dispersion formula, the measured polarizability, and the effective electron oscillator number correlations of Cambi et al.[17] Finally, in lieu of experimental high-energy molecular beam or high-temperature viscosity data, which are rarely available, the Tang and Toennies[15,16] potential model, together with the values of σ, ε, α, and C_6, is used to determine the repulsive potential parameters ρ^* and V^*. Because experimental polarizability and viscosity data are available for the homonuclear halogen diatomics, this approach was used to determine their potential parameters. For the halogen atoms and the interhalogen ICl, although measured polarizabilities and dipole moments are available, experimental viscosity data are unavailable, and an alternative, more empirical approach, based on the correlations

of Cambi et al.[17] to estimate the equilibrium separation r_M, the well-depth energy ε, and the effective dispersion coefficient C_6 from the measured polarizability was used. Then, given r_M, ε, and C_6, the Tang and Toennies[15,16] model was used to determine the potential parameters σ, ρ^*, and V^*.

1. Determination of σ and ε from Viscosity Data

For a nonpolar species, it is convenient to rescale the viscosity data according to

$$g(T) \equiv (16/5)N_A\eta(T)[\pi/(\pi WRT)^{\frac{1}{2}}]$$
$$= \left[1\Big/\sigma^2\Omega^{(2,2)^*}(T^*)\right]f_\eta(T^*) \tag{20}$$

and then fit the rescaled data $g(T)$ to the rightmost function of T in the identity (20) to obtain the potential parameters σ and ε. The domain of the fit is restricted to $1 \le T^* \le 10$ where the two-parameter correlation is applicable. For polar molecules, with Paul's potential model, the viscosity is given by

$$\eta = \frac{5}{16}\frac{1}{N_A}\frac{(\pi RTW_i)^{\frac{1}{2}}}{\pi\hat{\sigma}^2\Omega^{(2,2)^*}(\hat{T})}f_\eta(\hat{T}) \tag{21}$$

where the effective reduced temperature $\hat{T}$ is defined by $\hat{T} \equiv k_BT/\hat{\varepsilon}$ and the interaction potential collision diameter and well depth are given by Eqs. (12), $\hat{\sigma} \equiv \sigma\xi^{-1/6}$, $\hat{\varepsilon} \equiv \varepsilon\xi^2$, $\xi \equiv (1 + \chi^* + \delta^{*2}/6T^*)$, $\chi^* \equiv \alpha\mu^2/2\varepsilon\sigma^6 = 2\alpha\varepsilon\delta^{*2}/\mu^2$, and $\delta^* \equiv \mu^2/2\varepsilon\sigma^3$. In this case, it is convenient to rescale the data according to[13]

$$g(T) \equiv (16/5)N_A\eta(T)\left(\mu^2\Big/2k_BT\right)^{\frac{2}{3}}[\pi/(\pi WRT)^{\frac{1}{2}}]$$
$$= (\delta^*/T^*)^{\frac{2}{3}}(1 + 2\alpha\varepsilon\delta^{*2}/\mu^2 + \delta^{*2}/6T^*)^{\frac{1}{3}}$$
$$\times\left[1\Big/\Omega^{(2,2)^*}(\hat{T})\right]f_\eta(\hat{T}) \tag{22a}$$

$$\hat{T} \equiv k_BT/\hat{\varepsilon} = T^*/(1 + 2\alpha\varepsilon\delta^{*2}/\mu^2 + \delta^{*2}/6T^*)^2 \tag{22b}$$

and then fit the rescaled viscosity data $g(T)$ to the rightmost function of T in Eq. (22a) to determine the potential parameters ε and δ^*, again restricting the domain of the fit to $1 \le T^* \le 10$. Once ε and δ^* have been determined, σ can be found from Eq. (12c), that is, $\sigma \equiv (\mu^2/2\varepsilon\delta^*)^{1/3}$.

2. Cambi Correlations for r_M, ε, and C_6

In lieu of experimental viscosity data to determine the potential parameters σ and ε, a more empirical approach based on the correlations of Cambi et al.[17] expressing the equilibrium separation r_M and the well-depth energy ε, in terms of the polarizabilities α and effective dispersion coefficients C_6 of the interacting species, is employed. To obtain the dispersion coefficient when experimental data are unavailable, the well-known Slater–Kirkwood formula is used to express C_6 in terms of the species polarizabilities α and the effective number N_E of electron oscillators that cause the long-range dispersion interaction between the species. Cambi et al.[17] provide new, empirical, but especially easy to evaluate, expressions to estimate N_E and have extensively tested these correlations on practically all systems for which experimental data are available and found that the predicted values of r_M, ε, and C_6 compare very satisfactorily with the available experimental values. The advantage of their correlations is that only the polarizabilities and effective electron oscillator numbers of the interacting species are required to estimate the potential parameters r_M, ε, and C_6.

By considering the competition between long-range attractive and short-range repulsive forces, Cambi et al.[17] obtain the relation

$$r_M = 1.767\left[\left(\alpha_i^{\frac{1}{3}} + \alpha_j^{\frac{1}{3}}\right)\Big/(\alpha_i\alpha_j)^{0.095}\right] \tag{23}$$

The estimated uncertainties in the coefficient 1.767 and in the exponent 0.095 are ± 0.02 and ± 0.005, respectively. Here the numerator represents the effects due to molecular size, and the denominator represents the effects due to long-range attraction, which is roughly related to the product of the polarizabilities. The empirical value of the exponent determines the dependence of r_M on long-range attraction and accounts for dipole–dipole and higher-order terms in the dispersion interaction. Beginning with the preceding correlation between the equilibrium separation and the species polarizabilities and considering the near proportionality between ε and C_{6E}/r_M^6, Cambi et al.[17] then obtain the following correlation for the well-depth energy:

$$\varepsilon = 0.720\left(C_{6E}\Big/r_M^6\right) \tag{24}$$

where ε is in erg when C_{6E} is in erg $\cdot$ Å^6, and r_M is in Å. The constant C_{6E} is an effective long-range interaction coefficient that includes dipole–dipole, dipole–multipole, and multipole–multipole interactions between the species. It describes the overall attraction in the neighborhood of the potential well, and if C_{6E} takes into account the various multipole interactions, the near proportionality between the well-depth energy and the ratio of C_{6E} to r_M^6 is valid for any realistic potential model.[17] To obtain a simple correlation between the well-depth energy and the polarizabilities of the interacting species, an expression for C_{6E} in terms of the polarizabilities, whose reliability can be validated independently by comparison with experimental data, is required. The well-known Slater–Kirkwood formula for the long-range dispersion constant

$$C_{6E} = K\left\{\alpha_i\alpha_j\Big/\left[(\alpha_i/N_{Ei})^{\frac{1}{2}} + (\alpha_j/N_{Ej})^{\frac{1}{2}}\right]\right\} \tag{25}$$

can be used, provided good estimates of N_{Ei}, for each species are available. Here $K \equiv \frac{3}{2}(e^2/a_0)a_0^{3/2} \approx 2.5175 \times 10^{-11}$ and C_{6E} is in erg $\cdot$ Å^6 when α_i is in Å^3. The uncertainty in using the Slater–Kirkwood expression to estimate C_{6E} is about $\pm 1\%$ (see Refs. 11 and 15).

Although N_E is often approximated by the number of electrons in the outer shell of an atom or the number of electrons participating in the molecular bond, for many-electron systems this assumption tends to underestimate substantially the actual number of electrons that contribute to the dispersion forces. To circumvent this problem, Cambi et al.[17] take into account the roles played by the inner electrons in comparison to the outer electrons and develop a simple empirical expression with which to estimate N_E. For neutral atoms their result is

$$N_E/N_O = 1 + (1 - N_O/N_I)(N_I/N_T)^2 \tag{26}$$

where N_I and N_O are the total number of inner and outer electrons and $N_T = N_I + N_O$. Equation (26) expresses the deviation of the effective number of electron oscillators from the number of outer electrons as a product of two terms, the first of which gives the sign of the deviation. For many-electron systems, the ratio N_O/N_I is less than one, and therefore, N_E is greater than N_O, whereas for the elements B to Ne the ratio is greater than one and N_E is smaller than N_O. For the atomic halogens, $N_O = 7$ and $N_E \approx 6.14$, 7.73, 10.36, and 11.47 for F, Cl, Br, and I, respectively. For molecules made up of light atoms, the long-range interactions are caused, to first order, by the bond electrons, and the other remaining external electrons not involved in the bonds. The effective electron oscillator number is[17]

$$N_E/N_T = 1 - N_BN_{NB}\Big/N_T^2 \tag{27}$$

where N_B is the number of external bond electrons, N_{NB} is the number of external nonbond electrons, and $N_T = N_B + N_{NB}$. In this treatment, the remaining electrons are considered part of a hard inert core. Again, $N_E > N_B$, particularly as the number of noncore electrons, N_T, increases. In those molecules where all the external electrons bond, such as H_2 and the hydrocarbons, N_E coincides with N_T. For the diatomic halogens and interhalogens, $N_E \approx 12.29$, much greater than the number of bond electrons.

3. Tang–Toennies Potential Model

When σ and ε have been determined from a fit of viscosity data or r_M and ε from the correlations of Cambi et al.,[17] it remains to determine the Born–Mayer parameters ρ^* and V^* characterizing

the range and strength of the repulsive part of the intermolecular potential, respectively. To avoid elaborate self-consistent field (SCF) computations, these parameters are determined using the one-dimensional screened potential model of Tang and Toennies,[15,16] which is

$$U(r) = V\exp\left(-\frac{r}{\rho}\right) - \sum_{n\geq 3}^{\infty}\left[1 - \left(\sum_{k=0}^{2n}\frac{(r/\rho)^k}{k!}\right)\exp\left(-\frac{r}{\rho}\right)\right]\frac{C_{2n}}{r^{2n}} \tag{28}$$

The bracketed factor appearing in the sum of the attractive terms, which is an incomplete gamma function of order $2n+1$, is a (universal) damping function that accounts for the effects of charge overlap on the dispersion potential in the region of the potential well. In this region, it damps out the dispersion forces, whereas at large intermolecular separations this factor approaches unity. For a derivation of this damping factor as well as an extensive discussion of the model potential, see Tang and Toennies.[16] In their approach, knowledge of the well-depth energy ε, the equilibrium separation r_M, the asymptotic behavior of the potential at large intermolecular separations that is characterized by the van der Waals coefficients, and the boundary conditions

$$U(r_M) = -\varepsilon \tag{29a}$$

$$\left.\frac{\mathrm{d}U}{\mathrm{d}r}\right|_{r=r_M} = 0 \tag{29b}$$

provide two conditions that uniquely determine the Born–Mayer parameters ρ and V. The method is conceptually simple and mathematically convenient and has the advantage over more elaborate SCF calculations in that it directly incorporates the higher-order dispersion terms. Because the SCF calculations neglect these terms, they tend to underestimate the repulsive strength V^*, although the two methods tend to yield similar estimates of the repulsive range ρ^* (Refs. 15 and 16).

Although the dispersion C_6, C_8, and C_{10} coefficients are available for over 70 combinations of atoms,[16] for many species of interest in laser and combustion modeling, some or all of these dispersion coefficients may be unavailable. In these cases, the Slater–Kirkwood formula [Eq. (25)] was used to estimate C_6 from the polarizability and effective electron oscillator number, and to obtain C_8 and C_{10}, the correlations of Paul[13] and Thakkar and Smith[36]

$$C_8^* = \tfrac{4}{3}C_6^*(\alpha^*)^{\frac{1}{3}} \tag{30a}$$

$$C_{10}^* = (49/40)\left[\left(C_8^*\right)^2/C_6^*\right] \approx \tfrac{5}{4}\left(C_8^*\right)^2/C_6^* \tag{30b}$$

were used. In addition to the C_6, C_8, and C_{10} dispersion coefficients, the model requires the higher-order dispersion coefficients C_{2n} for $n \geq 6$, which fortunately it is not necessary to have accurate values of because they can be adequately estimated from the semi-empirical recursion relation

$$C_{2n}^* = \left(C_{2n-2}^*/C_{2n-4}^*\right)^3 C_{2n-6}^* \qquad n \geq 6 \tag{30c}$$

given by Tang and Toennies.[15,16]

Consider how to determine σ, ρ^*, and V^* given r_M, ε, C_{2n}, and the number of terms n to retain in the attractive part of the potential. To begin, it is convenient to normalize the potential by dividing $U(r)$ by the well-depth energy ε and introduce the dimensionless intermolecular separation $x = r/r_M$ to obtain

$$\tilde{U}(x) = \tilde{V}\exp\left(\frac{-x}{\tilde{\rho}}\right) - \sum_{n\geq 3}^{\infty}\left[1 - \left(\sum_{k=0}^{2n}\frac{(x/\tilde{\rho})^k}{k!}\right)\exp\left(-\frac{x}{\tilde{\rho}}\right)\right]\frac{\tilde{C}_{2n}}{x^{2n}} \tag{31}$$

With this choice of normalization, ε never explicitly enters the calculation. Differentiating $\tilde{U}$ with respect to x the condition (29b) implies that $\tilde{V}$ is

$$\tilde{V} = \exp\left(\frac{1}{\tilde{\rho}}\right)\sum_{n\geq 3}^{\infty}\left[1 - \left(\sum_{k=0}^{2n}\frac{(1/\tilde{\rho})^k}{k!}\right)\exp\left(\frac{-1}{\tilde{\rho}}\right)\right]2n\tilde{\rho}\tilde{C}_{2n} - \sum_{n\geq 3}^{\infty}\left[\frac{(1/\tilde{\rho})^{2n}}{(2n)!}\right]\tilde{C}_{2n} \tag{32}$$

Then, substituting this result into Eq. (31) and using the condition (29a) yields

$$\sum_{n\geq 3}^{\infty}\left[1 - \left(\sum_{k=0}^{2n}\frac{(1/\tilde{\rho})^k}{k!}\right)\exp\left(\frac{-1}{\tilde{\rho}}\right)\right](2n\tilde{\rho} - 1)\tilde{C}_{2n} - \exp\left(\frac{-1}{\tilde{\rho}}\right)\sum_{n\geq 3}^{\infty}\left[\frac{(1/\tilde{\rho})^{2n}}{(2n)!}\right]\tilde{C}_{2n} = -1 \tag{33}$$

which must be numerically solved for $\tilde{\rho}$, after which $\tilde{V}$ is determined from Eq. (32). At the zero-energy separation, $x_0 \equiv \sigma/r_M$, the reduced potential satisfies

$$\tilde{U}(x_0) \equiv \tilde{V}\exp\left(\frac{-x_0}{\tilde{\rho}}\right) - \sum_{n\geq 3}^{\infty}\left[1 - \left(\sum_{k=0}^{2n}\frac{(x_0/\tilde{\rho})^k}{k!}\right)\times\exp\left(\frac{-x_0}{\tilde{\rho}}\right)\right]\frac{\tilde{C}_{2n}}{x_0^{2n}} = 0 \tag{34}$$

and with both $\tilde{\rho}$ and $\tilde{V}$ known, this condition can be numerically solved to obtain x_0, the separation at which the attractive portion equals the repulsive portion of the reduced potential energy. Finally, with the solutions for x_0, $\tilde{\rho}$, and $\tilde{V}$, the potential parameters σ, ρ^*, and V^*, are given by

$$\sigma = x_0 r_M \tag{35a}$$

$$\rho^* \equiv \rho/\sigma = (\rho/r_M)(r_M/\sigma) = \tilde{\rho}/x_0 \tag{35b}$$

$$V^* \equiv V/\varepsilon = \tilde{V} \tag{35c}$$

which, in addition to ε and C_6^*, are the potential parameters required to evaluate the collision integrals. There is a slight complication if Paul[13] and Thakkar and Smith[36] scalings are used to obtain the coefficients C_8 and C_{10} from C_6 because then σ must be known. However, in this case, when started with an assumed value of σ, the required dispersion coefficients are computed, $\tilde{\rho}$, $\tilde{V}$, and a new estimate of σ are obtained using the described procedure, and then a self-consistent set of parameters σ, ρ^*, and V^* are determined by iteration. A good initial estimate for σ is the value for an L–J potential, $\sigma = r_M/2^{1/6}$. Finally, consider the problem when the zero-energy separation σ, instead of the equilibrium separation r_M, is given. When started with an estimate of r_M, the described procedure is used to determine $\tilde{\rho}$ and $\tilde{V}$, after which Eq. (34) is solved for x_0, and a new estimate of $r_M = \sigma/x_0$ is obtained. Then a self-consistent set of values of r_M, $\tilde{\rho}$, and $\tilde{V}$ is obtained by iteration, after which Eqs. (35) are used to obtain ρ^* and V^*. Again, a good initial estimate for r_M is the L–J value, $r_M = 2^{1/6}\sigma$. Unlike the first problem, the use of Paul[13] and Thakkar and Smith[36] scaling to obtain C_8 and C_{10} presents no intrinsic problem because σ is given and fixed throughout the procedure.

4. *Results*

For the halogen homonuclear diatomics F_2, Cl_2, Br_2, and I_2, experimental measurements of the viscosity were obtained from Touloukian et al.[37] and for high temperatures (those exceeding the temperatures of Touloukian et al.[37]) from Beaton and Hewitt.[38] Touloukian et al.[37] estimate the accuracy of the chlorine and bromine data to be about ±2% and the accuracy of the iodine data to be better than ±1%, but give no estimate of the accuracy of the fluorine data. Although Beaton and Hewitt[38] give no estimates of the accuracy of

their viscosity data, they were included because in all cases they more than doubled the range of T^* over which the fit was made. Because these molecules are nonpolar, the functional form (20) was used to determine σ and ε, ensuring that for the final fits only data satisfying $1 \le T^* \le 10$ were included. The maximum relative error of the fits was $\le 1.7\%$. The resulting potential parameters σ and ε are given in Table 1 and compared with those obtained by Svehla[39] for an L–J potential in Table 2. When it is considered that differences can be due to choice of data, procedure, and the fact that here the domain is limited to $1 \le T^* \le 10$, the overall trends and similarities are reassuring. Then, with these values for σ and ε, the ρ^* and V^* parameters were obtained using the Tang–Toennies potential model. To estimate the dispersion coefficient C_6, the Slater–Kirkwood formula (25) was used together with the polarizabilities taken from Miller[40] for F_2 and Br_2 and from the more recent measurements of Swift et al.[41] for Cl_2 and I_2. The effective electron oscillator number, obtained from the Cambi et al.[17] correlation, is 12.29 for each of these halogen diatomic molecules. The empirical correlations of Paul[13] and Thakkar and Smith,[36] Eqs. (30), were used to obtain C_8 and C_{10}. Following the recommendations of Tang and Toennies[16] because of the possible accumulation of errors when using the recurrence relation (30c), only attractive terms up to $n = 10$ were retained in the potential model. The resulting values of α, α^*, C_6, C_6^*, the repulsive parameters ρ^* and V^*, as well as the ratio σ/r_M are tabulated in Table 1. Observe that the computed ratio σ/r_M does not differ significantly from the L–J value of 0.8909. Because the halogen homonuclear diatomics are nonpolar, their dipole moments are zero and $\delta^* = 0$.

Comparisons of the present results for the viscosities of F_2, Cl_2, Br_2, and I_2 with the data of Touloukian et al.[37] and Beaton and Hewitt,[38] the recommended values of Svehla,[39] the recommended values of Vargaftik et al.,[42] of F_2 with the early estimates of Oerstavik and Storvick,[43] and of Cl_2 with the values obtained using the Sutherland model (see Ref. 44) are shown in Figs. 5–8. The percent deviation defined as

$$\Delta \equiv 100[(\eta - \eta_P)/\eta_P] \tag{36}$$

is shown where η is the viscosity to be compared to the viscosity η_P computed using the present algorithm and potential parameters. As would be expected, the viscosities agree quite well with those of Touloukian et al.[37] and Beaton and Hewitt[38] because the potential parameters were determined using these data. There is also good agreement of the present results with the recommended values from 300 to 1000 K of Svehla,[39] which were obtained using an L–J potential and parameters determined from viscosity data; for F_2, Cl_2, and I_2, the deviation from the present results is no more than about 2, 1, and 4%, respectively, increasing to 10% for Br_2. The agreement of the present results with the recommendations of Vargaftik et al.[42] is within 3% for F_2, for temperatures ranging from 90 to 1000 K and within 5% for I_2 for temperatures ranging from 400 to 1000 K. For F_2, the deviation of the results of Oerstavik and Storvick[43] from the present results is no more than 5%. For Cl_2 for temperatures ranging from about 200 to 1000 K, the deviation of the Sutherland model (see Ref. 44) is no more than 6%, although, because the deviation is nearly constant, a small adjustment of the reference viscosity would improve the agreement for temperatures above 200 K.

Also included in Table 1, as a check, are the potential parameters for H_2O computed using the same procedure. Following the procedure of Paul,[13] the viscosity data of Matsunaga and Nagashima[45] were used to determine σ and ε, and because water is a polar molecule, the data were fit to the functional form (22). The polarizability, 1.45 Å^3, and dipole moment, 1.8546 D, were taken

Table 2 Comparison of the parameters σ and ε for the molecular halogens with the values of Svehla[39]

	σ, Å		ε/k_B, K	
Species	Present work	Svehla	Present work	Svehla
F_2	3.340	3.357	118.7	112.6
Cl_2	4.313	4.235	284.7	300.0
Br_2	4.288	4.296	545.3	507.9
I_2	5.193	5.160	477.6	474.2

Table 1 Molecular weight and potential parameters for the halogen homonuclear diatomics and water

Species	W, g/mol	σ, Å	ε/k_B, K	ρ^*	$10^{-5}V^*$	C_6^*	α^*	$10^{60}C_6$, erg · cm^6	α, Å^3	σ/r_M
F_2	37.9968	3.340	118.7	0.0934	2.017	3.139	0.0370	71.5	1.38	0.8822
Cl_2	70.9054	4.313	284.7	0.0590	857.7	1.506	0.0525	381.2	4.21	0.9158
Br_2	159.8080	4.288	545.3	0.0729	40.78	1.753	0.0890	820.8	7.02	0.9038
I_2	253.80894	5.193	477.6	0.0691	87.4	1.580	0.0921	2044.5	12.9	0.9079
H_2O	18.01528	2.673	532.7	0.0674	118.3	1.621	0.0760	43.45	1.45	0.9087
H_2O (Ref. 13)	——	2.673	535.2	0.0640	350.0	1.612	0.0759	43.45	1.45	——

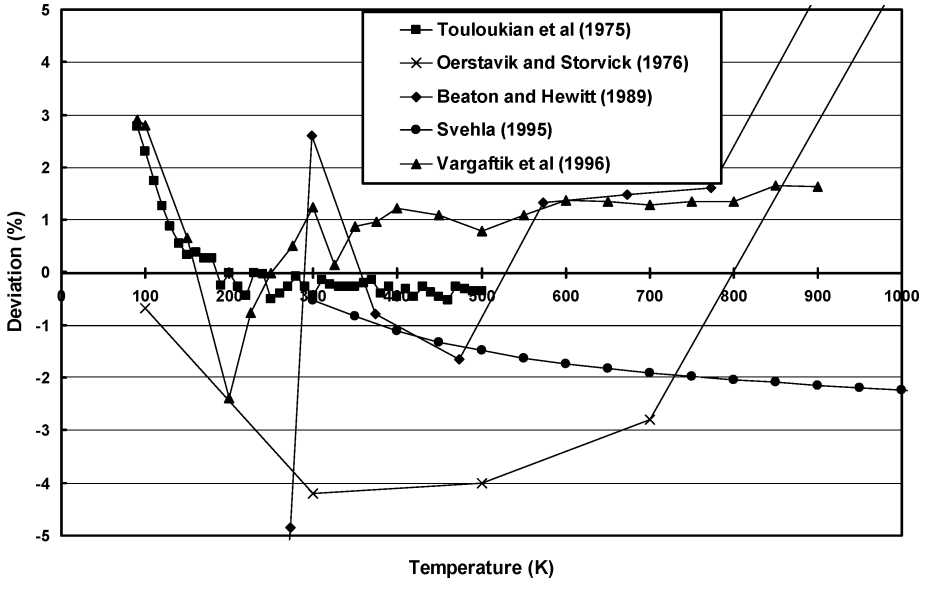

Fig. 5 Molecular fluorine viscosity deviation vs temperature.

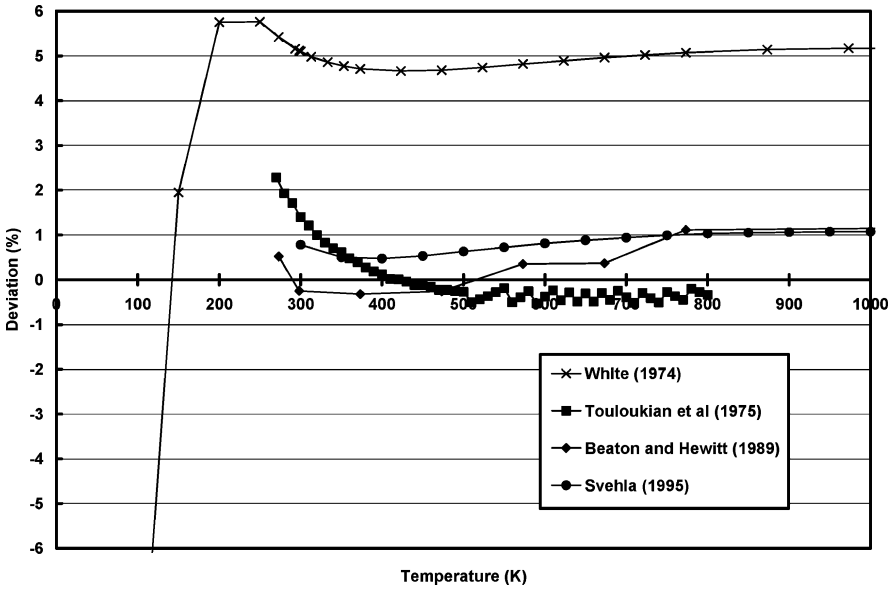

Fig. 6 Molecular chlorine viscosity deviation vs temperature.

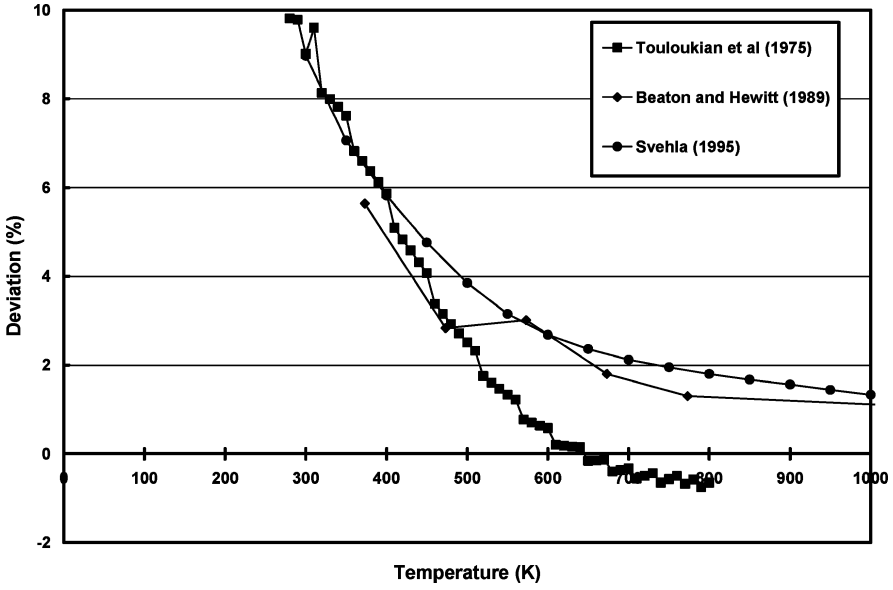

Fig. 7 Molecular bromine viscosity deviation vs temperature.

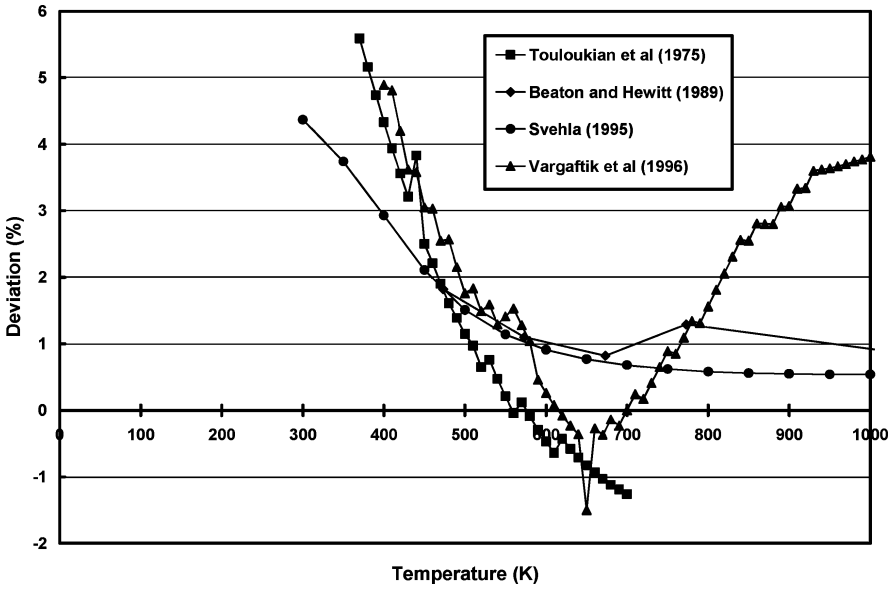

Fig. 8 Molecular iodine viscosity deviation vs temperature.

from Miller[40] and Lide,[46] respectively. The values $\sigma = 2.673$ Å and $\varepsilon/k_B = 532.7$ K were obtained from the fit, and the maximum relative error in the fit was $\leq 2.9\%$. These values agree very well with those of Paul[13] and Paul and Warnatz,[14] who obtained $\sigma = 2.673$ Å and $\varepsilon/k_B = 535.2$ K using 1.847 D for the dipole moment of water as well as a different polynomial extension for the required collision integral. For temperatures ranging from 100 to 5000 K, for which $T^* \leq 10$ and the two-parameter correlation applies, the computed values of the viscosity of water using either the parameters of Refs. 13 and 14 or the present parameters differed by less that 0.2%. However, when the experimental value of C_6 for water reported by Zeiss and Meath[47] was used, the values obtained in the present work for ρ^* and V^* are not in agreement with the values reported by Paul[13] and Paul and Warnatz[14] (Table 1). This is probably due to a different choice by Paul[13] and Paul and Warnatz[14] of the convergence tolerance used to determine r_M, ρ^*, and V^* and/or the number of attractive potential terms retained in the series, n, neither of which was reported. As pointed out by Tang and Toennies,[16] the error in determining V^* depends very sensitively on the errors in r_M; they found a 1% increase in r_M leads to a 100% increase in V^* but only a 5% increase in ρ^*. From a more practical point of view, the computed values of the viscosity of water using either the repulsive parameters of Paul[13] and Paul and Warnatz[14] or the present parameters differed by less that 0.2% over the temperature range from 5000 to 10,000 K for which T^* ranges from about 10 to 20. With the present values of the H_2O potential parameters, $\sigma = 2.673$ Å, $\varepsilon/k_B = 532.7$ K, and $\mu = 1.8546$ D, it follows that $\delta^* = 1.225$ and, hence, because $\delta^* > 1$, water is strongly polar. With Paul's model, this implies, at low temperatures, that the effects of potential well deepening are substantial. For example, at 100 K, $\xi \approx 2.42$ and σ decreases to about 2.306 Å, whereas ε/k_B increases to about 3130.0 K, a sixfold increase in well depth and, correspondingly, $\hat{T} \approx 0.032$. In Fig. 9, the present results for the viscosity of H_2O are compared with the values recommended by Touloukian et al.,[37] Svehla,[39] Matsunaga and Nagashima,[45] and Sengers and Watson.[48] It is clear from the deviation shown in Fig. 9 that the present values agree to within $\pm 3\%$ with the results of Svehla[39] and Sengers and Watson[48] and within $\pm 4\%$ with the results of Matsunga and Nagashima,[45] for the temperature ranges for which they provide values. The agreement with the data of Touloukian et al.[37] is not as good below 400 K.

For the atomic halogens F, Cl, Br, and I and the interhalogen ICl, the empirical correlations of Cambi et al.[17] were used to estimate r_M, ε, and C_6 from the polarizability and the effective number of electron oscillators. The polarizabilities of the halogen atoms were obtained from Miller,[40] whereas that for ICl was obtained from the more recent measurements of Swift et al.[41] With use of these values of r_M, ε, and C_6, the σ, ρ^*, and V^* potential parameters were obtained using the Tang–Toennies potential model, again using the correlations (30) and retaining $n = 10$ attractive terms; see Table 3. Again the ratio σ/r_M does not differ significantly from the L–J value. Because ICl has a dipole moment of[46] $\mu = 1.24$ D, it follows that $\delta^* = 0.209$, and hence, because $\delta^* \ll 1$, ICl is weakly polar. Although this procedure to determine the potential parameters is very straightforward, it should be apparent that σ, ε, ρ^*, V^*, and C_6^* for the halogen atoms and ICl have all been determined from the polarizability, the effective number of electron oscillators, and the Tang–Toennies model potential. This puts a very heavy burden on the correlations of Cambi et al.[17] because they have been used to determine the entire potential. However, because one might expect the halogen atom σ, ε, ρ^*, and V^* potential parameters to be similar to those for the noble gases,[9] a comparison is made in Table 4. The halogen atom potential parameters σ and ε are consistently somewhat larger than the corresponding parameters for the rare gases as would be expected because their polarizabilities are about 30% larger than those of the rare gases, whereas their van der Waals coefficients are almost twice those of the rare gases. That the halogen repulsive ranges ρ^* are consistently larger and the halogen repulsive strength V^* are consistently smaller than their rare gas counterparts is consistent with the expectation that the halogen atoms are less repulsive than the closed-shell noble gases. Overall, these trends and similarities are reassuring that the Cambi et al.[17] correlations provide reliable estimates.

Table 3 Molecular weights and potential parameters for the halogen atoms and the diatomic interhalogen ICl

Species	W, g/mol	N_E	σ, Å	ε/k_B, K	ρ^*	$10^{-5}V^*$	C_6^*	$10^{60}C_6$, erg · cm^6	α^*	α, Å^3	σ/r_M
F	18.9984	6.14	2.892	57.5	0.0837	6.281	2.797	13.0	0.0230	0.557	0.8900
Cl	35.4527	7.73	3.495	154.1	0.0915	2.540	2.902	112.5	0.0511	2.18	0.8844
Br	79.904	10.36	3.662	221.3	0.0936	2.046	2.930	215.9	0.0621	3.05	0.8830
I	126.90447	11.47	3.956	334.0	0.0973	1.423	2.983	527.2	0.0864	5.35	0.8804
ICl	162.35717	12.29	4.073	395.1	0.0988	1.246	3.004	748.1	0.0977	6.60	0.8794

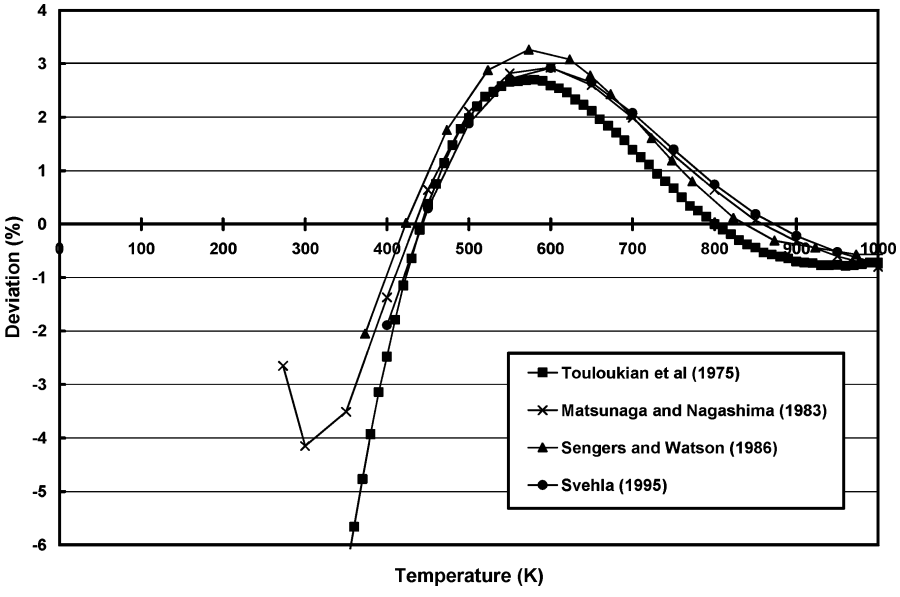

Fig. 9 Water viscosity deviation vs temperature.

Because experimental data are unavailable for the atomic halogens and the interhalogen ICl, their viscosities have been compared in Fig. 10 with early estimates made by Svehla[49] using an L–J potential model and parameters that he estimated using various empirical rules and correlations. For the atomic halogens, Svehla[49] estimated their monatomic collision diameter σ_M from the corresponding diatomic diameter σ_D using the rule $\sigma_M = 0.75\sigma_D + 0.45$. The potential well-depth energy for atomic fluorine was taken equal to that of diatomic fluorine, whereas those of the remaining atomic halogens were estimated using Brandt's correlation and the value of σ_M. For ICl, Svehla[49] obtained its collision diameter from the arithmetic mean of the values for I_2 and Cl_2 and its well-depth energy from the boiling point temperature using the empirical rule $\varepsilon/k_B = 1.18T_B$. The present parameters σ and ε are compared to those used by Svehla[49] in Table 5, and deviation plots of the viscosities computed using the Svehla[49] parameters from the present results are shown in Fig. 10. For both F and ICl, the agreement with the present values, which are believed to be more reliable, is poor. For F and ICl, the deviation in Fig. 10 shows that, regardless of temperature, the Svehla values are about 15 and 25% low compared to the present values, whereas for Cl and Br the deviations from present estimates are within 5%, and for I the deviations are within 10%. For an L–J potential, Kunc[50] has shown that the dependence of the viscosity on the potential parameters and temperature is given approximately by

$$\eta \propto (k_B T)^{\frac{3}{4}} \Big/ \sigma^2 \varepsilon^{\frac{1}{4}} \tag{37}$$

and, hence, for a constant temperature, the deviation of Svehla's estimate from the present estimate is approximately

$$\Delta \approx 100\left[(\sigma/\sigma_{SV})^2(\varepsilon/\varepsilon_{SV})^{\frac{1}{4}} - 1\right] \tag{38}$$

in an obvious notation. The corresponding computed deviations (Table 5) are consistent with the deviations observed in Fig. 10. Also shown in Table 5 is a comparison of the present potential parameters with the values for F and Cl recommended by Gray and Gubbins[51] and the values for Br and I that Hayhurst and Springett[52] inferred from flame photometric measurements of their diffusion coefficients in H_2, N_2, and O_2 mixtures, assuming a linear mixing rule and an L–J potential model. It is apparent that the recommended values for F and I are in reasonable agreement with the present estimates, whereas those for Cl and Br are less so.

C. Potential Parameters for COIL

For the species of interest to the COIL, the molecular weights and pure species potential parameters needed for the transport model are summarized in Table 6. For the rare gases, N_2, and O_2, the values were obtained from Bzowski et al.[11] For H_2O, the present values are recommended, whereas for H_2O_2, the values were obtained from Paul[13] and Paul and Warnatz.[14] Observe that ICl and H_2O_2 are weakly polar in comparison to H_2O. The Q column is indicative of the quality of the potential parameters: A indicates highest quality, based on as much viscosity and molecular beam data as available; B+ indicates that σ and ε were based on fits to viscosity data but that the database is much less extensive than for A; C+ indicates the potential parameters were derived entirely from the species polarizability and effective electron oscillator number but that the parameter trends are in good agreement with those for the rare gases; and C is same as C+ but for which no comparative

Table 5 Comparison of parameters σ and ε for atomic halogens and ICl with the values of other workers

	σ, Å			ε/k_B, K			
Species	Present work	Svehla[49]	Other	Present work	Svehla[49]	Other	Δ, %
F	2.982	2.968	2.982[a]	57.5	112.6	54.9[a]	−14.7
Cl	3.495	3.613	3.353[a]	154.1	130.8	258.5[a]	−2.5
Br	3.662	3.672	3.490[b]	221.3	236.6	740.0[b]	−2.2
I	3.956	4.320	4.360[b]	334.0	210.7	300.0[b]	−5.9
ICl	4.073	4.688	——	395.1	437.3	——	−26.4

[a]Reference 51. [b]Reference 52.

Table 4 Comparison of parameters σ, ε, ρ^*, and V^* for atomic halogens and noble gases[9]

	σ, Å		ε/k_B, K		ρ^*		$10^{-5}V^*$	
Species	Halogen	Rare gas	Halogen	Rare gas	Halogen	Rare gas	Halogen	Rare gas
F	2.982	2.755	57.5	42.0	0.0837	0.0784	6.281	11.09
Cl	3.495	3.350	154.1	141.5	0.0915	0.0836	2.540	5.117
Br	3.662	3.571	221.3	197.8	0.0936	0.0831	2.046	4.491
I	3.956	3.885	334.0	274.0	0.0973	0.0854	1.423	3.898

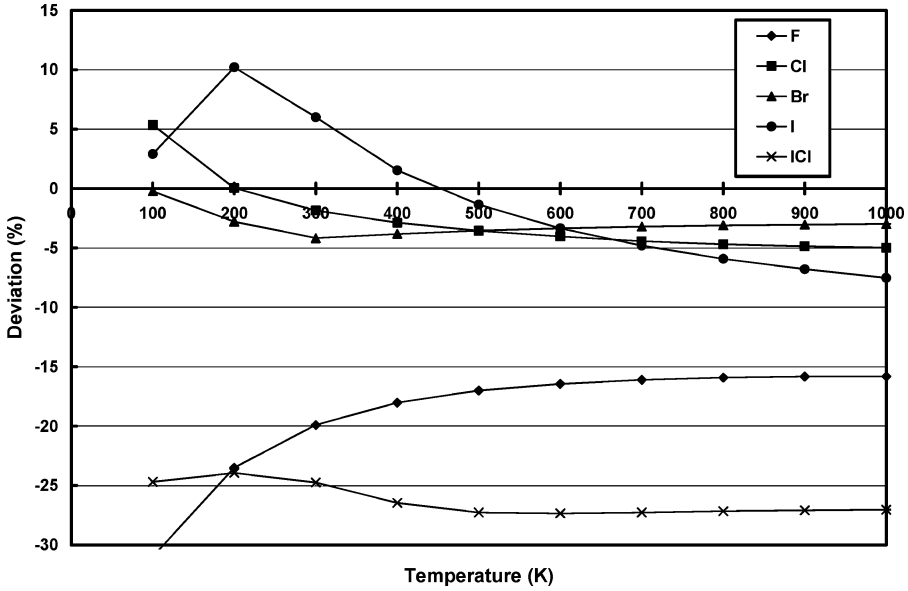

Fig. 10 Atomic halogen and iodine chloride viscosity deviation versus temperature.

Table 6 Molecular weight and potential parameters for species of interest to COIL

Species	Q	W, g/mol	σ, Å	ε/k_B, K	ρ^*	$10^{-5}V^*$	C_6^*	α^*	δ^*	μ, D
He	A	4.0026	2.610	10.4	0.0797	8.50	3.090	0.0115	0	0
Ne	A	20.1797	2.755	42.0	0.0784	11.09	2.594	0.0189	0	0
Ar	A	39.948	3.350	141.5	0.0836	5.117	2.210	0.0437	0	0
Kr	A	83.800	3.571	197.8	0.0831	4.491	2.164	0.0547	0	0
Xe	A	131.29	3.885	274.0	0.0854	3.898	2.162	0.0690	0	0
N_2	A	28.01348	3.652	98.4	0.1080	0.5308	2.180	0.0357	0	0
O_2	A	31.9988	3.407	121.1	0.0745	13.22	2.270	0.0397	0	0
H_2O	B+	18.01528	2.673	532.7	0.0674	118.3	1.621	0.0760	1.225	1.8546
H_2O_2	C	34.01468	3.499	368.1	0.0830	8.23	2.322	0.0521	0.568	1.573
Cl_2	B+	70.90540	4.313	284.7	0.0590	857.7	1.506	0.0525	0	0
I_2	B+	253.80894	5.193	477.6	0.0691	87.4	1.580	0.0921	0	0
ICl	C	162.35717	4.073	395.1	0.0988	1.246	3.004	0.0977	0.209	1.24
Cl	C+	35.4527	3.495	154.1	0.0915	2.540	2.902	0.0511	0	0
I	C+	126.90447	3.956	334.0	0.0973	1.423	2.983	0.0864	0	0

Table 7 Potential interaction parameters σ_{ij}, Å (above the diagonal) and ε_{ij}/k_B, K, (below the diagonal) for COIL mixtures

Species	He	Ne	Ar	Kr	Xe	N_2	O_2	H_2O	H_2O_2	Cl_2	I_2	ICl	Cl	I
He	——	2.691	3.084	3.267	3.533	3.243	3.096	2.632	3.188	3.682	4.327	3.582	3.159	3.494
Ne	19.44	——	3.119	3.264	3.488	3.253	3.118	2.696	3.200	3.665	4.265	3.563	3.175	3.481
Ar	30.01	64.17	——	3.460	3.660	3.499	3.378	2.993	3.430	3.861	4.392	3.750	3.423	3.680
Kr	31.05	67.32	165.80	——	3.753	3.610	3.493	3.117	3.534	3.954	4.462	3.840	3.534	3.774
Xe	29.77	67.25	182.60	225.40	——	3.779	3.665	3.299	3.692	4.100	4.581	3.982	3.702	3.921
N_2	23.42	52.97	117.67	139.41	159.29	——	3.529	3.132	3.569	4.001	4.527	3.888	3.572	3.820
O_2	27.94	61.78	130.86	152.82	171.70	108.83	——	3.017	3.457	3.889	4.422	3.779	3.452	3.709
H_2O	73.89	145.69	268.88	300.51	320.73	220.20	248.82	——	3.101	3.523	4.065	3.422	3.069	3.347
H_2O_2	44.49	103.76	214.11	250.66	284.06	183.08	200.78	372.15	——	3.908	4.402	3.795	3.497	3.731
Cl_2	31.32	73.84	186.33	230.09	276.86	161.05	172.94	313.92	298.76	——	4.784	4.193	3.923	4.134
I_2	24.42	59.63	187.39	247.59	323.36	167.01	173.10	287.37	294.54	331.06	——	4.653	4.444	4.605
ICl	34.50	80.73	213.80	267.52	326.87	185.73	197.99	354.58	332.82	333.14	406.36	——	3.811	4.016
Cl	30.11	67.33	147.17	173.57	197.39	123.35	136.31	272.94	227.54	199.61	205.01	229.27	——	3.743
I	34.13	79.28	202.51	250.56	301.97	174.79	187.57	342.61	315.29	307.49	362.46	362.27	216.25	——

Table 8 Potential interaction parameters ρ_{ij}^* (above the diagonal) and $10^{-5}V_{ij}^*$ (below the diagonal) for COIL mixtures

Species	He	Ne	Ar	Kr	Xe	N_2	O_2	H_2O	H_2O_2	Cl_2	I_2	ICl	Cl	I
He	——	0.0788	0.0791	0.0772	0.0764	0.0929	0.0746	0.0737	0.0782	0.0628	0.0655	0.0852	0.0835	0.0849
Ne	10.60	——	0.0795	0.0786	0.0785	0.0938	0.0753	0.0735	0.0791	0.0642	0.0674	0.0868	0.0844	0.0863
Ar	9.74	9.24	——	0.0833	0.0835	0.0964	0.0790	0.0769	0.0832	0.0692	0.0727	0.0910	0.0876	0.0903
Kr	10.89	9.93	4.85	——	0.0837	0.0957	0.0788	0.0765	0.0831	0.0697	0.0735	0.0910	0.0872	0.0903
Xe	13.37	11.20	4.88	4.34	——	0.0961	0.0799	0.0776	0.0843	0.0715	0.0754	0.0922	0.0880	0.0914
N_2	2.55	2.05	1.30	1.25	1.30	——	0.0918	0.0917	0.0959	0.0811	0.0832	0.1025	0.1000	0.1020
O_2	15.47	14.64	8.06	7.60	7.35	1.79	——	0.0719	0.0787	0.0653	0.0693	0.0868	0.0831	0.0861
H_2O	25.17	29.66	15.11	14.35	13.38	2.04	29.13	——	0.0759	0.0617	0.0663	0.0851	0.0815	0.0844
H_2O_2	15.37	13.00	7.01	6.50	6.10	1.58	11.18	25.31	——	0.0697	0.0737	0.0913	0.0872	0.0905
Cl_2	219.72	185.95	62.01	51.45	40.42	8.71	114.69	437.20	78.59	——	0.0641	0.0783	0.0732	0.0773
I_2	172.16	125.30	37.38	29.38	22.17	7.54	61.54	157.62	43.59	258.61	——	0.0818	0.0764	0.0808
ICl	7.55	5.71	2.65	2.34	2.13	0.87	3.82	5.78	3.13	15.95	9.81	——	0.0947	0.0980
Cl	7.07	6.12	3.54	3.34	3.31	1.04	5.32	8.60	4.55	33.74	22.51	1.93	——	0.0941
I	7.38	5.72	2.77	2.47	2.28	0.89	4.02	6.16	3.31	18.15	11.35	1.34	2.00	——

trends are available. The corresponding binary interaction potential parameters σ_{ij} and ε_{ij}/k_B are in Table 7. The single species and interaction rigid-core parameters have not been given because they are easily obtained from Eq. (6) and are not directly needed. The binary interaction potential Born–Mayer parameters ρ_{ij}^* and V_{ij}^* and dispersion coefficients C_{6ij}^* are in Tables 8 and 9, respectively. With these potential parameters, reliable estimates of the pure species viscosity and binary mass diffusion coefficients as well as the viscosity and multicomponent mass fluxes of COIL mixtures can be made. Furthermore, the rare gases, N_2, and O_2, which dominate typical COIL gas mixtures, have the most reliable values of the potential parameters, whereas the trace species I, Cl, I_2, Cl_2, ICl, H_2O, and H_2O_2, although having somewhat less reliable potential parameter values, do not contribute as much to the mixture viscosity and diffusion coefficients.

For those species that dominate COIL mixtures, the rare gases, N_2, and O_2, Kestin et al.[9] and Boushehri et al.[10] provide detailed deviation plots of their recommended values from experimental data and, in conjunction with these plots, provide an assessment of the uncertainty of the values computed using their transport algorithms. The present implementation of the collision integral functionals and viscosity and diffusion transport algorithms for the pure species has been thoroughly checked against the tables provided by Kestin et al.[9] and Boushehri et al.[10] and found to agree with their tabulated values to within 0.1% or better. For the viscosity of the pure rare gases, Kestin et al.[9] estimate the accuracy to be no worse than 0.3% for temperatures of 50–1000 K. Similarly, for N_2, Boushehri et al.[10] estimate the accuracy of the viscosity to be no worse than 0.8% for temperatures ranging from 100 to 1300 K and for O_2 the accuracy is no worse than 0.6% for temperatures of 130–1400 K.

The viscosity of H_2O_2 vapor, computed using the present model and potential parameters of Paul[13] and Paul and Warnatz,[14] was compared with the measurements of Satterfield et al.,[53] the Stiel–Thodos[54] viscosity correlation, and the recommendations of Yaws.[55]

Table 9 Potential interaction parameter C^*_{6ij} for COIL mixtures

Species	He	Ne	Ar	Kr	Xe	N_2	O_2	H_2O	H_2O_2	Cl_2	I_2	ICl	Cl	I
He	3.090	2.940	2.681	2.498	2.346	2.594	2.648	2.237	2.679	2.094	2.142	3.047	2.995	3.036
Ne		2.594	2.429	2.424	2.204	2.377	2.427	2.057	2.454	1.917	1.957	2.791	2.744	2.782
Ar			2.210	2.426	2.053	2.195	2.240	1.928	2.265	1.790	1.817	2.577	2.532	2.568
Kr				2.164	2.051	2.172	2.216	1.918	2.242	1.780	1.804	2.550	2.506	2.541
Xe					2.162	2.171	2.215	1.931	2.241	1.792	1.812	2.548	2.505	2.540
N_2						2.180	2.224	1.924	2.250	1.791	1.817	2.560	2.515	2.551
O_2							2.270	1.956	2.296	1.817	1.844	2.611	2.567	2.602
H_2O								1.621	1.985	1.554	1.611	2.286	2.216	2.272
H_2O_2									2.322	1.839	1.863	2.641	2.596	2.632
Cl_2										1.506	1.550	2.122	2.058	2.109
I_2											1.580	2.142	2.087	2.130
ICl												3.004	2.953	2.993
Cl													2.902	2.942
I														2.983

The viscosity computed using the Paul parameters is about 18% larger than the values recommended by Satterfield et al.,[53] which were based on measurements of hydrogen peroxide and water mixtures in the vapor state at 1 atm for temperatures ranging from 170 to 240°C, which were then extrapolated to obtain the viscosity of pure hydrogen peroxide vapor as a function of temperature. The present author has been unable to find any additional experimental determination of the H_2O_2 vapor viscosity in the open literature, and, indeed, every source of peroxide vapor viscosity appears to trace back to the Satterfield et al. work. Yaws[55] simply fit these data. Stiel and Thodos[54] examined the viscosity of 11 polar gases that exhibit hydrogen bonding and developed a correlation in terms of the critical constants using dimensional analysis. Their correlation, which included water but not hydrogen peroxide data, predicts values within about 5% of the Satterfield work.[53] Paul[13] and Paul and Warnatz[14] did not provide references for the viscosity data they used to determine the potential parameters. Although hydrogen peroxide is a minor species in most combustion process and its viscosity contributes little to the mixture, its presence can critically affect the diffusive flame structure. Thus, the lack of reliable measurements of hydrogen peroxide vapor viscosity over a broad range of temperatures is unfortunate because the inferred potential parameters are needed to reliably estimate its diffusion coefficient.

III. Thermal Conductivity

A. Review

Thijsse et al.[18] obtained an expression for the thermal conductivity of a pure species by expanding the solution of the linearized Boltzmann equation in terms of two orthonormal trial functions, one containing the total energy and the other containing the difference between the translational and total internal energy. It was then shown that a greatly simplified expression for the conductivity could be obtained by retaining only the basis vector proportional to the total energy. Subsequent work by van der Oord and Korving[19] and Millat et al.[20] confirmed the applicability of this approximation for pure gases, including many polyatomic species. As discussed by Thijsse et al.,[18] van der Oord and Korving,[19] and Millat et al.,[20] in the absence of a magnetic field, the conductivity of a single polyatomic gas species can be expressed as[19,20]

$$\lambda = (k_B T/\nu_0)(C_P/W)(1/\mathfrak{S}_{10E})[1/(1-\alpha)] \tag{39a}$$

$$\nu_0 = (16RT/\pi W)^{\frac{1}{2}} \tag{39b}$$

$$\alpha = \left(\mathfrak{S}^{10E}_{10D}\right)^2 \Big/ \mathfrak{S}_{10E}\mathfrak{S}_{10D} \tag{39c}$$

$$\mathfrak{S}_{10E} = [1/(1+r^2)]\left[\mathfrak{S}_{1010} - 2r\mathfrak{S}^{1010}_{100\varepsilon} + r^2\mathfrak{S}_{100\varepsilon}\right] \tag{39d}$$

$$\mathfrak{S}^{10E}_{10D} = [1/(1+r^2)]\left[r\mathfrak{S}_{1010} + (1-r^2)\mathfrak{S}^{1010}_{100\varepsilon} - r\mathfrak{S}_{100\varepsilon}\right] \tag{39e}$$

$$\mathfrak{S}_{10D} = [1/(1+r^2)]\left[r^2\mathfrak{S}_{1010} + 2r\mathfrak{S}^{1010}_{100\varepsilon} + \mathfrak{S}_{100\varepsilon}\right] \tag{39f}$$

where the species index has been suppressed for clarity and the deviation of α from zero measures the extent to which the total energy expansion function is not an eigenfunction of the linearized Boltzmann collision operator (see Ref. 19) and, hence, heat conduction in a pure polyatomic gas mixture cannot be characterized solely by a single effective relaxation time of the total energy. Here r^2 measures the deviation of the species heat capacity from that of an ideal monatomic gas and is given by

$$r^2 = C_{\text{int}} \Big/ C_P^{(M)} = \tfrac{2}{5}(C_P/R) - 1 \tag{40}$$

where $C_P \equiv C_P^{(M)} + C_{\text{int}}$ and $C_P^{(M)} \equiv \frac{5}{2}R$. The ordinary shear viscosity, volume viscosity, mass self-diffusion coefficient, internal energy diffusion coefficient, and total internal energy collision number can be expressed in terms of the Thijsse cross sections as[19,20,56–58]

$$\eta \equiv (k_B T/\nu_0)(1/\mathfrak{S}_{20}) \tag{41}$$

$$\eta_V \equiv \tfrac{2}{3}(k_B T/\nu_0)(C_{\text{int}}/C_V)^2(1/\mathfrak{S}_{0010}) = \tfrac{2}{3}\eta(C_{\text{int}}/C_V)^2(\mathfrak{S}_{20}/\mathfrak{S}_{0010}) \tag{42}$$

$$D \equiv (k_B T/\rho\nu_0)(1/\mathfrak{S}_{1000}) = (\eta/\rho)(\mathfrak{S}_{20}/\mathfrak{S}_{1000}) \tag{43}$$

$$D_{\text{int}} \equiv (k_B T/\rho\nu_0)\left(1\Big/\left[\mathfrak{S}_{100\varepsilon} - \tfrac{1}{2}\mathfrak{S}_{0001}\right]\right) = (\eta/\rho)\left(\mathfrak{S}_{20}\Big/\left[\mathfrak{S}_{100\varepsilon} - \tfrac{1}{2}\mathfrak{S}_{0001}\right]\right) \tag{44}$$

$$Z_{\text{int}} \equiv (k_B T/\eta\nu_0)(4/\pi)(1/\mathfrak{S}_{0001}) = (4/\pi)(\mathfrak{S}_{20}/\mathfrak{S}_{0001}) \tag{45}$$

where ρ denotes the species mass density and the last equalities in Eqs. (42–45) follow from Eq. (41). (Note that the sign convention in Ref. 58 is not the same as that used in Ref. 19.)

Van der Oord and Korving[19] and Millat et al.[20] present convincing experimental evidence and theoretical analysis demonstrating that for many polyatomic molecules $\alpha \approx 0$, so that the thermal conductivity is approximately given by

$$\lambda_0 \approx (k_B T/\nu_0)(C_P/W)(1/\mathfrak{S}_{10E}) \tag{46}$$

From the fact that $\alpha \approx 0$, van der Oord and Korving[19] infer that the coupling cross section $\mathfrak{S}^{10E}_{10D}$ between the total and difference energy fluxes satisfies $\mathfrak{S}^{10E}_{10D} \approx 0$. Then, assuming $\mathfrak{S}^{10E}_{10D} \equiv 0$ and using the following identities satisfied by the Thijsse cross sections (see Refs. 20 and 59)

$$\mathfrak{S}_{1010} = \tfrac{2}{3}\mathfrak{S}_{20} + (25/18)r^2\mathfrak{S}_{0001} \tag{47a}$$

$$\mathfrak{S}^{1010}_{100\varepsilon} = \tfrac{5}{6}r\mathfrak{S}_{0001} \tag{47b}$$

$$\mathfrak{S}_{0010} = \tfrac{5}{3}r^2\mathfrak{S}_{0001} \tag{47c}$$

they derive an expression for the cross section for the total energy flux $\mathfrak{S}_{10E}$ in terms of the cross sections for momentum transfer, $\mathfrak{S}_{20}$,

and translational and internal energy exchange, $\mathfrak{S}_{0010}$. Inserting this result into approximation (46), and eliminating the Thijssen cross sections in favor of the shear and volume viscosities, they finally obtain for the thermal conductivity of a polyatomic species

$$(C_P/W)/\lambda_0 = \tfrac{2}{3}(1/\eta) + \tfrac{2}{9}(C_{\text{int}}/C_V)^2(1/\eta_V) \tag{48}$$

Van der Oord and Korving[19] tested expression (48) for a few, relatively simple molecules with a small value of vibrational specific heat because of insufficient data for the volume viscosity of more complicated polyatomic molecules. The agreement between the experimental and calculated thermal conductivity was very satisfactory. However, because of the lack of volume viscosity data and the difficulty of estimating it from the second viral coefficient, the simple thermal conductivity expression (48) is not very useful for a priori estimating and/or predicting the thermal conductivity of an arbitrary molecule. Another disadvantage is that one can not estimate the correction factor α because the derivation of expression (48) presumes α is identically zero. The purpose of van der Oord and Korving[19] was more to demonstrate the validity of the expression (46) for thermal conductivity than to provide a means of estimating the conductivity for arbitrary molecules.

Instead of the approach of van der Oord and Korving,[19] here we assume that $\alpha = 0$ in the first approximation but do not use this to infer that $\mathfrak{S}_{10D}^{10E} = 0$. Rather we use the expression for $\mathfrak{S}_{10E}$ as is and estimate the cross section $\mathfrak{S}_{100\varepsilon}$ from the diffusion coefficient for internal energy. A potential advantage of this approach is that one can estimate α and apply the correction factor $(1-\alpha)^{-1}$ if necessary. Using the definition (44), first an expression for $\mathfrak{S}_{100\varepsilon}$ is obtained in terms of the cross sections for momentum transfer and internal energy relaxation and the internal energy diffusion coefficient. Substituting this result and the identities (47) into Eqs. (39) and using definition (45) of the total internal collision number yields

$$\mathfrak{S}_{10E} = \frac{\frac{2}{3}\mathfrak{S}_{20}}{1+r^2}\left[1 + r^2\left(\frac{1}{\frac{2}{3}\rho D_{\text{int}}/\eta} + \frac{4}{3\pi}\frac{1}{Z_{\text{int}}}\right)\right] \tag{49a}$$

$$\mathfrak{S}_{10D}^{10E} = \frac{\frac{2}{3}\mathfrak{S}_{20}}{1+r^2} r\left[1 - \frac{1}{\frac{2}{3}\rho D_{\text{int}}/\eta} + \left(\frac{5}{3}r^2 + 1\right)\frac{2}{\pi}\frac{1}{Z_{\text{int}}}\right] \tag{49b}$$

$$\mathfrak{S}_{10D} = \frac{\frac{2}{3}\mathfrak{S}_{20}}{1+r^2}\left[\frac{1}{\frac{2}{3}\rho D_{\text{int}}/\eta} + r^2 + 3\left(\frac{5}{3}r^2 + 1\right)^2\frac{1}{\pi Z_{\text{int}}}\right] \tag{49c}$$

Finally, substituting Eq. (49a) into Eq. (39) yields, after some algebra, an expression for the thermal conductivity when α is zero, or

$$\lambda_0 = \lambda^{(M)}\left\{(1+r^2)^2 \Big/ \left[1 + r^2\left(\frac{1}{\frac{2}{3}\rho D_{\text{int}}/\eta} + \frac{4}{3\pi}\frac{1}{Z_{\text{int}}}\right)\right]\right\} \tag{50a}$$

$$\lambda^{(M)} = \frac{15}{4}\frac{R}{W}\eta \tag{50b}$$

where $\lambda^{(M)}$ is a hypothetical thermal conductivity as if the molecule behaved like a ideal monatomic gas and α is given by a rather imposing expression[3] which will not be given here. This expression for λ_0, unlike the corresponding expression (48) of van der Oord and Korving,[19] accounts for the diffusion of internal energy.

To obtain the final formal expression for the thermal conductivity used here, two additional refinements are necessary. First, the monatomic conductivity must be modified to account for the higher-order Kihara corrections. Second, to account for spin-polarization effects in polyatomic molecules, an additional multiplicative correction factor, $(1+\Delta_{\text{spn}})$, must introduced.[21] Physically, the spin-polarization correction Δ_{spn} occurs because collisions of nonspherical molecules in the presence of temperature gradients produce a partial alignment of the molecular angular momentum. Because this alignment has the effect of decreasing slightly the orientation-averaged cross section, the spin-polarization correction increases the conductivity slightly.[21] For a monatomic species, this correction is absent. By considering a diamagnetic rigid rotator, making reasonable approximations for the temperature dependence of the required cross sections, and assuming that internal energy diffusion and collisional relaxation are dominated by rotational processes, Uribe et al.[21] have shown that Δ_{spn} can be approximated by[3]

$$\Delta_{\text{spn}} \approx C_{\text{spn}}\frac{5}{3}\frac{\mathfrak{S}_{20}}{\mathfrak{S}_{10E}} = \frac{5}{2}C_{\text{spn}}\left(\left[(1+s^2)\frac{\rho D_{\text{ROT}}}{\eta}\right] \Big/ \left\{\left(1 + s^2\left[\frac{4}{3\pi}\frac{1}{Z_{\text{rot}}}\right]\right)\frac{\rho D_{\text{ROT}}}{\eta} + \frac{3}{2}s^2\right\}\right) \tag{51a}$$

$$s^2 \equiv \frac{C_{\text{rot}}}{C_P^{(M)}} = \frac{2}{5}\frac{C_{\text{rot}}}{R} \tag{51b}$$

where s^2 is defined analogous to r^2, D_{ROT} denotes the uncorrected rotational energy diffusion coefficient [discussed following Eq. (56)], and C_{spn} is a dimensionless, empirical constant of the order $10^{-3} - 10^{-2}$ characterizing the strength of the spin-polarization interaction, which must be derived from measurement. This correction, whose temperature dependence is largely determined by that of $\rho D_{\text{ROT}}/\eta$, is small, amounting to only about 1.5% at most, and is very nearly independent of temperature.[21,22] In the present work, the spin-polarization correction has been included in the conductivity of N_2 and O_2 for which data are available and neglected for all remaining species. With these refinements, the thermal conductivity of a pure polyatomic species can be written as

$$\lambda = \lambda^{(M)}\left\{(1+r^2)^2 \Big/ \left[1 + r^2\left(\frac{1}{\frac{2}{3}\rho D_{\text{int}}/\eta} + \frac{4}{3\pi}\frac{1}{Z_{\text{int}}}\right)\right]\right\}\frac{(1+\Delta_{\text{spn}})}{1-\alpha} \tag{52a}$$

$$\lambda^{(M)} = \frac{15}{4}\frac{R}{W}\eta\frac{f_\lambda}{f_\eta} \tag{52b}$$

where the correction factors f_η and $f_\lambda = 1 + (3/42)(8E^* - 7)^2$ are very nearly unity.[26] For all species of present interest, except for the strongly polar molecule H_2O, for which near-resonant rotational exchange collisions are important at low temperatures, it was found that the relaxation time correction α was small, less than 0.005.

B. Thermal Conductivity Model

When Eqs. (52) are used to estimate the thermal conductivity of a species, the most difficult problems are how to estimate the internal energy collision number Z_{int} and diffusion coefficient D_{int}. The internal energy collision number Z_{int}, which represents the number of collisions required to equilibrate the internal energy distribution, or more prosaically, the number of collisions required to exchange a quantum of the molecules internal energy with its translational energy, must account for the combined effects of internal rotational, vibrational, and electronic energy relaxation. Similarly, the internal energy diffusion coefficient D_{int} must account for the combined effects of internal rotational, vibrational, and electronic energy diffusion. Because these properties are sensitive to the details of the internal molecular degrees of freedom and to the details of both elastic and inelastic energy transfer, at present no single model or correlation that includes a number of different molecules in a single comprehensive scheme has been developed, although it has been possible to develop representations for the conductivity of individual species over fairly wide temperatures ranges with good accuracy.[12] Nevertheless, there has been some progress, and recently Uribe et al.[21,22] developed a correlation for a number of small, non- or weakly polar molecules. The crucial feature of their analysis was the development of a subcorrelation by which the uncorrected rotational energy diffusion coefficient D_{ROT} could be determined from the rotational collision number Z_{rot} and the reduced temperature T^*.

We employ the approximate but common assumption of mechanically independent modes of internal motion so that[20,32,60]

$$C_{\text{int}}/Z_{\text{int}} = C_{\text{rot}}/Z_{\text{rot}} + C_{\text{vib}}/Z_{\text{vib}} + C_{\text{ele}}/Z_{\text{ele}} \tag{53a}$$

$$C_{\text{int}}/D_{\text{int}} = C_{\text{rot}}/D_{\text{rot}} + C_{\text{vib}}/D_{\text{vib}} + C_{\text{ele}}/D_{\text{ele}} \tag{53b}$$

Although C_{rot}, C_{vib}, and C_{ele} can be obtained from well-founded thermochemical theory and/or tabulated values,[61] here the simplifying engineering approximation[62] is used that C_{rot} is given by its classical, high-temperature value so that $C_{rot} = 0$, $C_{rot} = R$, and $C_{rot} = \frac{3}{2}R$ for monatomic, linear, and nonlinear molecules, respectively. This is a good approximation when $T \gg \theta_R$, which is satisfied for all molecules and temperatures of present interest. For very light molecules, for example, H_2, at low temperatures one must include higher-order terms in the rotational energy expansion. Separate estimates of C_{vib} and C_{ele} are not required, as will be seen.

Generally speaking, collision numbers for vibrational energy relaxation are on the order of 10^4 or greater, and those for electronic energy relaxation are also expected to be quite large. However, collision numbers for rotational energy exchange are often much smaller, typically 10 or less at ordinary temperatures. Thus it is assumed that

$$Z_{rot} \ll Z_{vib}, Z_{ele} \tag{54}$$

Furthermore, when the collision number is large and resonant exchange of internal energy is negligible, it is reasonable to approximate the internal energy diffusion coefficient by the mass self-diffusion coefficient, denoted here by D. Thus, for the vibration and electronic degrees of freedom, it is assumed that the vibrational and electronic diffusion coefficients are given by

$$\rho D_{vib}/\eta = \rho D_{ele}/\eta = \rho D/\eta = \tfrac{6}{5}A^* \tag{55}$$

where A^* is a dimensionless ratio of collision integrals, which is of order unity. However, because collision numbers for rotational energy exchange are much smaller, a more accurate estimate of the rotational energy diffusion coefficient D_{rot} is required. As indicated earlier, it is the influence of inelastic collisions that is important. However, there is an important correction to D_{rot} that accounts for the near-resonant exchange of rotational energy that can be accurately estimated theoretically because the exchange is mediated by the long-range anisotropic interactions between the permanent dipoles and quadrupoles of the molecules. When these interactions, which always reduce D_{rot}, are taken into account, the diffusion coefficient D_{rot} can be expressed as[21]

$$D_{rot} = D_{ROT}/(1+\Delta) = D_{ROT}/(1+\Delta_{\mu\mu}+\Delta_{\mu\Theta}+\Delta_{\Theta\Theta}) \tag{56a}$$

where D_{ROT} is the diffusion coefficient uncorrected for the near-resonant rotational exchange interaction, $\Delta \equiv \Delta_{\mu\mu}+\Delta_{\mu\Theta}+\Delta_{\Theta\Theta}$ and $\Delta_{\mu\mu}$, $\Delta_{\mu\Theta}$, and $\Delta_{\Theta\Theta}$ are the exchange correction terms for dipole–dipole, dipole–quadrupole, and quadrupole–quadrupole interactions, respectively, which in addition to temperature depend on the dipole and quadrupole moments and moments of inertia of the molecules. For linear molecules, the exchange correction terms for dipole–dipole, $\Delta_{\mu\mu}$, dipole–quadrupole, $\Delta_{\mu\Theta}$, and quadrupole–quadrupole interactions, $\Delta_{\Theta\Theta}$, are[3,21,63]

$$\Delta_{\mu\mu} = 0.44 g^{\mu\mu}(3\pi^2/2)(\pi/2)^{\frac{1}{2}}(\mu^2/\hbar)(\eta/k_BT)(\rho D_{ROT}/\eta)(\theta_R/T)^{\frac{3}{2}} \tag{56b}$$

$$\Delta_{\mu\Theta} = 0.51 g^{\mu\Theta}(56\pi^2/45)(3/5)^{\frac{1}{2}}(\pi^2/6)^{\frac{1}{3}}(\mu|\Theta|/\hbar)^{\frac{2}{3}} \times (RT/W)^{\frac{1}{6}}(\eta/k_BT)(\rho D_{ROT}/\eta)(\theta_R/T)^{\frac{3}{2}} \tag{56c}$$

$$\Delta_{\Theta\Theta} = 1.31 g^{\Theta\Theta}(7\pi^{\frac{3}{2}}/2)\Gamma(7/4)(|\Theta|^2/\hbar)^{\frac{1}{2}}(RT/W)^{\frac{1}{4}}(\eta/k_BT) \times (\rho D_{ROT}/\eta)(\theta_R/T)^{\frac{3}{2}} \tag{56d}$$

Note that it is the uncorrected rotational energy diffusion coefficient D_{rot} that appears in these expressions. These resonant exchange corrections rise from zero at low temperatures to attain a maximum and then decrease with a further increase in temperature. Because it is important to use accurate g values, these factors have been obtained by linear interpolation of the tables of Nyeland et al.[63] for $T/\theta_R < 10$, whereas the asymptotic formulas of Nyeland et al.[63] are sufficient to estimate these factors for $T/\theta_R \geq 10$. Analytic expressions for the exchange corrections for asymmetric tops and polyatomic molecules are unavailable. However, to estimate the resonant exchange correction terms for water and hydrogen peroxide molecules, which are nonlinear and polar, these molecules can be approximated as if they were nearly prolate symmetric tops[32] for which $\theta_A \gg \theta_B \approx \theta_C$, where θ_i is the rotational temperature parameter corresponding to the ith principle axis. Then the resonant exchange correction terms are identical to those for linear polar molecules except that $(\theta_R/T)^{3/2}$ is replaced by $(\theta_{BC}/T)^{3/2}[\theta_A/(\theta_A-\theta_{BC})]$, where $\theta_{BC} = (\theta_B\theta_C)^{1/2}$ and g is evaluated using $\theta_R = (\theta_A\theta_B\theta_C)^{1/3}$. The resonant exchange corrections are largest for strongly polar molecules with low moments of inertia such as HCl, NH_3, and H_2O and are of marginal significance for weakly polar molecules with large moments of inertia such as ICl and H_2O_2 or nonpolar diatomic molecules such as N_2, O_2, I_2, or Cl_2 with relatively large moments of inertia.

With the approximation (54) for the collision numbers and the expressions (55) and (56) for the internal energy diffusion coefficients, it follows from Eqs. (53) that

$$Z_{int} \approx (C_{int}/C_{rot})Z_{rot} = (r^2/s^2)Z_{rot} \tag{57a}$$

$$1/D_{int} = [(1+\Delta)s^2/r^2]\big/D_{ROT} + [1-s^2/r^2]/D \tag{57b}$$

The essence of approximation (57a), which ignores the details of inelastic and/or resonate vibrational or electronic collisions and their effect on the relaxation times, is that the internal energy collision number scales with the rotational energy collision number by the excess of a molecules vibrational and electronic energy over its rotational energy. This approximation is still valid, even if the vibrational and electronic contributions to the specific heat are comparable to that from the rotational contribution, as long as the approximation (54) holds. Also, it is evident from Eq. (57b) that, when the vibrational and electronic contributions to the heat capacity are small in comparison to the rotational contribution, $r^2 \approx s^2$ and $D_{int} \approx D_{ROT}/(1+\Delta) \equiv D_{rot}$, whereas if the rotational contributions to the heat capacity are small in comparison to vibrational and electronic contributions, then $s^2 \ll r^2$ and $D_{int} \approx D$.

To estimate the rotational collision number, we proceed in a manner similar to that used by Uribe et al.[21] For homonuclear diatomic molecules, in the approximation that the rotational relaxation can be characterized by a single relaxation time, the temperature dependence of rotational collision number Z_{rot} has been derived classically, assuming a modified Morse potential, by Parker[23] and Brau and Jonkman,[24] who obtain

$$Z_{rot}(T) = Z_{rot}^{\infty}\Big/\left(1+\frac{\pi^{\frac{3}{2}}}{2}\frac{1}{(T^*)^{\frac{1}{2}}}+\left(\frac{\pi^2}{4}+2\right)\frac{1}{(T^*)}+\frac{\pi^{\frac{3}{2}}}{(T^*)^{\frac{3}{2}}}\right) \tag{58}$$

where Z_{rot}^{∞} denotes the rotational collision number in the high-temperature limit. Following Uribe et al.,[21] because the scatter of the experimental measurements of Z_{rot} for most molecules is sufficiently large, Z_{rot}^{∞} is treated as an adjustable parameter whose value is only moderately constrained by such measurements. Furthermore, the result (58) is assumed to apply to all molecules considered, not merely to homonuclear diatomics. Evidence to support this contention is presented, for a few molecules, in Fig. 2 of Uribe et al.[21] Here, unlike the model of Uribe et al.,[21] an additional requirement is imposed on the value of Z_{rot} as suggested by Brokaw.[64] If Z_{rot}, as computed from Eq. (58), is less than unity, then Z_{rot} is set to unity, that is, we take $Z_{rot} \geq 1$ to ensure that at low temperatures at least a single quantum of rotational energy is exchanged with the translational degree of freedom. As with the model of Uribe et al.,[21] the present correlation is a one–parameter fit of the conductivity data (if available) for which the adjustable parameter is Z_{rot}^{∞}. In the absence of conductivity data, the model can used in a predictive mode if Z_{rot}^{∞} can be obtained either from experiment, estimated from theory, or obtained from a correlation, for example, see Brokaw.[64]

To estimate the rotational energy diffusion coefficient, we proceed as described by Uribe et al.[21] By inspecting the pertinent kinetic-theory cross sections for rotational energy diffusion, which shows that D_{ROT} should depend upon Z_{rot}, T, and possibly other molecular parameters, they were able to develop a correlation for D_{ROT} in terms

of Z_{rot} and T^*, which is

$$\frac{\rho D_{\text{ROT}}}{\eta} = \begin{cases} \left(Z_{\text{rot}}^{\infty}\right)^{\frac{1}{4}}(1.122 + 4.552/T^*)\left(Z_{\text{rot}}/Z_{\text{rot}}^{\infty}\right) & T^* \le T_{\text{crs}}^* \\ \frac{6}{5}A^*\left(1 + 0.27/Z_{\text{rot}} - 0.44/Z_{\text{rot}}^2 - 0.90/Z_{\text{rot}}^3\right) & T^* \ge T_{\text{crs}}^* \end{cases} \tag{59}$$

where T_{crs}^* is the temperature at which the correlation switches from the phenomenological low-temperature correlation of Uribe et al.[21] to the high-temperature result of Sandler.[25] Given Z_{rot}^{∞} and the functions Z_{rot} and A^*, it is straightforward to compute the crossover temperature T_{crs}^* by determining the value of T^* at which the low-temperature expression for $\rho D_{\text{ROT}}/\eta$ equals the high-temperature expression for $\rho D_{\text{ROT}}/\eta$.

For the noble gases, r^2, Δ_{spn}, and α are identically zero, λ reduces to $\lambda^{(M)}$ as it should, and only the species molecular weight and potential parameters are needed to compute the conductivity. For a monatomic species, such as the atomic halogens, for which there may be electronic, but not rotational or vibrational, contributions to the heat capacity, $r^2 > 0$, and because the number of collisions required to relax the internal electronic energy distribution is large, that is, $Z_{\text{int}} \gg 1$, we may assume $Z_{\text{int}} \to \infty$ and take $\rho D_{\text{int}}/\eta \approx \rho D/\eta = \frac{6}{5}A^*$ to obtain

$$\lambda \approx \lambda^{(M)}\left[(1 + r^2)^2/\left(1 + \tfrac{5}{4}r^2/A^*\right)\right] \tag{60}$$

because $\alpha \ll 1$. In this case, in addition to the potential parameters needed to compute the viscosity, only the molar specific heat capacity is needed to compute the conductivity. Finally, to compute the conductivity of a diatomic or polyatomic species using Eqs. (52) requires, in addition to the potential parameters needed to compute the viscosity, the molar specific heat capacity C_P, the dipole and quadrupole moments μ and Θ, the rotational temperature(s) θ_R, the high-temperature rotational collision number Z_{rot}^{∞}, the spin-polarization constant C_{spn}, and the crossover temperature T_{crs}^*.

C. Molecular Parameters for the Halogens

For the homonuclear halogens and the interhalogen ICl, the potential parameters needed to compute the viscosity are summarized in Tables 1 and 3, respectively. For these species, the molar specific heat capacity was obtained from the NIST–JANAF thermochemical tables.[61] For the homonuclear halogen molecules, the quadrupole moments were obtained from the review and tabulation of Gray and Gubbins.[51] For ICl, the dipole moment was obtained from Lide,[46] and, in lieu of experimental measurement or theoretical estimates, its quadrupole moment was crudely estimated by averaging the quadrupole moments of I_2 and Cl_2. The halogen rotational temperatures were determined using the ground state rotational constants obtained from Chase.[61] These additional molecular parameters are summarized in Table 10. Also tabulated are the reduced dipole and quadrupole moments, μ^* and $|\Theta^*|$, respectively. For the diatomic halogens, the correlation parameter Z_{rot}^{∞} was determined by an iterative process. For F_2, Cl_2, and Br_2, conductivity data were obtained from Touloukian et al.,[65] who estimated the accuracy in their recommended F_2 and Cl_2 values to be 10 and 5%, respectively, but gave no recommendation as to the accuracy of their recommended values for Br_2. For I_2, conductivity data were obtained from the more recent measurements of Umanskii et al.,[66] who estimated the errors in their measurements were no greater than 2.5%. Their data are thought to be the most reliable measurements of I_2 conductivity to date. To begin, estimates of the rotational collision number at 298.15 K, Z_{rot}^{298}, were obtained from Brokaw's empirical correlations,[64] which were developed from an examination of acoustical, nuclear magnetic resonance (NMR), and recovery data for a wide variety of molecules but were largely limited to ordinary, near-room, temperatures. These values were then simply scaled by a constant multiplicative factor, after which the conductivity was computed as a function of temperature and compared to the aforementioned conductivity data. Good agreement was obtained for all of the homonuclear species, within the error estimates of the data, for a scaling factor of 3.5, which was also assumed to apply to ICl. The resulting values of Z_{rot}^{298} and Z_{rot}^{∞} are given in Table 10. The value of $Z_{\text{rot}}^{\infty} = 78.4$ obtained here for Cl_2 agrees quite well with that reported by Mason and Monchick[32] if their value is recomputed using the correct expression for the rotational relaxation collision number, Eq. (58). That is, with their well-depth energy $\varepsilon/k_B = 300$ K and room-temperature collision number $Z_{\text{rot}}^{300} = 5.6$, which is consistent with experiment, one obtains $Z_{\text{rot}}^{\infty} = 78.1$.

Comparisons of the homonuclear halogen conductivities computed using the present model with several data sources are shown in Figs. 11–14. As expected by the choice of Z_{rot}^{∞} the agreement

Table 10 Molecular parameters for homonuclear halogens and interhalogen ICl

Species	μ, D	μ^*	$\lvert\Theta\rvert$, B	$\lvert\Theta^*\rvert$	θ_R, K	Z_{rot}^{∞}	Z_{rot}^{298}	T_{crs}^*
F_2	0	0	1.5	0.575	1.271	58.1	9.80	2.73
Cl_2	0	0	4.2	0.548	0.351	78.4	5.95	1.95
Br_2	0	0	4.78	0.458	0.118	121.5	4.55	1.26
I_2	0	0	5.61	0.356	0.054	96.6	4.20	1.57
ICl	1.24	0.646	4.9	0.627	0.163	91.4	4.90	1.66

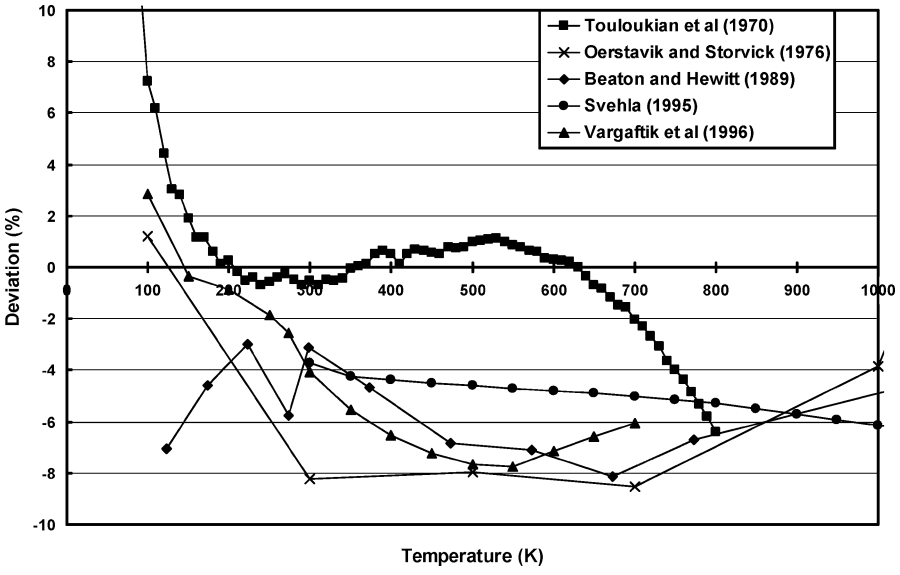

Fig. 11 Molecular fluorine conductivity deviation vs temperature.

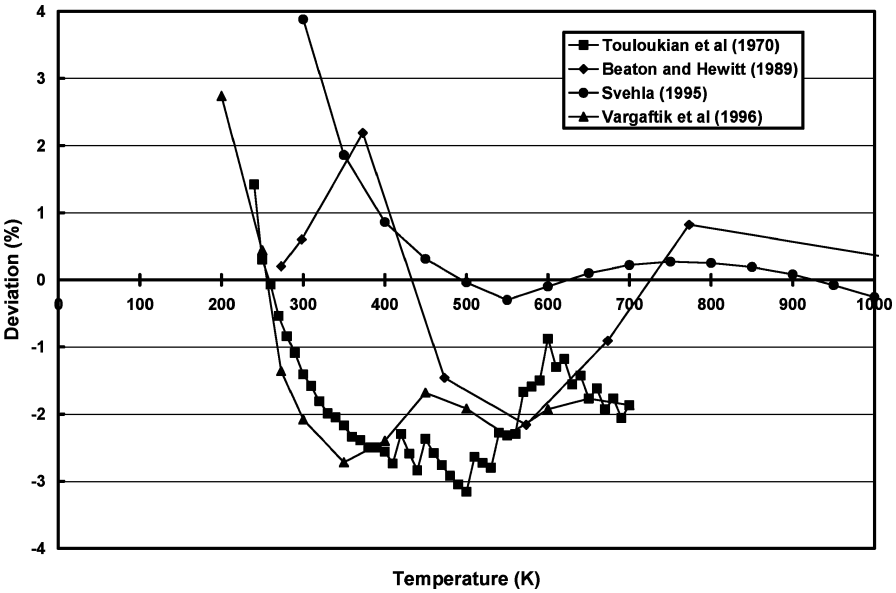

Fig. 12 Molecular chlorine conductivity deviation vs temperature.

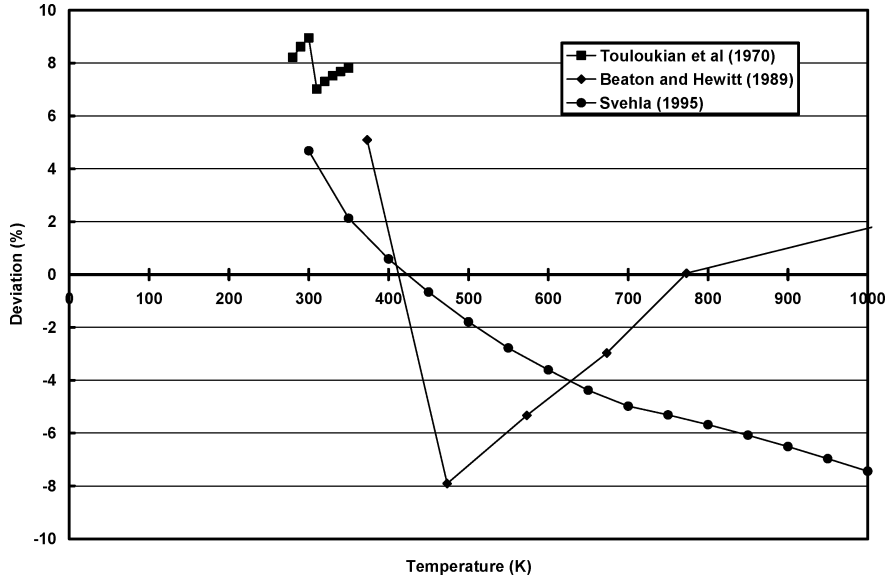

Fig. 13 Molecular bromine conductivity deviation vs temperature.

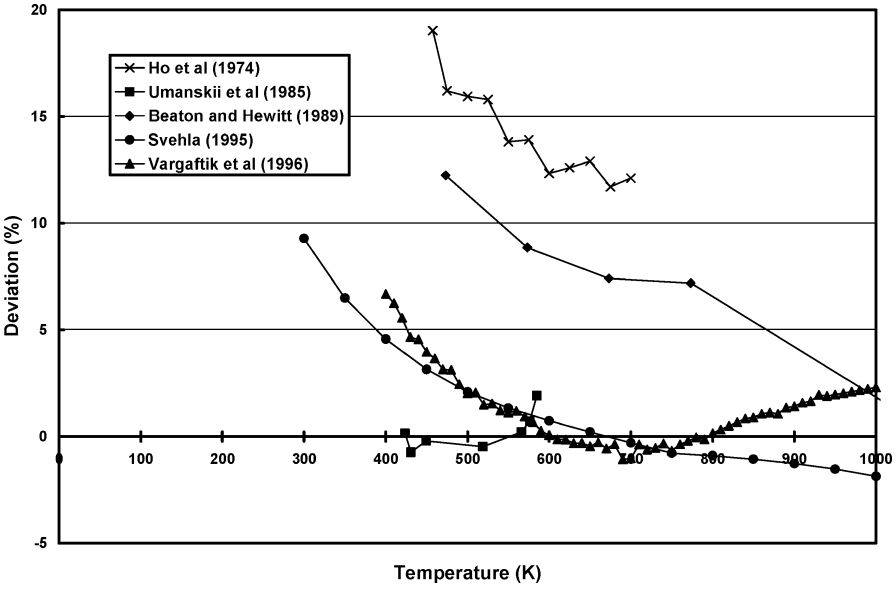

Fig. 14 Molecular iodine conductivity deviation vs temperature.

of the F_2 conductivity computed using the present model with the values of Touloukian et al.[65] is well within 6% over most of the temperature range, as shown in Fig. 11, and well within their reported uncertainty of 10%. Also, as shown in Fig. 11, the values reported by Beaton and Hewitt,[38] Svehla,[39] and Vargaftik et al.[42] are consistently about 4–8% low. The early estimates of Oerstavik and Storvick[43] are also consistently low over most of the temperature range. For Cl_2, the agreement of the conductivity computed using the present model with the values reported by Beaton and Hewitt,[38] Svehla,[39] Vargaftik et al.,[42] and Touloukian et al.[65] is quite good, as shown in Fig. 12; over their respective temperature ranges, the deviations are all within about 3%. Of course, the agreement with Touloukian et al.[65] is expected because Z_{rot}^{∞} was determined by fitting these data. For Br_2 the agreement with the values reported by Beaton and Hewitt,[38] Svehla,[39] and Touloukian et al.,[65] none of whom provided an estimate of the uncertainty in their recommended values, is within about 8%, as shown in Fig. 13. In Fig. 14, the I_2 conductivity computed using the present model is compared with the values recommended by Beaton and Hewitt,[38] Svehla,[39] Vargaftik et al.,[42] Umanskii et al.,[66] and Ho et al.[67] The present values of I_2 conductivity agree quite well with the measurements of Umanskii et al.[66] as expected because the value of Z_{rot}^{∞} was chosen to obtain a fit of these data. Ho et al.[67] estimated that the error in their recommended values could be as much as 25%, and so the disagreement with the present model would not be unexpected. Also note that above 400 K the present values agree to within 5% or better with the values recommended by Svehla[39] and within about 6% or better with the values recommended by Vargaftik et al.[42] Because the present conductivity model should be most applicable to diatomic molecules, it is satisfying that a good fit of the conductivity data vs temperature for all of the diatomic halogens can be achieved by such a simple scaling of Brokaw's correlation for Z_{rot}^{298}. For the atomic halogens and the interhalogen ICl, experimental conductivity data are unavailable and, again, comparisons of their conductivities, computed using the present model, were made with the early estimates of Svehla.[49] Because the trends were very similar to those observed when comparing the viscosities, the deviation plots are omitted. As with the viscosities, the present estimates of the halogen conductivities are believed to be more reliable.

D. Molecular Parameters for COIL

As already mentioned, to compute the conductivity of the rare gases all that is required are the previously determined species and potential parameters, which were obtained from Kestin et al.[9] and are given in Table 6. For the conductivity of the pure rare gases, Kestin et al.[9] estimate the accuracy to be no worse that 0.7% for temperatures ranging from 50 to 1000 K. For the molecular species of interest to COIL, the potential parameters needed to compute the viscosity are summarized in Table 6, and the additional molecular parameters to compute the conductivity are summarized in Table 11. For all species, with the exception of H_2O_2, the molar specific heat capacity was obtained from the NIST–JANAF thermochemical tables.[61] For hydrogen peroxide for temperatures less than or equal to 300 K, C_P was obtained from values reported in Ref. 61, whereas for temperature greater than 300 K, it was obtained from Ref. 68. For N_2, the molecular parameters were obtained from Uribe et al.,[22] whereas for O_2 the revised molecular parameters recommended by Mason and Uribe[12] were used. For the conductivity of N_2, Uribe et al.[22] estimate the uncertainty in their correlation to be 1.5% for temperatures ranging from 300 to 500 K, deteriorating to 3% at lower and higher temperatures. For O_2, they estimate the uncertainty to be 3% from 300 to 500 K rising to 5% outside these temperatures. Note that, although we have employed the potential parameters of Boushehri et al.,[10] the N_2 molecular parameters of Uribe et al.,[22] and the O_2 molecular parameters of Mason and Uribe,[12] the present model by which the conductivity is computed differs from that of Uribe et al.[21,22] In spite of this, the conductivity values computed using the present model do not differ from their tabulated values by more than 0.4%.

For water, the dipole moment was obtained from Lide.[46] The magnitude of the quadrupole tensor, required to estimate the near-resonant rotational exchange corrections, is by definition [Ref. 51, Eq. (2.119)]

$$|\Theta| = \left[\tfrac{2}{3}\left(\Theta_{xx}^2 + \Theta_{yy}^2 + \Theta_{zz}^2\right)\right]^{\frac{1}{2}} \tag{61}$$

where Θ_{ii}, $i = \{x, y, z\}$ denote the principle quadrupole moments. From Gray and Gubbins (Ref. 51, Table D.3), we find for water $\Theta_{xx} = +2.63$ B, $\Theta_{yy} = -2.50$ B, and $\Theta_{zz} = -0.13$ B from which $|\Theta| \simeq 2.96$ B. Matsunaga and Nagashima[45] give the rotational temperatures corresponding to each of the principle moments of inertia as $\theta_A = 39.99$ K, $\theta_B = 20.88$ K, and $\theta_C = 13.37$ K so that the effective rotational temperatures are $\theta_R = 22.35$ K and $\theta_{BC} = 16.71$. Finally, using Brokaw's rotational collision number correlations,[64] we have estimated $Z_{\text{rot}}^{298} \approx 4$, which is in reasonable agreement with the value reported by Lambert.[33] Because the Uribe et al.[21,22] rotational diffusion correlation is not applicable to strongly polar molecules, H_2O was treated by assuming that its rotational collision number was temperature independent and using the Sandler high-temperature expression for the rotational diffusion coefficient.[25] For water, as mentioned earlier, the relaxation time correction factor α was significant at low temperatures, ranging from a little more than 10% at 300 K to a little more than 60% at 100 K. With the present model this is due to the decrease in the internal energy diffusion coefficient because of the increasing importance of rotational exchange corrections at low temperatures. In consequence, the computed conductivities corrected for relaxation times are about 10–20% lower for temperatures ranging from 300 to 100 K than would be obtained with the linearized Hirschfelder–Eucken model used by Uribe et al.[21,22] but are identical to those obtained with the nonlinear Monchick et al.[60] model from which the linearized Hirschfelder–Eucken model is derived. Thus, although the present conductivity model for water is in agreement with the expectation[32] that the conductivity of strongly polar species is less than would be expected from the Eucken model, it must be viewed as only qualitatively correct because of the uncertainties inherent in both the models for the rotational collision number and the internal energy diffusion coefficient. In view of these limitations, it is satisfying that the model agrees as well as it does, within 10%, with the recommendations of Svehla,[39] Matsunaga and Nagashima,[45] and Sengers and Watson[48] over the range of temperatures for which they provide values (Fig. 15). The agreement with the data of Touloukian et al.[65] is not as good above 800 K.

Table 11 Molecular parameters for species of interest to COIL

Species	μ, D	μ^*	$\lvert\Theta\rvert$, B	$\lvert\Theta^*\rvert$	θ_R, K	Z_{rot}^{∞}	Z_{rot}^{298}	$10^3 C_{\text{spn}}$	T_{crs}^*
N_2	0	0	1.4	0.470	2.88	29.5	5.75	5.7	6.70
O_2	0	0	0.39	0.141	2.07	28.0	4.64	6.4	7.30
H_2O	1.8546	1.565	2.96	0.934	22.35[a]	4.0[a]	4.0	——	——
H_2O_2	1.573	1.066	2.82	0.546	2.732[a]	86.2	5.00	——	1.76
Cl_2	0	0	4.2	0.548	0.351	78.4	5.95	——	1.95
I_2	0	0	5.61	0.356	0.054	96.6	4.20	——	1.57
ICl	1.24	0.646	4.9	0.627	0.163	91.4	4.90	——	1.66

[a]See text.

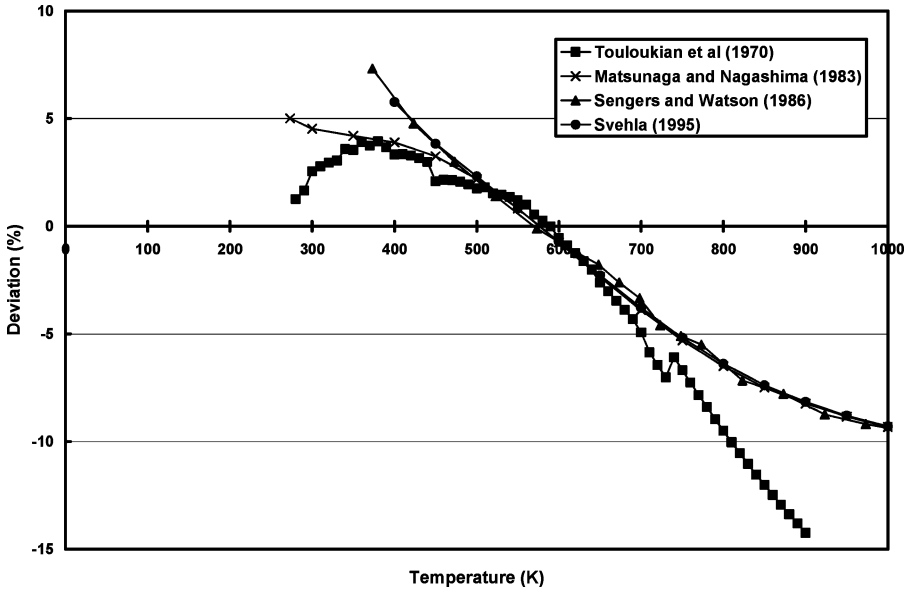

Fig. 15 Water conductivity deviation vs temperature.

For hydrogen peroxide, H_2O_2, the dipole moment was obtained from Lide.[46] In the absence of experimental measurements, the atom dipole method of Gierke et al.[69] has been used to estimate the quadrupole moment tensor of H_2O_2. With this method, the total dipole and quadrupole moments of the molecule relative to the molecules center of mass are the vector and tensor sums of the atom dipole and quadrupole moments, respectively, or

$$\boldsymbol{\mu} = \sum_a \boldsymbol{\mu}_a \tag{62}$$

$$\boldsymbol{\Theta} = \sum_a \boldsymbol{\Theta}_a = \sum_a (3\boldsymbol{R}_a \otimes \boldsymbol{\mu}_a - \boldsymbol{R}_a \cdot \boldsymbol{\mu}_a \boldsymbol{I}) \tag{63}$$

where $\boldsymbol{v} \otimes \boldsymbol{u}$ and $\boldsymbol{v} \cdot \boldsymbol{u}$ are the tensor and dot product of the vectors $\boldsymbol{v}$ and $\boldsymbol{u}$, respectively, and $\boldsymbol{I}$ is the unit tensor. Once the quadrupole tensor has been determined relative to the c.m. coordinate system, the principle quadrupole moments can be found by solving the characteristic polynomial

$$\det(\boldsymbol{\Theta} - \lambda \boldsymbol{I}) = 0 \tag{64}$$

for its eigenvalues, $\lambda_i \equiv \Theta_{ii}$, $i = \{x, y, z\}$, after which the magnitude of the quadrupole tensor is given by Eq. (61). The O–O and O–H bond lengths were taken to be 1.48 Å and 0.98 Å, respectively, whereas the O–O–H bond angle and the dihedral angle were taken to be 102 and 90 deg, respectively.[70] The resulting value of the H_2O_2 dipole moment was 1.859 D, which is about 18% higher than the value, 1.573 D, reported by Lide.[46] This uncertainty is consistent with the uncertainty between the calculated and experimental molecular dipole moments.[69] Because of the simple linear relationship between the atom dipoles and the molecular quadrupole moment and the assumption that the O and H atom dipoles are collinear (but oppositely polarized), we can simply rescale the atom dipole moments by the ratio of the experimental to estimated molecular dipole moment and recompute both the molecular dipole and quadrupole moments. When this is done, the calculated magnitude of the H_2O_2 quadrupole moment is 2.820 B, with an uncertainty of about 15%. For the rotational temperatures, we have taken the principle moments of inertia to be[70] $I_A = 2.83 \times 10^{-40}\,\mathrm{g \cdot cm^2}$, $I_B = 33.6 \times 10^{-40}\,\mathrm{g \cdot cm^2}$, and $I_C = 33.7 \times 10^{-40}\,\mathrm{g \cdot cm^2}$ to obtain $\theta_A = 14.232$ K, $\theta_B = 1.199$ K, and $\theta_C = 1.195$ K from which it follows that $\theta_R = 2.732$ K and $\theta_{BC} = 1.197$ K. Using Brokaw's rotational collision number correlations,[64] we have estimated $Z_{\mathrm{rot}}^{298} \approx 5$. Comparison of the present result for the conductivity of H_2O_2 with that of Paul[13] and Paul and Warnatz[14] is very good; the deviation is no more that 4% for temperatures ranging from 300 to 1000 K, which is somewhat remarkable because they did not provide any details regarding their estimate other than to state that they used the Uribe et al.[21,22] model. Not surprisingly, a comparison with the values recommended by Yaws,[55] based on the Eucken model, is poor; the deviation ranges from −10% at 300 K to more than −25% for temperatures above 700 K.

IV. Viscosity and Thermal Conductivity of COIL Mixtures

Within the framework of the Chapman–Enskog theory of transport processes in dilute gases, the viscosity and thermal conductivity of a mixture of polyatomic gases can be expressed as (see Ref. 4)

$$\mathcal{P} = \tilde{\boldsymbol{p}}^T \boldsymbol{x} \tag{65a}$$

$$G\tilde{\boldsymbol{p}} = \boldsymbol{x} \tag{65b}$$

where $\boldsymbol{x} = \{x_i | i = 1, \ldots, N_S\}$ is the column vector of mole fractions, $\tilde{\boldsymbol{p}}$ is a column vector, and G is an $N_S \times N_S$ symmetric, positive definite matrix. For the viscosity, the elements of the matrix G, now called H, are

$$H_{ii} = \frac{x_i^2}{\eta_i} - \sum_{j \neq i} H_{ij} \frac{\left(5/3A_{ij}^* + W_j/W_i\right)}{\left(5/3A_{ij}^* - 1\right)} \tag{66a}$$

$$H_{ij} = -\frac{x_i x_j}{2(\eta_i \eta_j)^{\frac{1}{2}}} S_{ij}^* M_{ij}^3 \left(\frac{5}{3A_{ij}^*} - 1\right) = H_{ji} \qquad j \neq i \tag{66b}$$

$$S_{ij}^* = \frac{\hat{\sigma}_{ij}^2 \Omega_{ij}^{(2,2)^*}}{\left(\hat{\sigma}_i^2 \Omega_i^{(2,2)^*} \hat{\sigma}_j^2 \Omega_j^{(2,2)^*}\right)^{\frac{1}{2}}} = S_{ji}^* \tag{66c}$$

$$M_{ij} = \left(\frac{4W_i W_j}{(W_i + W_j)^2}\right)^{\frac{1}{4}} \tag{66d}$$

Similarly, for the thermal conductivity, within the Thijsse formulation and making the spherical potential approximation,[4,71] the

elements of the matrix G, now called F to avoid confusion, are

$$F_{ii} = \frac{x_i^2}{\lambda_i} - \sum_{j\neq i} F_{ij}\frac{\left(1+r_j^2\right)}{\left(1+r_i^2\right)}\left\{\left[\frac{15}{4}\frac{W_i^2}{A_{ij}^*} + \frac{25}{8}\frac{W_j^2}{A_{ij}^*} - \frac{3}{2}W_j^2\frac{B_{ij}^*}{A_{ij}^*} + 2W_iW_j + \frac{5}{4}(W_i+W_j)^2\frac{r_i^2}{A_{ij}^*}\right]\Big/ W_iW_j\left[\frac{55}{8A_{ij}^*} - \frac{3}{2}\frac{B_{ij}^*}{A_{ij}^*} - 2\right]\right\} \tag{67a}$$

$$F_{ij} = -\frac{x_ix_j}{4\left(\lambda_i^{(M)}\lambda_j^{(M)}\right)^{\frac{1}{2}}}S_{ij}^*M_{ij}^5\frac{1}{\left(1+r_i^2\right)\left(1+r_j^2\right)} \times\left[\frac{55}{8A_{ij}^*} - \frac{3}{2}\frac{B_{ij}^*}{A_{ij}^*} - 2\right] = F_{ji} \qquad j\neq i \tag{67b}$$

The off-diagonal elements of H and F characterize the interaction between unlike molecules. The matrices S^* and M are symmetric and dimensionless, and because S^* is a ratio of collision cross sections, we will call it the scattering matrix. The primary temperature and molecular collision dynamics dependence enters through the S^* matrix because the temperature dependence of A^* and B^* are relatively weak. Once the matrices H and F have been evaluated, the viscosity and thermal conductivity of the dilute polyatomic gas mixture can be determined by solving the linear equations (65) using either Gaussian elimination or the more efficient preconditioned conjugate-gradient method suggested by Ern and Giovangigli.[72] Evaluating the matrices H and F requires the pure species viscosities, thermal conductivities, specific heats, and the interaction matrices S^*, A^*, and B^*, which in turn requires the binary interaction potential matrices $\hat{\sigma}$, $\hat{\varepsilon}$, $\hat{\rho}$, $\hat{V}$, and $\hat{C}_6$.

In practical CFD computations, approximations are often made in one or more of these steps to evaluate mixture transport properties. In particular, simplified approximate solutions of Eqs. (65) are often employed together with suitable approximations for the G matrix, which require only the pure species properties and not the binary interaction parameters to compute. For example, Ern and Giovangigli[72] suggested using a single iteration of the preconditioned conjugate-gradient method to obtain a useful analytical formula for the viscosity or conductivity. In this case, the solution of Eqs. (65) is[4,72]

$$\mathcal{P} = (y^Tx)^2/y^TGy \tag{68}$$

where $y = x/D$ and D is the diagonal of the matrix G. A significant advantage[4] of this solution is that it retains to first order the off-diagonal elements of G. Copeland[4] employed this solution together with several simplifying approximations for the interaction matrices S^*, A^*, and B^* to obtain new, efficient rules for computing the viscosity and conductivity of dilute polyatomic mixtures that outperform the popular Wilke rules. Here, for the present potential model, these rules are summarized. First, using the well-known approximations[73] $A_{ij}^* \approx 10/9$ and $B_{ij}^* \approx 10/9$, the elements of the matrix H for the viscosity become

$$H_{ii} = \frac{x_i^2}{\eta_i} - \sum_{j\neq i} H_{ij}\left[1 + 2\left(\frac{W_i+W_j}{W_i}\right)\right] \tag{69a}$$

$$H_{ij} = -\frac{1}{4}\frac{x_ix_j}{(\eta_i\eta_j)^{\frac{1}{2}}}S_{ij}^*M_{ij}^3 = H_{ji} \qquad j\neq i \tag{69b}$$

and, similarly, the elements of the matrix F for the conductivity become

$$F_{ii} = \frac{x_i^2}{\lambda_i} - \sum_{j\neq i} F_{ij}\frac{\left(1+r_j^2\right)}{\left(1+r_i^2\right)} \times\frac{\left[54W_i^2 + 21W_j^2 + 32W_iW_j + 18(W_i+W_j)^2r_i^2\right]}{43W_iW_j} \tag{70a}$$

$$F_{ij} = -\frac{43}{64}\frac{x_ix_j}{\left(\lambda_i^{(M)}\lambda_j^{(M)}\right)^{\frac{1}{2}}}S_{ij}^*M_{ij}^5\frac{1}{\left(1+r_i^2\right)\left(1+r_j^2\right)} = F_{ji} \qquad j\neq i \tag{70b}$$

Finally, using Brokaw's approximation[64] that $\Omega^{(2,2)^*}(\hat{T}) \approx \frac{4}{5}(1+1/\hat{T})$ together with the approximations $\sigma_{ij} = \sqrt{\sigma_i\sigma_j}$ and

Table 12 Viscosity fit coefficients and value in μPa · s at 300 K[a]

Species	c_0	c_1	c_2	c_3	c_4	Value
He	−5.881317	4.570221	−1.111076	0.138729	−0.006410	20.04
	−0.079454	0.313448	0.060944	−0.004778	0.000183	
Ne	−6.910251	4.311269	−0.736251	0.063654	−0.001956	32.10
	−15.054384	9.538815	−1.993374	0.197898	−0.007328	
Ar	7.466858	−4.906335	1.112053	−0.056096	−0.002006	22.82
	−13.066112	6.566178	−1.025533	0.077325	−0.002119	
Kr	−43.940121	37.370172	−11.728686	1.655533	−0.086547	25.60
	−14.663582	7.090179	−1.061278	0.075749	−0.001950	
Xe	−15.071143	12.014936	−3.430945	0.455786	−0.021990	23.16
	−16.534599	7.600784	−1.089473	0.073496	−0.001767	
N_2	23.916182	−21.444507	6.964601	−0.941834	0.046745	17.96
	−11.694545	6.076253	−0.997073	0.080032	−0.002351	
O_2	52.224840	−43.464911	13.352716	−1.759703	0.085838	20.78
	−12.401723	6.322807	−1.006470	0.077775	−0.002189	
H_2O	26.819092	−25.265446	8.479538	−1.203228	0.063336	10.36
	−512.255746	332.907251	−80.895808	8.731121	−0.352044	
H_2O_2	29.547819	−27.166960	9.110301	−1.309291	0.070298	11.35
	39.647930	−29.446364	7.826738	−0.869054	0.035300	
Cl_2	−60.437386	49.542065	−15.164362	2.075235	−0.105135	13.52
	−17.287763	7.661112	−1.092434	0.073194	−0.001745	
I_2	14.307421	−13.904839	4.900400	−0.721555	0.039722	13.08
	166.099320	−106.414076	25.397916	−2.650965	0.103055	
ICl	−2.487312	0.012470	0.687687	−0.159914	0.011937	18.48
	21.645928	−17.143142	4.798357	−0.541621	0.022148	
Cl	45.286190	−36.274280	10.697659	−1.345008	0.062473	19.18
	−13.666191	6.699626	−1.035324	0.077002	−0.002078	
I	−39.911376	31.750323	−9.316343	1.229102	−0.059707	19.62
	−17.832207	7.914330	−1.104237	0.071882	−0.001651	

[a]Coefficients in first row for 50–300 K and in second row for 300–1000 K.

Table 13 Conductivity fit coefficients and value in mW/m · K at 300 K[a]

Species	c_0	c_1	c_2	c_3	c_4	Value
He	−3.862637	4.583445	−1.110316	0.138070	−0.006353	156.68
	1.983293	0.311852	0.060979	−0.004764	0.000182	
Ne	−6.216152	4.107644	−0.677883	0.056423	−0.001627	49.78
	−15.051939	9.780543	−2.043193	0.202430	−0.007482	
Ar	7.574985	−5.200403	1.203877	−0.068932	−0.001329	17.83
	−12.822666	6.258315	−0.954757	0.070246	−0.001857	
Kr	−45.189800	37.586804	−11.794414	1.664208	−0.086968	9.52
	−14.869641	6.622435	−0.958001	0.065754	−0.001591	
Xe	−16.760203	12.210635	−3.486355	0.462575	−0.022294	5.50
	−16.834563	6.945485	−0.949377	0.060302	−0.001304	
N_2	13.389245	−13.435145	4.669037	−0.642808	0.032008	25.88
	48.660601	−29.619355	6.919710	−0.697551	0.026324	
O_2	81.142293	−68.242100	21.176554	−2.841436	0.141417	25.99
	−90.860071	59.751942	−14.608922	1.612263	−0.066700	
H_2O	31.619085	−28.972097	9.610465	−1.358913	0.071813	17.66
	−358.243593	236.425871	−58.303781	6.389202	−0.260951	
H_2O_2	−186.130260	152.444950	−46.718885	6.352337	−0.320556	19.00
	108.425440	−73.530856	18.231886	−1.937381	0.075857	
Cl_2	−98.850664	81.372429	−25.276301	3.499087	−0.179573	9.02
	137.509721	−94.047472	23.713714	−2.597539	0.105480	
I_2	47.347075	−43.336449	13.890934	−1.911663	0.097888	2.60
	171.267135	−110.264290	26.133285	−2.702879	0.103896	
ICl	28.967735	−25.922991	8.069978	−1.066706	0.052913	5.55
	134.889266	−89.722061	21.933441	−2.327174	0.091508	
Cl	37.649908	−30.280037	8.941153	−1.122261	0.052247	17.67
	65.587838	−45.747747	11.842465	−1.315680	0.053935	
I	−42.297465	32.545462	−9.554797	1.260555	−0.061248	4.82
	−24.665154	11.384956	−1.933014	0.159467	−0.005106	

[a]Coefficients in first row for 50–300 K and in second row for 300–1000 K.

$\varepsilon_{ij} = \sqrt{\varepsilon_i \varepsilon_j}$ to avoid computing the binary interaction parameters σ_{ij} and ε_{ij}, we obtain for the S^* matrix

$$S^*_{ij} \cong \left(\frac{\sqrt{\xi_i \xi_j}}{\xi_{ij}}\right)^{\frac{1}{3}} \frac{\left(\xi^2_{ij} + \sqrt{T^*_i T^*_j}\right)}{\left[\left(\xi^2_i + T^*_i\right)\left(\xi^2_j + T^*_j\right)\right]^{\frac{1}{2}}} \tag{71a}$$

$$\xi_{ij} = 1 + \chi^*_{ij} + \frac{\delta^*_i \delta^*_j}{6\sqrt{T^*_i T^*_j}} \tag{71b}$$

$$\chi^*_{ij} = \frac{1}{2}\left(\alpha^*_i \delta^*_j \sqrt{\frac{\varepsilon_j}{\varepsilon_i}} + \alpha^*_j \delta^*_i \sqrt{\frac{\varepsilon_i}{\varepsilon_j}}\right) \tag{71c}$$

Following Brokaw,[64,73] when computing mixture viscosities (but not mixture conductivities) Eq. (71) is used if either δ^*_i or δ^*_j is greater than 0.1, whereas S^*_{ij} is taken to be unity if both δ^*_i and δ^*_j are less than 0.1. Here the scattering matrix S^* is based on Paul's thermally averaged potential, Eq. (12), and not the Stockmayer potential (see Ref. 4) although if one expands ξ^2_{ij} and retains only the lowest-order dipole–dipole interaction corrections, Brokaw's S^* matrix is obtained if γ is three-eighths, not one-fourth. The preceding approximate rules with this new interaction matrix have been tested using the same methodology and database reported in Ref. 4 with polarizabilities taken from Miller[40] and found to perform better than the EG-B rule for viscosity and as well as the EG-TSB rule for conductivity.[4]

To facilitate using the preceding equations to compute the mixture properties and because tables of the viscosity and thermal conductivity for the fourteen species He, Ne, Ar, Kr, Xe, N_2, O_2, H_2O, H_2O_2, Cl_2, I_2, ICl, Cl, and I for temperatures ranging from 50 to 1000 K are quite large, parametric representations of the data are provided. The considerations that guide the choice of a functional form with which to fit transport property data for the purposes of CFD have been discussed elsewhere.[3] For each species, the logarithm of the transport property as a function of the logarithm of the temperature is represented by a fourth-degree polynomial in each of two contiguous temperature ranges (T_L, T_C) and (T_C, T_F). Suppressing the species index for clarity, the functional representation is

Table 14 Maximum and minimum relative errors in the viscosity and conductivity fits

	Viscosity, %		Conductivity, %	
Species	Maximum	Minimum	Maximum	Minimum
He	0.001	−0.001	0.000	−0.001
Ne	0.001	−0.001	0.001	−0.001
Ar	0.112	−0.137	0.109	−0.133
Kr	0.022	−0.018	0.017	−0.014
Xe	0.047	−0.038	0.049	−0.040
N_2	0.042	−0.034	0.084	−0.141
O_2	0.067	−0.055	0.124	−0.101
H_2O	0.544	−0.442	0.466	−0.379
H_2O_2	0.140	−0.114	0.384	−0.468
Cl_2	0.063	−0.051	0.089	−0.183
I_2	0.070	−0.055	0.111	−0.187
ICl	0.082	−0.067	0.098	−0.166
Cl	0.029	−0.035	0.036	−0.033
I	0.076	−0.062	0.083	−0.067
Overall	0.544	−0.442	0.466	−0.468

$$\ell_n(\mathcal{P}) = \sum_{i=0}^{4} c_i [\ell_n(T)]^i \tag{72}$$

The units of e^{c_0} are the dimensions of the transport property, whereas the units of c_i are $[\ell_n(T)]^{-i}$, $i = 1, \ldots, 4$. The procedure used to determine the fit coefficients ensured that the derivative was continuous at the crossover temperature T_C. Thus, for each species, there are five required coefficients in each of two temperature ranges for a total of 10 coefficients. Although, compared to evaluating a polynomial, evaluating the form (72) is more complicated, a significant reduction in fit error is achieved. For viscosity, Table 12 lists the coefficients for each species in each of the two temperature ranges (50, 300 K) and (300, 1000 K) and its value at 300 K; the units of viscosity are μP · s. Similarly Table 13 provides the coefficients for the conductivity; the units of conductivity are mW/m · K. For each

species, the maximum and minimum relative errors in the viscosity and conductivity fits over the entire range from 50 to 1000 K are tabulated in Table 14. Overall, for viscosity the relative fit error was about ±0.6% at worst, whereas for conductivity it was about ±0.5% at worst. The largest fit errors occurred for H_2O and H_2O_2, whereas those for the remaining species were much smaller. For all species, the fit errors were less than the uncertainty in the experimental data from which the viscosity and conductivity were determined.

V. Summary

Models to compute the mass diffusivity, viscosity, and thermal conductivity coefficients of several species and their mixtures pertinent to COIL performance modeling have been developed. The species diffusivity and viscosity models are based upon the Chapman–Enskog theory and the corresponding states correlation of Kestin et al.,[9] Boushehri et al.,[10] Bzowski et al.,[11] and Mason and Uribe[12] for the transport properties of the rare gases and several non- or weakly polar molecules and Paul's[13] extension of these correlations to strongly polar molecules. For the present application, because the molecular collision integrals are required for reduced temperatures down to ~0.01, new polynomial extensions were developed to allow their computation for $0 < T^* \leq 1$. Conditions under which Paul's thermally averaged interaction potential model can be used to extend the collision integral functionals to describe strongly polar species were briefly discussed, and it was shown that the most severe constraint on the lower temperature bound was due to the neglect of higher-order orientation–averaged terms in the interaction potential. For the species of present interest, this restriction is most severe for water, requiring that $T > 140$ K, although the model is at least qualitatively correct for temperatures below this bound. Of course the real justification of any such model is a posteriori by how well it fits and correlates the available experimental data. By these criteria, the model is quite good for the present species and temperature ranges of interest.

The required potential-well parameters for the homonuclear halogens were determined from fits of viscosity data, whereas the Born–Mayer repulsive potential parameters were derived using the Tang–Toennies screened potential model together with the measured polarizabilities and the Cambi et al.[17] electron oscillator number correlations to estimate the effective van der Waals coefficient. For the homonuclear halogens, good agreement between the present results and those of Svehla[39] for the potential parameters and resulting viscosities was obtained; for F_2, Cl_2, and I_2, the deviation from the present results is no more than 4%, increasing to 10% for Br_2. For the atomic halogens and the interhalogen ICl, the potential parameters were obtained using the Tang–Toennies[15,16] potential model and the Cambi et al.[17] correlations for the potential equilibrium separation, well-depth energy, and effective dispersion coefficient. Comparison of the resulting atomic halogen potential parameter trends with those for the noble gases were in accord with the expectation that the halogens would have somewhat deeper potential wells but not as repulsive a potential wall as the rare gases. Overall, these trends are reassuring that reliable estimates of the atomic halogen interaction potential parameters have been determined, even though the Cambi et al.[17] correlations and Tang–Toennies screened potential model have been used to determine all of the potential parameters from the atomic polarizabilities. Comparison of the computed viscosities with the early estimates of Svehla[49] shows agreement with his results within 5% for Cl and Br and 10% for I but poor agreement for F and ICl, which was explained in terms of Svehla's[49] estimates for their potential parameters. The present potential parameter estimates for the halogens are believed to be more reliable.

The thermal conductivity model for non- or weakly polar molecules is based on the Thijsse total energy expression (see Refs. 18–20) for conductivity, assumes the internal energy modes are independent, and uses the Uribe et al.[21,22] rotational energy diffusion correlation, and the Parker[23] Brau–Jonkman[24] expression for rotational collision number. Corrections for near-resonant rotational exchange collisions on the rotational diffusion coefficient and the small spin-polarization effects have been included as appropriate when experimental data were available. With this model, the high-temperature rotational collision number Z_{rot}^{∞} is treated as an adjustable parameter to obtain a one-parameter correlation. For the molecular species treated by the model of Uribe et al.,[21,22] which was based on the more traditional Hirschfelder–Eucken expression for conductivity, the present model with their recommended molecular parameters gives results essentially identical to theirs. For the halogen diatomics, the required molecular parameters were obtained from the literature with the exception of Z_{rot}^{∞}, which was obtained by scaling Brokaw's[64] room temperature correlations for Z_{rot}. When the same scaling factor was used for all of the halogen diatomic species, the model provides a very satisfactory correlation of the thermal conductivity for all of the halogen homonuclear diatomics, as shown by comparison to both experimental and theoretical data. These results demonstrate, for the temperature range of interest, that rotational energy relaxation in the homonuclear halogens can be adequately described a single effective relaxation time, which is an important assumption of both the Thijsse conductivity (see Ref. 19) and Parker[23] Brau–Jonkman[24] rotational collision number models. For the atomic halogens, the model accounts for diffusion of internal electronic energy and provides estimates of their conductivities. For the polyatomics H_2O and H_2O_2, the molecular parameters were obtained from the literature or estimated as necessary. For the weakly polar polyatomic H_2O_2 molecule, the model provides an estimate of the conductivity that is in reasonable agreement, within 5%, with that of Paul[13] over the temperature range of 300–1000 K. Finally, although the Uribe et al.[21] rotational diffusion coefficient correlation does not apply to strongly polar molecules, a reasonable correlation, within about 3%, of the Matsunaga and Nagashima[45] and Sengers and Watson[48] recommendations for the thermal conductivity of H_2O, was obtained by assuming that the rotational diffusion coefficient was given by Sandler's[25] high-temperature correlation and a constant, temperature-independent rotational collision number. Together with the molecular and potential parameters supplied in Refs. 9–12, for the rare gases, N_2, and O_2, the present model and set of halogen parameters provides a reliable means of estimated the species viscosity for temperatures ranging from about 50 to 5000 K and thermal conductivities from about 50 to 1000 K, although for the purposes of ejector COIL modeling there is interest only for temperatures less than 1000 K. Comparisons of the viscosities and conductivities computed using the present model with those computed using the Sutherland model shows that the latter only describes these transport properties over a limited temperature range (see Ref. 3). The present work suggests a need to develop a rotational energy diffusion correlation for strongly polar molecules, analogous to that which Uribe et al.[21] devised for non- or weakly polar molecules and improved models and/or correlations for the rotational and internal collision numbers.

The Chapman–Enskog theory of the viscosity and conductivity of dilute gas mixtures was summarized, and the appropriate binary interaction potential parameters for 14 species of interest to COIL performance modeling was provided. The mixture formulas were cast in a useful form from which to develop approximate mixture rules and, for the present thermally averaged potential model, new approximate rules for the viscosity and conductivity that outperform the well-known Wilke rules were summarized. These approximate rules are more than adequate for most practical applications. Finally, the present work serves, in part, as a guide and, with judicious care in estimating the required interaction potential and molecular parameters, can be used to correlate, estimate, and predict the transport properties of other neutral, dilute gases comprised of atomic or small polyatomic species.

Appendix: Noble and Molecular Collision Integrals

This Appendix summarizes the correlations for the noble and molecular collision integral functionals and the approach used to obtain the molecular collision integral polynomial extensions. The definitions of several important collision integral ratios and the recursion relation for the reduced collision integrals are also briefly discussed.

A. Noble Gases

0 < T < 1.2*

For $0 < T^* \leq 1.2$, the noble gas collision integrals $\Omega^{(1,1)^*}$ and $\Omega^{(2,2)^*}$ depend only on T^* and C_6^* and are given by[11]

$$\Omega^{(1,1)^*} = 1.1874\left(C_6^*/T^*\right)^{\frac{1}{3}}\left[1 + a_1(T^*)^{\frac{1}{3}} + a_2(T^*)^{\frac{2}{3}} + a_3(T^*) + a_4(T^*)^{\frac{4}{3}} + a_5(T^*)^{\frac{5}{3}} + a_6(T^*)^2\right] \quad \text{(A1a)}$$

$$\Omega^{(2,2)^*} = 1.1943\left(C_6^*/T^*\right)^{\frac{1}{3}}\left[1 + b_1(T^*)^{\frac{1}{3}} + b_2(T^*)^{\frac{2}{3}} + b_3(T^*) + b_4(T^*)^{\frac{4}{3}} + b_5(T^*)^{\frac{5}{3}} + b_6(T^*)^2\right] \quad \text{(A1b)}$$

where $a_1 = 0, a_2 = 0, b_1 = 0.18$, and $b_2 = 0$ and the other coefficients are given by

$$a_3 = +10.0161 - 10.5395\left(C_6^*\right)^{-\frac{1}{3}} \quad \text{(A1c)}$$

$$a_4 = -40.0394 + 46.0048\left(C_6^*\right)^{-\frac{1}{3}} \quad \text{(A1d)}$$

$$a_5 = +44.3202 - 53.0817\left(C_6^*\right)^{-\frac{1}{3}} \quad \text{(A1e)}$$

$$a_6 = -15.2912 + 18.8125\left(C_6^*\right)^{-\frac{1}{3}} \quad \text{(A1f)}$$

$$b_3 = -1.20407 - 0.195866\left(C_6^*\right)^{-\frac{1}{3}} \quad \text{(A1g)}$$

$$b_4 = -9.86374 + 20.2221\left(C_6^*\right)^{-\frac{1}{3}} \quad \text{(A1h)}$$

$$b_5 = +16.6295 - 31.3613\left(C_6^*\right)^{-\frac{1}{3}} \quad \text{(A1i)}$$

$$b_6 = -6.73805 + 12.6611\left(C_6^*\right)^{-\frac{1}{3}} \quad \text{(A1j)}$$

1.2 ≤ T ≤ 10*

For $1.2 \leq T^* \leq 10$, the noble gas collision integrals $\Omega^{(1,1)^*}$ and $\Omega^{(2,2)^*}$ depend only on T^* and are represented by[11]

$$\Omega^{(i,i)^*} = \exp[P^{(i,i)^*}(z)] = \exp\left(\sum_{k=0}^{4} c_k^{(i,i)^*} z^k\right) \quad \text{(A2a)}$$

$$P^{(1,1)^*} = +0.357588 - 0.472513z + 0.0700902z^2 + 0.0165741z^3 - 0.00592022z^4 \quad \text{(A2b)}$$

$$P^{(2,2)^*} = +0.466410 - 0.569910z + 0.1959100z^2 - 0.0387900z^3 + 0.00259000z^4 \quad \text{(A2c)}$$

where $z = \ell_n(T^*)$.

T ≥ 10*

For $T^* \geq 10$, the collision integrals $\Omega^{(1,1)^*}$ and $\Omega^{(2,2)^*}$ depend only on T^*, ρ^*, and V^* and are[11,12]

$$\Omega^{(1,1)^*} = (\rho^*\alpha)^2\left[0.89 + a_2(T^*)^{-2} + a_4(T^*)^{-4} + a_6(T^*)^{-6}\right] \quad \text{(A3a)}$$

$$\Omega^{(2,2)^*} = (\rho^*\alpha)^2\left[1.04 + b_2 z^{-2} + b_3 z^{-3} + b_4 z^{-4}\right] \quad \text{(A3b)}$$

where $\alpha = \ell_n(V^*/T^*)$, $z = \ell_n(T^*)$, and the coefficients a_i and b_i, which depend only on ρ^* and V^*, are[11,12]

$$a_2 = -267.00 + \left(\alpha_{10}\rho^*\right)^{-2} \times \left[201.570 + (174.672/\alpha_{10}) + (7.36916/\alpha_{10})^2\right] \quad \text{(A3c)}$$

$$a_4 = +26700 - \left(\alpha_{10}\rho^*\right)^{-2} \times \left[19226.5 + (27693.8/\alpha_{10}) + (3295.59/\alpha_{10})^2\right] \quad \text{(A3d)}$$

$$a_6 = -8.9 \times 10^5 + \left(\alpha_{10}\rho^*\right)^{-2}\left[6.31013 \times 10^5 + \left(10.2266 \times 10^5/\alpha_{10}\right) + \left(2.33033 \times 10^5/\alpha_{10}\right)^2\right] \quad \text{(A3e)}$$

$$b_2 = -33.0838 + \left(\alpha_{10}\rho^*\right)^{-2} \times \left[20.0862 + (72.1059/\alpha_{10}) + (8.27648/\alpha_{10})^2\right] \quad \text{(A3f)}$$

$$b_4 = +101.571 - \left(\alpha_{10}\rho^*\right)^{-2} \times \left[56.4472 + (286.393/\alpha_{10}) + (17.7610/\alpha_{10})^2\right] \quad \text{(A3g)}$$

$$b_4 = -87.7036 + \left(\alpha_{10}\rho^*\right)^{-2} \times \left[46.3130 + (277.146/\alpha_{10}) + (19.0573/\alpha_{10})^2\right] \quad \text{(A3h)}$$

and $\alpha_{10} = \ell_n(V^*/10)$ denotes the value of α at the matching point of $T^* = 10$.

B. Molecular Gases

0 < T ≤ 0.1*

When the polynomial extensions that follow for $0.1 \leq T^* \leq 1$ and the known scaling behavior of the collision integrals for T^* near zero[29,74] were used, the functional $\chi^{(i,i)^*} \equiv T^{*1/3}\Omega^{(i,i)^*}$ was linearly extrapolated to obtain $\Omega^{(1,1)^*}$ and $\Omega^{(2,2)^*}$, which are given by

$$T^{*\frac{1}{3}}\Omega^{(1,1)^*} \equiv 1.73603 - 0.27870(T^* - 0.1) \quad \text{(A4a)}$$

$$T^{*\frac{1}{3}}\Omega^{(2,2)^*} \equiv 1.90328 + 0.04700(T^* - 0.1) \quad \text{(A4b)}$$

0.1 < T ≤ 1*

To extend the collision integrals given by Bzowski et al.[11] from $T^* = 1$ down to $T^* = 0.1$, we assume that the collision integrals, denoted Ω_E, can be represented by

$$\Omega_E = \exp[P_E(z)] = \exp\left(\sum_{k=0}^{5} a_{Ek} z^k\right) \quad \text{(A5)}$$

where, following Paul,[13] the polynomial extension is assumed to be one degree higher than the original representation of Bzowski et al.[11] The continuity of the collision integrals and their first and second derivatives at $T^* = 1$ require that $a_{Ek} \equiv c_k$ for $k = 0, 1, 2$, where c_k are the coefficients of the polynomial of the particular collision integral under consideration. Assume that values of required collision integral, denoted Ω_i, are known at three additional reduced temperatures, $T_i^* < 1$, for $i = 0, 1, 2$. From representation (A5), the continuity requirements, and these known values, it then follows that the remaining three coefficients a_{Ek}, $k = 3, 4, 5$, are determined by

$$\begin{bmatrix} z_0^3 & z_0^4 & z_0^5 \\ z_1^3 & z_1^4 & z_1^5 \\ z_2^3 & z_2^4 & z_2^5 \end{bmatrix}\begin{bmatrix} a_{E3} \\ a_{E4} \\ a_{E5} \end{bmatrix} = \begin{bmatrix} b_0 \\ b_1 \\ b_2 \end{bmatrix} \quad \text{(A6)}$$

where $b_i = \ell_n(\Omega_i^*) - (c_0 + c_1 z_i + c_2 z_i^2)$ and $z_i = \ell_n(T_i^*)$, which can be solved using Cramer's rule. The required values of the collision integrals $\Omega^{(1,1)^*}$ and $\Omega^{(2,2)^*}$ were obtained by appropriately scaling the values of the collision integrals for an L–J potential at $T^* = 0.1$, 0.2, and 0.3 (Ref. 75). At the crossover point of $T^* = 1$, the values of the Bzowski et al.[11] universal molecular collision integrals (discussed subsequently) are $\Omega^{(1,1)^*} = 1.34367$ and $\Omega^{(2,2)^*} = 1.59426$. Because the corresponding L–J values are[75] $\Omega_{L-J}^{(1,1)^*} = 1.4398$ and $\Omega_{L-J}^{(2,2)^*} = 1.5929$, only $\Omega^{(1,1)^*}$ is scaled down

by 0.9332. The resulting polynomial extensions are

$$P^{(1,1)^*} = +0.295402 - 0.510069z + 0.189395z^2 + 0.304101z^3 + 0.151527z^4 + 0.0262932z^5 \quad \text{(A7a)}$$

$$P^{(2,2)^*} = +0.466410 - 0.569910z + 0.195910z^2 + 0.488907z^3 + 0.281443z^4 + 0.0517421z^5 \quad \text{(A7b)}$$

The deviation of these extensions for the molecular collision integrals $\Omega^{(1,1)^*}$ and $\Omega^{(2,2)^*}$ from those of Paul[13] are less than 1.5 and 2%, respectively, over the entire range $0.2 \le T^* \le 1$ for which he provided extensions. These differences are quite small considering that the present polynomial extensions span a larger reduced temperature range.

$1 \le T^* \le 10$

For $1 \le T^* \le 10$, the molecular collision integrals $\Omega^{(1,1)^*}$ and $\Omega^{(2,2)^*}$ again depend only on T^* and are represented using Eq. (A2), but now $P^{(1,1)^*}$ is given by[11]

$$P^{(1,1)^*} = +0.295402 - 0.510069z + 0.189395z^2 - 0.045427z^3 + 0.0037928z^4 \quad \text{(A8)}$$

$\Omega^{(2,2)^*}$ is identical to that for the noble gases, although the range of T^* over which it applies is different; see Eq. (A2).

$T^* \ge 10$

For $T^* \ge 10$, the collision integrals $\Omega^{(1,1)^*}$ and $\Omega^{(2,2)^*}$, which depend only on ρ^*, V^*, and T^*, are identical to those used for the noble gases; see Eqs. (A3).

C. Collision Integral Ratios and Recursion Relations

Finally, consider the collision integral ratios A^*, B^*, C^*, and E^*, which are defined by

$$A^* = \frac{\Omega^{(2,2)^*}}{\Omega^{(1,1)^*}} \quad \text{(A9)}$$

$$B^* = \frac{\left(5\Omega^{(1,2)^*} - 4\Omega^{(1,3)^*}\right)}{\Omega^{(1,1)^*}} = 1 + 3C^* - 3(C^*)^2 - \frac{(T^*)^2}{3} \times \frac{\mathrm{d}^2 \ell_n\left(\Omega^{(1,1)^*}\right)}{\mathrm{d}(T^*)^2} = 4C^* - 3(C^*)^2 - \frac{1}{3}\frac{\mathrm{d}^2 \ell_n\left(\Omega^{(1,1)^*}\right)}{\mathrm{d}z^2} \quad \text{(A10)}$$

$$C^* = \frac{\Omega^{(1,2)^*}}{\Omega^{(1,1)^*}} = 1 + \frac{T^*}{3}\frac{\mathrm{d}\,\ell_n\left(\Omega^{(1,1)^*}\right)}{\mathrm{d}T^*} = 1 + \frac{1}{3}\frac{\mathrm{d}\,\ell_n\left(\Omega^{(1,1)^*}\right)}{\mathrm{d}z} \quad \text{(A11)}$$

$$E^* = \frac{\Omega^{(2,3)^*}}{\Omega^{(2,2)^*}} = 1 + \frac{T^*}{4}\frac{\mathrm{d}\,\ell_n\left(\Omega^{(2,2)^*}\right)}{\mathrm{d}T^*} = 1 + \frac{1}{4}\frac{\mathrm{d}\,\ell_n(\Omega^{(2,2)^*})}{\mathrm{d}z} \quad \text{(A12)}$$

where, as earlier, $z = \ell_n(T^*)$ and the recursion relation

$$\Omega^{(l,s+1)^*} = \Omega^{(l,s)^*}\left[1 + \frac{1}{s+2}\frac{\mathrm{d}\,\ell_n\left(\Omega^{(l,s)^*}\right)}{\mathrm{d}z}\right] \quad \text{(A13)}$$

has been used to relate each ratio to derivatives of the collision integrals $\Omega^{(1,1)^*}$ and $\Omega^{(2,2)^*}$. For the noble gases, these relations and the expressions for $\Omega^{(1,1)^*}$ and $\Omega^{(2,2)^*}$ can be used to compute the collision integral ratios for $T^* > 0$. B^* will not have a continuous first derivative at the matching points because only the continuity of the functionals through the second derivative has been demanded. For the molecular gases, application of the recursion relations is somewhat more limited. With the present representations of the molecular collision integrals $\Omega^{(1,1)^*}$ and $\Omega^{(2,2)^*}$, the ratios B^*, C^*, and E^* do not have continuous first derivatives below $T^* = 0.3$ because we have not imposed any restrictions on the derivatives of the polynomial extensions at the endpoints T_i^*, $i = 0, 1, 2$, but only demanded that the polynomials agree with the known values of the collision integrals at these points. To improve the smoothness of the representations of B^*, C^*, and E^* below $T^* = 0.3$, the similarity of the values of these ratios with those for the L–J potential suggests that below 0.3 we simply use the L–J values and fit a cubic polynomial to these values and the values obtained with the polynomial extensions at 0.3. The resulting expressions for $T^* \le 0.3$ are

$$B^* = 32/27 + 0.040105T^* + 0.691019T^{*2} - 0.105864T^{*3} \quad \text{(A14a)}$$

$$C^* = \tfrac{8}{9} + 0.046837T^* - 0.925111T^{*2} + 1.428519T^{*3} \quad \text{(A14b)}$$

$$E^* = 11/12 - 0.019839T^* + 0.305667T^{*2} - 0.829444T^{*3} \quad \text{(A14c)}$$

Acknowledgments

The author would like to thank Phillip H. Paul for several useful discussions and comments during the course of this work and the AIAA reviewers for their careful, critical review and useful suggestions regarding this work.

References

[1]Palaniswamy, S., Chakravarthy, S. R., and Ota, D. K., "Finite Rate Chemistry for USA–Series Codes: Formulation and Applications," AIAA Paper 89-0200, Jan. 1989.

[2]Drummond, J. P., Rogers, R. C., and Hussaini, M. Y., "A Numerical Model for Supersonic Reacting Mixing Layers," *Computer Methods in Applied Mechanics and Engineering*, Vol. 64, 1987, pp. 39–60.

[3]Copeland, D. A., "Transport Properties for COIL," AIAA Paper 2004-2261, June–July 2004.

[4]Copeland, D. A., "New Approximate Formulas for Viscosity and Thermal Conductivity of Dilute Gas Mixtures," *AIAA Journal*, Vol. 41, No. 3, 2003, pp. 525–537.

[5]Palmer, G. E., and Wright, M. J., "Comparison of Methods to Compute High-Temperature Gas Viscosity," *Journal of Thermophysics and Heat Transfer*, Vol. 17, No. 2, 2003, pp. 232–239.

[6]Palmer, G. E., and Wright, M. J., "Comparison of Methods to Compute High–Temperature Gas Thermal Conductivity," AIAA Paper 2003-3913, June 2003.

[7]Kang, S. H., and Kunc, J. A., "Viscosity of High-Temperature Iodine," *Physical Review A: General Physics*, Vol. 44, No. 6, 1991, pp. 3596–3605.

[8]Wakeham, W. A., "Transport Properties of Polyatomic Gases," *International Journal of Thermophysics*, Vol. 7, No. 1, 1986, pp. 1–35.

[9]Kestin, J., Knierim, K., Mason, E. A., Najafi, B., Ro, S. T., and Waldman, M., "Equilibrium and Transport Properties of the Noble Gases and Their Mixtures at Low Density," *Journal of Physical and Chemical Reference Data*, Vol. 13, No. 1, 1984, pp. 229–303.

[10]Boushehri, A., Bzowski, J., Kestin, J., and Mason, E. A., "Equilibrium and Transport Properties of Eleven Polyatomic Gases at Low Density," *Journal of Physical and Chemical Reference Data*, Vol. 16, No. 3, 1987, pp. 445–466; also Errata in Journal of Physical and Chemical Reference Data, Vol. 17, No. 1 (1988), page 255.

[11]Bzowski, J., Kestin, J., Mason, E. A., and Uribe, F. J., "Equilibrium and Transport Properties of Gas Mixtures at Low Density: Eleven Polyatomic Gases and Five Noble Gases," *Journal of Physical and Chemical Reference Data*, Vol. 19, No. 5, 1990, pp. 1179–1232.

[12]Mason, E. A., and Uribe, F. J., "The Corresponding States Principle: Dilute Gases," *Transport Properties of Fluids Their Correlation, Prediction, and Estimation*, edited by J. Millat, J. J. Dymond, and C. A. Nieto de Casto, Cambridge Univ. Press, Cambridge, England, U.K., 1996, Chap. 11, pp. 250–282.

[13]Paul, P. H., "DRFM: A New Package for the Evaluation of Gas–Phase Transport Properties," Sandia National Labs., Rept. SAND98-8203, UC-1409, Livermore, CA, Nov. 1997.

[14]Paul, P. H., and Warnatz, J., "A Re-Evaluation of the Means used to Calculate Transport Properties of Reacting Flows," *Twenty-Seventh Symposium (International) in Combustion*, Combustion Inst., Pittsburgh, PA, 1998, pp. 495–504.

[15]Tang, K. T., and Toennies, J. P., "New Combining Rules for Well Parameters and Shapes of the van der Waal Potential of Mixed Rare Gas Systems," *Z. Phys. D-Atoms, Molecules, and Clusters*, Vol. 1, 1986, pp. 91–101.

[16]Tang, K. T., and Toennies, J. P., "An Improved Simple Model for the van der Waals Potential Based on Universal Damping Functions for the Dispersion Coefficients," *Journal of Chemical Physics*, Vol. 80, No. 8, 1984, pp. 3726–3741.

[17]Cambi, R., Cappelletti, D., Liuti, G., and Pirani, F., "Generalized Correlations in Terms of Polarizability for van der Waals Interaction Potential Parameter Calculations," *Journal of Chemical Physics*, Vol. 95, No. 3, 1991, pp. 1852–1861.

[18]Thijsse, B. J., Hooft, G. W., Coombe, D. A., Knapp, H. F. P., and Beenakker, J. J. M., "Some Simplified Expressions for the Thermal Conductivity in an External Field," *Physica*, Vol. 98A, 1979, pp. 307–312.

[19]van der Oord, R. J., and Korving, J., "The Thermal Conductivity of Polyatomic Molecules," *Journal of Chemical Physics*, Vol. 89, No. 7, 1988, pp. 4333–4338.

[20]Millat, J., Vesovic, V., and Wakeham, W. A., "On the Validity of the Simplified Expression for Thermal Conductivity of Thijsse et al.," *Physica*, Vol. 148A, 1988, pp. 153–164.

[21]Uribe, F. J., Mason, E. A., and Kestin, J., "A Correlation Scheme for the Thermal Conductivity of Polyatomic Gases at Low Density," *Physica A*, Vol. 156, 1989, pp. 467–491.

[22]Uribe, F. J., Mason, E. A., and Kestin, J., "Thermal Conductivity of Nine Polyatomic Gases at Low Density," *Journal of Physical and Chemical Reference Data*, Vol. 19, No. 5, 1990, pp. 1123–1136.

[23]Parker, J. G., "Rotational and Vibrational Relaxation in Diatomic Gases," *Physics of Fluids*, Vol. 2, No. 4, 1959, pp. 449–462.

[24]Brau, C. A., and Jonkman, R. M., "Classical Theory of Rotational Relaxation in Diatomic Gases," *Journal of Chemical Physics*, 52, No. 2, 1970, pp. 477–484.

[25]Sandler, S. I., "Thermal Conductivity of Polyatomic Molecules," *Physics of Fluids*, Vol. 11, No. 12, 1968, pp. 2549–2555.

[26]Hirschfelder, J. O., Curtiss, C. F., and Bird, R. B., *Molecular Theory of Gases and Liquids*, Corrected Printing with Notes Added, Wiley, New York, 1964, Chap. 8, Appendix A.

[27]Marrero, T. R., and Mason, E. A., "Gaseous Diffusion Coefficients," *Journal of Physical and Chemical Reference Data*, Vol. 1, No. 1, 1972, pp. 3–118.

[28]Kestin, J., Ro, S. T., and Wakeham, W. A., "An Extended Law of Corresponding States for the Equilibrium and Transport Properties of the Noble Gases," *Physica*, Vol. 58, 1972, pp. 165–211.

[29]Najafi, B., Mason, E. A., and Kestin, J., "Improved Corresponding States Principle for the Noble Gases," *Physica*, Vol. 119A, 1983, pp. 387–440.

[30]Bzowski, J., Mason, E. A., and Kestin, J., "On Combination Rules for Molecular van der Waals Potential–Well Parameters," *International Journal of Thermophysics*, Vol. 9, No. 1, 1988, pp. 131–143.

[31]Maitland, G. C., Rigby, M., Smith, E. B., and Wakeham, W. A., *Intermolecular Forces Their Origin and Determination*, Clarendon, Oxford, 1987.

[32]Mason, E. A., and Monchick, L., "Heat Conductivity of Polyatomic and Polar Gases," *Journal of Chemical Physics*, Vol. 36, No. 6, 1962, pp. 1622–1639.

[33]Lambert, J. D., *Vibrational and Rotational Relaxation in Gases*, Clarendon, Oxford, 1977, Table 5.3, 123.

[34]Singh, Y., and Das Gupta, A., "Transport Properties of Polar–Quadrupolar Gas Mixtures," *Journal of Chemical Physics*, Vol. 33, No. 4, 1970, pp. 3055–3063.

[35]Singh, Y., and Das Gupta, A., "Transport and Equilibrium Properties of Polar Gases," *Journal of Chemical Physics*, Vol. 33, No. 4, 1970, pp. 3064–3067.

[36]Thakkar, A. J., and Smith, V. H., Jr., "On a Representation of the Long-Range Interatomic Interaction Potential," *Journal of Physics B, Atomic and Molecular Physics*, Vol. 7, No. 10, 1974, pp. L321–L325.

[37]Touloukian, Y. S., Saxena, S. C., and Hestermanns, P., "Viscosity," *Thermophysical Properties of Matter*, Vol. 11, Plenum, New York, 1975, Tables 2–G(T), 3–G(T), 5–G(T), 8–G(T), 23–G(T).

[38]Beaton, C. F., and Hewitt, G. F., *Physical Property Data for the Design Engineer*, Hemisphere, New York, 1989, pp. 262–265.

[39]Svehla, R. A., "Transport Coefficients for the NASA Lewis Chemical Equilibrium Program," NASA TM, 4647, April 1995.

[40]Miller, T. H., "Atomic and Molecular Polarizabilities," *Handbook of Chemistry and Physics*, 82nd ed., edited by D. R. Lide, CRC Press, Boca Raton, FL, 2001.

[41]Swift, K. M., Schlie, L. A., and Rathge, R. D., "Dispersion of Gases in Atomic Iodine Lasers at 1.315 μm," Preprint, Jan. 1988.

[42]Vargaftik, N. B., Vinogradov, Y. K., Yargin, V. S., "Handbook of Physical Properties of Liquids and Gases Pure Substances and Mixtures," 3rd and augmented ed., Begell House, New York, 1996.

[43]Oerstavik, K. I., and Storvick, T. S., "Viscosity and Heat Conductivity of Fluorine Gas; Computed Values from 100–2500 K and 0.25–2.0 Atmospheres," *Thermal Conductivity 14*, edited by P. G. Klemens and T. K. Chu, Plenum Press, New York, 1976, pp. 361–365.

[44]White, F. M., *Viscous Fluid Flow*, McGraw–Hill, New York, 1974.

[45]Matsunaga, N., and Nagashima, A., "Prediction of the Transport Properties of Gaseous H_2O and Its Isotopes at High Temperatures," *Journal of Physical Chemistry*, Vol. 87, No. 25, 1983, pp. 5268–5279.

[46]Lide, D. R., "Dipole Moments," *Handbook of Chemistry and Physics*, 82nd ed., edited by D. R. Lide, CRC Press, Boca Raton, FL, 2001.

[47]Zeiss, G. D., and Meath, W. J., "Dispersion Energy Constants $C_6(A, B)$, Dipole Oscillator Strength Sums, and Refractivities for Li, N, O, H_2, N_2, O_2, NH_3, H_2O, NO, and N_2O," *Molecular Physics*, Vol. 33, 1977, pp. 1155–1176.

[48]Sengers, J. V., and Watson, J. T. R., "Improved International Formulations for the Viscosity and Thermal Conductivity of Water Substance," *Journal of Physical and Chemical Reference Data*, Vol. 15, No. 4, 1986, pp. 1291–1314.

[49]Svehla, R. A., "Estimated Viscosities and Thermal Conductivities of Gases at High Temperatures," NASA TR R-132, 1962.

[50]Kunc, J. A., "Analytical Dependence of the Viscosity Cross Sections and Viscosity Coefficients on Parameters of Intermolecular Potentials," *Journal of Chemical Physics*, Vol. 99, No. 6, 1993, pp. 4705–4717.

[51]Gray, C. G., and Gubbins, K. E., *Theory of Molecular Fluids, Volume 1: Fundamentals*, Clarendon, Oxford, 1984, Eq. (2.119), Table D.3.

[52]Hayhurst, A. N., and Springett, M. J., "Flame Photometric Determination of Diffusion Coefficients Part 6.—Results for Carbon Monoxide and Free Atoms of Bromine, Iodine, and Thallium," *Journal of the Chemical Society, Faraday Transactions I*, Vol. 74, No. 3, 1978, pp. 715–719.

[53]Satterfield, C. N., Wentworth, R. L., and Demetriades, S. T., "The Viscosity of Vapor Mixtures of Hydrogen Peroxide and Water," *Journal of the American Chemical Society*, Vol. 76, No. 10, 1954, pp. 2633–2637.

[54]Stiel, L. I., and Thodos, G., "The Viscosity of Polar Gases at Normal Pressures," *AIChE Journal*, Vol. 8, No. 2, 1962, pp. 229–232.

[55]Yaws, C. L., *Chemical Properties Handbook*, McGraw–Hill, New York, 1999, p. 474.

[56]Millat, J., and Wakeham, W. A., "The Thermal Conductivity of Nitrogen and Carbon Monoxide in the Limit of Zero Density," *Journal of Physical and Chemical Reference Data*, Vol. 18, No. 2, 1989, pp. 565–581.

[57]Viehland, L. A., Mason, E. A., and Sandler, S. I., "Effect of Spin Polarization on the Thermal Conductivity of Polyatomic Gases," *Journal of Chemical Physics*, Vol. 68, No. 1, 1972, pp. 5277–5282.

[58]Millat, J., Vesovic, V., and Wakeham, W. A., "Transport Properties of Dilute Gases and Gaseous Mixtures," *Transport Properties of Fluids: Their Correlation, Prediction, and Estimation*, edited by J. Millat, J. H. Dymond, and C. A. Nieto de Castro, Cambridge Univ. Press, Cambridge, 1996, pp. 29–65.

[59]Moraal, H., and Snider, R. F., "Kinetic Theory Collision Integrals for Diatomic Molecules," *Chemical Physics Letters*, Vol. 9, No. 5, 1971, pp. 401–405.

[60]Monchick, L., Pereira, A. N. G., and Mason, E. A., "Heat Conductivity of Polar and Polyatomic Gases and Gas Mixtures," *Journal of Chemical Physics*, Vol. 42, No. 9, 1965, pp. 3241–3256.

[61]Chase, M. W., Jr., "Journal of Physical and Chemical Reference Data," Monograph No. 9, *NIST–JANAF Thermochemical Table*, 4th ed., American Chemical Society and the American Institute of Physics, Woodbury, NY, 1998.

[62]Kee, R. J., Warnatz, J., and Miller, J. A., "A FORTRAN Computer Code Package for the Evaluation of Gas-Phase Viscosities, Conductivities, and Diffusion Coefficients," Sandia National Labs., Rept. SAND83-8209, Livermore, CA, March 1983.

[63]Nyeland, C., Mason, E. A., and Monchick, L., "Thermal Conductivity and Resonant Multipole Interactions," *Journal of Chemical Physics*, Vol. 56, No. 12, 1972, pp. 6180–6192.

[64]Brokaw, R. S., "Predicting Transport Properties of Dilute Gases," *Industrial and Engineering Chemistry*, Vol. 8, No. 2, 1969, pp. 240–253.

[65]Touloukian, Y. S., Liley, P. E., and Saxena, S. C., "Thermal Conductivity," *Thermophysical Properties of Matter*, Vol. 3, Plenum, New York, 1970, Tables 2 (Br_2), 3 (Cl_2), 5 (F_2), and 24 (H_2O).

[66]Umanskii, A. S., Vladimirov, V. I., and Gorshkov, Yu. A., "Thermal Conductivity of Molecular Iodine Vapors," *High Temperature*, Vol. 22, No. 6, 1984, pp. 842–849.

[67]Ho, C. Y., Powell, R. W., and Liley, P. E., "Thermal Conductivity of the Elements: A Comprehensive Review," *Journal of Physical and Chemical Reference Data*, Vol. 3, Supplement No. 1, 1974, Table 75 (I_2).

[68]Kee, R. J., Rupley, F. M., and Miller, J. A., "The Chemkin Thermodynamic Data Base," Sandia National Labs., Rept. SAND87-8215B UC-4, Livermore, CA, March 1990.

[69]Gierke, T. D., Tigelaar, H. L., and Flygare, W. H., "Calculation of Molecular Electric Dipole and Quadrupole Moments," *Journal of American Chemical Society*, Vol. 94, No. 2, 1972, pp. 330–338.

[70]*Hydrogen Peroxide Physical Properties Data Book*, 2nd ed., Becco Chemical Div., FMC Corp., New York, 1954, p. 30, Table 30.

[71]Schreiber, M., Vesovic, V., and Wakeham, W. A., "Thermal Conductivity of Multicomponent Dilute Gas Mixtures," *International Journal of Thermophysics*, Vol. 18, No. 4, 1997, pp. 925–938.

[72]Ern, A., and Giovangigli, A., "Fast and Accurate Multicomponent Transport Property Evaluation," *Journal of Computational Physics*, Vol. 120, 1995, pp. 519–536.

[73]Brokaw, R. S., "Approximate Formulas for the Viscosity and Thermal Conductivity of Gas Mixtures," *Journal of Chemical Physics*, Vol. 42, No. 4, 1965, pp. 1140–1146.

[74]Kunc, J. A., "Transport Integrals $\Omega^{(l,s)}(T)$ for Binary Collisions of Open–Shell Atoms with Uncertain Interaction Potentials," *Physical Review E*, Vol. 58, No. 4, 1998, pp. 4960–4966.

[75]Ferziger, J. H., and Kaper, H. G., *Mathematical Theory of Transport Processes in Gases*, North–Holland, Amsterdam, 1972, pp. 526, 527.